DEVELOPMENTAL MECHANISMS REGULATING SPECIFICATION OF PREPLACODAL ECTODERM AND ITS MORPHOGENESIS INTO SENSORY PLACODES IN ZEBRAFISH

A Dissertation

by

NEHA BHAT

Submitted to the Office of Graduate Studies of
Texas A&M University
in partial fulfillment of the requirements for the degree of

DOCTOR OF PHILOSOPHY

Approved by:

Chair of Committee,	Bruce B. Riley
Committee Members,	Brian Perkins
	Robyn Lints
	Tina Guimnney
Head of Department,	U.J.McMahan

May 2013

Major Subject: Biology

ABSTRACT

Preplacodal ectoderm (PPE) is a contigous horse-shoe shaped domain that enwraps the anterior neural plate towards the end of gastrulation and eventally resolves into a number of focal epithelial thickenings called placodes. These placodes together with Neural Crest (NC), contributes to the peripheral nervous system in vertebrates. PPE and NC arise at the neural-non neural interface by distinct mechanisms during development. However, a general idea in the field was that a Bmp signaling gradient specifies different ectodermal fates: high Bmp levels specify epidermis, intermediate levels PPE and NC and no Bmp signaling is required for neural fate specification. We showed that while NC responds to intermediate levels of Bmp signals, PPE is specified by a distinct mechanism that involves a two step model for PPE specification. In the first step, Bmp is positively required to activate four competence factors, *tfap2a*, *tfap2c*, *foxi1* and *gata3* throughout the ventral ectoderm and renders this domain competent to respond to inductive factors. In the second step, inductive factors Fgf and Bmp antagonists act to completely block all Bmp signaling to specify PPE at neural-non neural interface. These Bmp-activated competence factors do not need Bmp for subsequent maintenance because they positively cross-regulate and autoregulate each other's expression forming a gene regulatory network. This network is sufficient to rescue both PPE and NC in the complete absence of Bmp.

The subsequent resolution of PPE into discerte placodal thickenings was hypothesized to involve localized migration of placodal progenitors and one of the

molecules that could play an important role during cell migration was extracellular matrix binding molecule, *integrin alpha 5* (*itga5*) because it was expressed at the right time and place. Knockdown of *itga5* results in disorganised trigeminal, epibranchial ganglia and smaller otic placodes. Tracing the cell trajectories of placodal progenitors revealed that cells failed to migrate directionally. Additionally, we observed elevated levels of cell death in *itga5* morphants which could be rescued by overexpression of Fgf ligands suggesting that Itga5 and Fgf pathways cooperate during placodal development. All together, this dissertation reveals novel genetic mechanisms that regulate placodal development from late-blastula to mid-somitogenesis stages.

DEDICATION

I would like to dedicate my dissertation to my mother, father and brother who have provided incessant and unconditional support throughout my graduate school without exactly knowing what I really do in the lab!

ACKNOWLEDGMENTS

I am grateful to my Ph.D advisor, Dr. Bruce Riley, for his continued support, encouragement and guidance throughout my research. I have matured as a person and as a researcher until his guidance. I would also like to thank my committee member, Dr. Brian Perkins for allowing me to use his compound and dissecting microscope for time-lapse imaging and for all the helpful advice all through the graduate school. I am also thankful to Dr. Robyn Lints and Dr. Tina Gumienny for their support and suggestions.

I am thankful to former and current Riley lab members for their support and helpful suggestions. I would especially like to mention Biwei Guo for sharing the interest for scientific and philosophical conversations. I had my best time in the lab with her. I especilly thank Dr. Hye-Joo Kwon for her work on the first chapter of this dissertation. Additionally, I learned how to work smartly and efficiently from her. I am also thankful to Dr. Elly Sweet and Dr. Bonny Millimaki for their useful comments and constructive criticisms on my research. Thanks to Dr. Mary C. Mullins for valuable suggestions on studies in ChapterII especially her idea of misexpressing competence factors in the dorsal ectoderm and also for sharing *Tg (hs:chd)* with us. Also, thanks to Johann Eberhart for sharing the *itga5* mutant line.

I am also thankful to former and current members of the Lekven lab: Anand Narayanan, Kevin Baker, Amy Whitener, JoAnne Fleming and current and previous members of Perkins lab: Bryan Krock and Michelle Ramsey for their continous support and useful suggestions. Thanks Amy for swiching that TA proctoring with me just a few

days before my defense. Thanks to Rhonda Patterson and all student workers for taking care of our fish. Thanks to all my friends, James, Sharvani, Mahesh Guruswamy, Bijay Shah, Dhara Shah, Miguel Zarate, Anand Narayanan and many others for making my stay in College Station a rewarding experience.

I am immensely grateful to all my teachers and mentors through high school and undergrad who provided me with an environment in which I could flourish and grow. I would not have been here without my teachers. I would especially like to mention Mr. S.K. Sangal, Mr. Pachijha, Dr. Renu Saxena, Dr. Nimisha Sharma, Dr N. Raghuram, Dr. Krishnamoorty Kannan and Dr. P.C. Sharma.

Last but not the least; I would like to thank my parents and my brother for their incessant support, prayers and love throughout my graduate career. Please don't ever change, Ma. I would also like to thank all my extended family back in India for their constant support and encouragement. Thank you all for your help.

TABLE OF CONTENTS

LIST OF FIGURES

Page

LIST OF TABLES

CHAPTER I

INTRODUCTION

This dissertation focusses on the molecular mechanisms responsible for the specification of Preplacodal ectoderm (PPE) and its subsequent resolution into cranial placodes. The cranial placodes make significant contributions to the sensory organs and ganglia in the vertebrate head. Since the specification of PPE is interlinked with the establishment of dorsal and ventral axis established during gastrulation, I will briefly review early embryonic patterning followed by a description of the known factors required for the specification of PPE and cranial placodes. Next, I will summarize the molecular events that lead to morphogenesis of PPE into individual placodes and describe why integrins could be interesting candidates for mediating morphogenesis.

EARLY EMBRYONIC PATTERNING AND THE ROLE OF BMP LIGANDS

The anterior-posterior and dorsal-ventral axes of most metazoans are established during gastrula stages in early embryogenesis. The seminal work done by Hans Spemann in early 1900's laid the foundation for understanding this basic mechanism in nature. One of his most famous experiments included transplantation of dorsal blastopore lip of a pigmented *Xenopus*gastrula embryo onto a less pigmented ventral side of another embryo. He found that this transplanted tissue was able to induce the surrounding regions of the host embryo to acquire a dorsal fate eventually leading to the twinning of

dorsal axes of *Xenopus* embryos (Spemann and Mangold 1924). This phenotype stimulated many investigators over the years to find the "mystery" molecule secreted by the dorsal region of *Xenopus*that has the ability to induce/ organize tissues around it. With the advent of feasible molecular techniques in late 1980's Edward De Robertis and other groups discovered that *Xenopus* organizer is a rich source of molecules such as: chordin, noggin and follistatin. It was subsequently found that these molecules can directly bind to Bmp ligands and prevent it from binding to its receptor. Bmp is expressed at high levels on the future ventral side and gets extracellularly inhibited by the Bmp antagonists secreted by the organizer creating a gradient of Bmp activity across the dorsal-ventral axes of the embryo (Figure 1.1; De Robertis 2006).

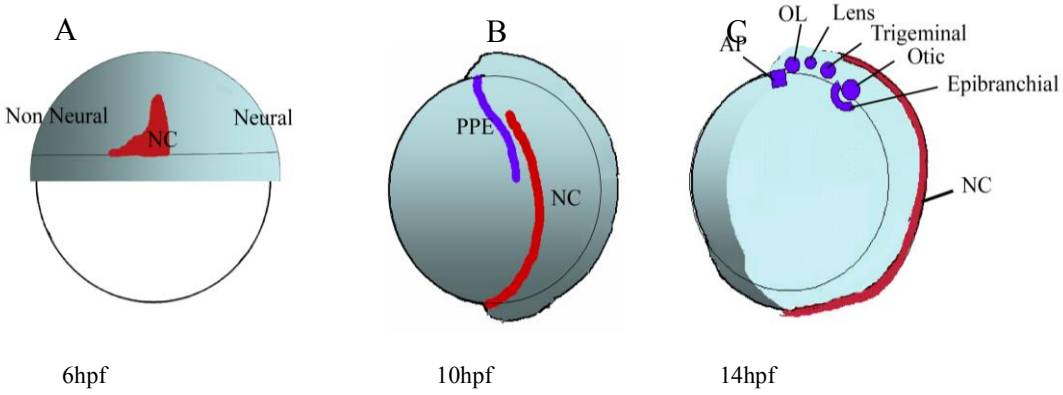

Figure 1.1: Relative location of NC and PPE with respect to the Bmp gradient. Panels A-C show relative position of neural (light blue), non neural, neural crest (NC, red), preplacodal ectoderm (PPE, dark blue), and specific placodes (blue): anterior pituitary (AP), olfactory (OL), lens, trigeminal, otic and epibranchial placodes at 6hpf (A), 10hpf (B) and 14hpf (C). Bmp gradient in the ectoderm is shown as a blue-gray color, with light blue representing least Bmp signal. At 6hpf, the gradient is evident across the dorsal (neural)-ventral axis while at 10hpf the gradient develops from posterior to anterior (Tucker et al., 2008). At 14hpf, higher levels of Bmp are evident in the prospective tail and epidermal domain. All panels show lateral views.

ELUCIDATION OF BMP PATHWAY

The genetic screens conducted in *Drosophila melanogaster* and *C. elegans* combined with biochemical approaches lead to the elucidation of the Bmp pathway, which is described as follows: dimeric Bmp ligand binds to tetrameric Bmp receptors that are composed of two types I and two type II Ser/Thr kinase receptors. Upon ligand binding, type II constitutively active receptor transphosphorylates type I receptor which then phosphorylates Smad1/5/8 proteins. The phosphorylated Smads 1/5/8 complexes with Smad4 protein and translocates to the nucleus. The dimeric complex of Smad 1/5/8 and Smad 4 binds to specific regulatory sequences leading to changes or maintenance of gene expression (Nakayama et al., 2000; Figure1.2).

BMP AS A MORPHOGEN

The TGFβ subfamily of ligands includes some of the first morphogens to be discovered. Gradients of both Bmp and Nodal were shown to induce formation of different fates along the dorso-ventral axis (Schier and Talbot, 2005). They satisfied three primary requirements of morphogen: (i) Different fates in the gastrula embryo show distinct concentration-dependent thresholds (ii) graded activity of these factors was directly visualized (iii) can act long-range to specify different fates (Rogers and Schier, 2011; Barkai and Shilo, 2009; Jones and Smith, 1998; Tucker et al., 2008).

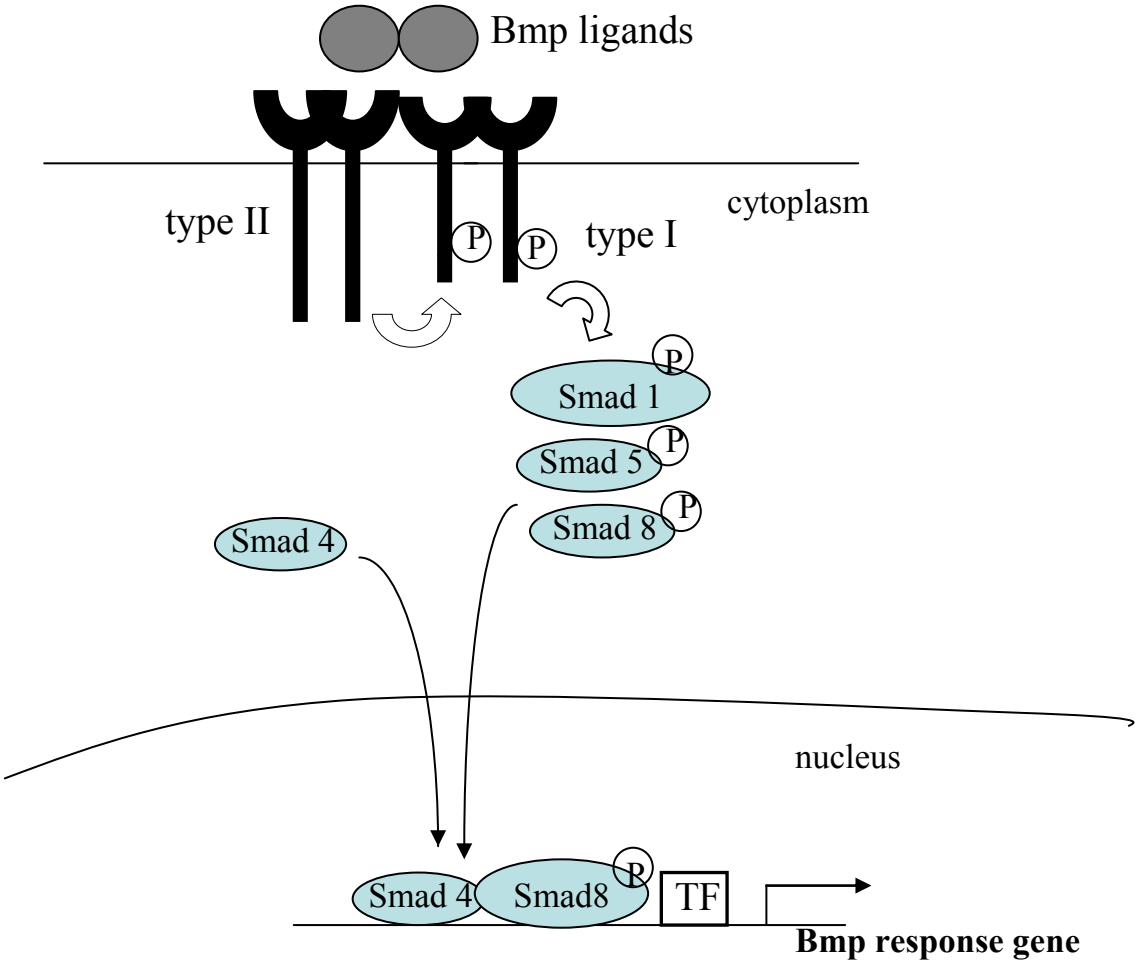

Figure 1.2: Bmp signal transduction pathway. Dimeric Bmp ligands bring constitutively active type II receptor in close proximity to type I receptor which gets phosphorylated at several serine-threonine residues. This phosphorylated type I receptor then phosphorylates Smad 1/5/8 which then forms a complex with Smad4 and translocates to the nucleus where it binds specific regulatory regions to cause activation of specific genes.

A gradient of Bmp signaling has been demonstrated to specify different fates along the dorsal-ventral axis of the embryo. In the mesoderm, high levels of Bmp specify blood; intermediate levels specify pronephros and somites while no Bmp signaling is required for specifying dorsally located notochord. These studies make Bmp a classic morphogen during mesodermal patterning (Neave et al., 1997; Wilson et al., 1997; Marchant 1998; Nguyen et al., 1998; Tucker et al., 2008; Dosch et al., 1997). Bmp also acts as a morphogen during ectodermal fate specification, where Bmp has to be inhibited to promote neural fates and high levels of Bmp specify epidermal fates. Intermediate levels of Bmp specify neural crest at the neural-non neural interface. In embryos hypomorphic for Bmp signaling, neural crest expands throughout the ventral ectoderm at the expense of epidermal fates (Nguyen et al., 1998; Tucker et al., 2008; Marchant et al., 1998; Barth et al., 1998; Figure1.1). However, the role of Bmp in specifying another dorsolateral fate, preplacodal ectoderm has been controversial and will be discussed below and also in Chapter II.

MOLECULAR REQUIREMENTS FOR NEURAL CREST SPECIFICATION

Neural crest (NC) is a vertebrate specific multipotent cell type that gives rise to diverse tissues such as cartilage, bone, connective tissue, neurons and glial cells of peripheral nervous system, pigment cells of skin, mesenchyme and smooth muscle cells of cardiovascular system (Northcutt, 2005; Donoghue et al., 2008). NC is induced at the lateral edges of the neural plate and as the neural tube closes, neural crest cells delaminate from the dorsal neural tube and then migrate in a highly stereotyped fashion

to different regions of the vertebrate body guided by both attractive and repulsive cues such as neuropilin, VEGF, semaphorins, Ephrins, cxcr4s etc (Huang and Saint-Jeannet, 2004; McLennan et al., 2012; Kulesa et al., 2010; Minoux and Rijli, 2010; Toyofuku et al., 2008; McLennan et al., 2010).

Studies in different model systems including chick, zebrafish and *Xenopus*indicate that NC is specified at early gastrula stages even though definitive NC markers are only evident by the end of gastrulation (Steventon et al., 2009; Basch et al., 2006; Mayor, 1995; Patthey et al., 2009; Tucker et al., 2008). Based on the fate mapping studies, it is apparent that the ectodermal domain contributing to the NC correlates with the domain that experiences intermediate levels of Bmp signaling in the ectoderm (Figure1.1 A, Tucker et al., 2008; Steventon et al., 2009; Basch et al., 2007). Most studies in vertebrate model systems concur that intermediate levels of Bmp signals specify NC. In zebrafish hypomorphic Bmp mutants NC expands at the expense of epidermal domain strongly suggesting that intermediate levels of Bmp specify NC (Tucker et al., 2008; Nguyen et al., 1998; Marchant et al., 1997;, Patthey et al., 2008; Patthey et al., 2009; Barembaum and Bronner-Fraser, 2005; Wawersick et al., 2004; Tribulo et al., 2003; Mayor et al., 1995; Wilson et al., 1997). After its initial specification by intermediate levels of Bmp, higher levels of Bmp signaling are required for subsequent NC differentiation (Stuhlmiller et al., 2012; Steventon et al., 2005; Figure1.1).

Gain and loss of function studies have also revealed an essential role for both Fgf and Wnt signaling for NC induction. Interestingly, tissues that induce this domain differ

among vertebrates: in chick and *Xenopus* paraxial mesoderm is the primary inducer while in zebrafish ectoderm is the major inducer (Monsoro-Burq, 2003; Villanueva et al., 2002; Lewis et al., 2004; Patthey et al., 2008; Patthey et al., 2009; Steventon et al., 2009; Carmona-Fontaine et al., 2007;, Stuhlmiller and Garcia-Castro, 2012; Bastidas et al., 2004). Additionally, Notch signaling also plays an important role in specification of NC. Cornell and Eisen showed that trunk NC and Rohan-Beard neurons are specified from an equivalence group where lateral inhibition by Notch prevents ngn1 expression in prospective NC cells (Cornell and Eisen, 2000; Cornell and Eisen, 2002).

SPECIFICATION OF PREPLACODAL ECTODERM

Preplacodal ectoderm is specified lateral to NC at neural-non neural interface at the end of gastrulation (Figure1.1; Patthey et al., 2009; Tucker et al., 2008; Steventon et al., 2009; Basch et al., 2006; Mayor, 1995). PPE eventually resolves into bilaterally located cranial placodes which together with neural crest, contribute to the peripheral nervous system in the head. Gene families belonging to *six*, *eya* and *dlx* are specifically upregulated in the PPE (Akimenko et al., 1994; Sahly et al., 1999; Kobayashi et al., 2000).

Since PPE arises at the neural-nonneural interface, a distinct intermediate level of Bmp signaling was assumed to specify PPE akin to NC (described above). This idea was supported by animal-cap explants in *Xenopus*where treatment with an intermediate dose of Bmp inhibitor Noggin, leads to induction of preplacodal markers in the explants (Brugmann et al., 2004). Glavic et al. 2004 showed that overexpression of Bmp inhibitor,

chordin can expand the PPE domain. These studies were interpreted as an evidence for Bmp morphogen model. In contrast, more recent studies by Litsiou et al. 2005; Ahrens and Schlosser, 2005 indicated that Bmp has to be attenuated for PPE specification. These studies never quantified the level of Bmp inhibition in their experiments making it difficult to assess whether intermediate levels or complete inhibition of Bmp signaling is required for PPE specification. The Bmp attenuation model does not completely discredit the Bmp morphogen model since Bmp could be attenuated to some intermediate level while *Xenopus*explant studies do not recapitulate the in-vivo conditions. Interpretation of these studies is further complicated by the fact that in zebrafish Bmp null mutant, *swirl*, PPE is completely lost indicting a positive requirement for Bmp. However, no zebrafish hypomorphic Bmp mutants have been discovered that would expand PPE throughout the ventral ectoderm similar to NC expansion in hypomorphic Bmp mutants (Nguyen et al., 1998). Altogether, Bmp is required for PPE specification but it was not clear whether intermediate levels directly specify PPE. We will show evidence in Chapter II against the Bmp gradient model and instead propose a different model showing temporally distinct roles for Bmp during PPE specification: first during blastula stages when Bmp establishes preplacodal competence throughout the ventral ectoderm irrespective of the Bmp gradient and second at the end of gastrulation when Bmp has to be completely inhibited.

In addition to Bmp attenuation, other reports have suggested that Fgf signaling also plays a crucial role in specification of PPE. Combination of Fgf together with Bmp antagonists have been shown to induce ectopic PPE markers on the ventral side of the

ectoderm indicating that both of these signals are sufficient to induce PPE markers (Litsiou et al., 2005; Ahrens and Schlosser, 2005). The temporal requirements for Fgf signaling during PPE specification will be addressed in Chapter II.

NEURAL PLATE BORDER MODEL FOR PPE AND NC SPECIFICATION

As mentioned above, NC and PPE are the two dorsolateral fates in the ectoderm. They share many common properties such as extensive cell migration (delamination of neurogenic placodal cells and NC cells), ability to form neurons, common requirement of certain transcription factors such as *tfap2a*, requirement for Fgf signaling. Several investigators have proposed that these two domains are specified together at the neural-nonneural border while other reports indicate that NC and PPE have distinct molecular requirements and are specified at different times during gastrulation. While Wnt and Bmp signaling are required for NC specification, PPE seems to be specified by Bmp inhibitors and Wnt inhibitors at the end of gastrulation. Lineage tracing of the neural plate border at early gastrula stages would reveal whether NC and PPE fates are derived from a common neural plate border domain or whether they are specified at different times in gastrulation. (Litsiou et al., 2005; Ahrens and Schlosser, 2005; Brugmann et al., 2004; Patthey et al., 2009; Tucker et al., 2008; Steventon et al., 2009; Basch et al., 2006; Mayor, 1995). In summary, the role of Bmp for PPE specification remains an unresolved problem. This problem is further complicated by other studies showing that both Bmp and a number of Bmp targets are positively required for specification of preplacodal ectoderm suggesting that Bmp has a positive role during PPE specification.

BMP TARGET GENES AND THEIR ROLE IN PLACODAL DEVELOPMENT

Bmp activates a number of genes in the nonneural ectoderm, out of which four transcription factors, *tfap2a*, *tfap2c*, *foxi1, gata3* are implicated in placodal development in different vertebrates (Li and Cornell, 2007;, Neave et al., 1995; Solomon et al., 2003; Lee et al., 2003; Solomon et al., 2003; Nissen et al., 2003; Sun et al., 2007;, Karis et al., 2001). These four transcription factors are expressed throughout the non neural ectoderm starting late blastula stages with *tfap2a* and *tfap2c* extending slightly more medially than *foxi1* and *gata3* suggesting that *tfap2a* and *tfap2c* might be sensitive to lower levels of Bmp signaling than *foxi1* and *gata3*. Since these factors had previously been implicated in placode development (see below) we sought to understand whether the broad expression of these transcription factors in the nonneural ectoderm has any biological relevance for preplacodal development. In contrast to the above mentioned transcription factors, *p63*, another Bmp target coinduced in the ventral ectoderm is critical for epidermal specification but plays no role in PPE development (Bakkers et al., 2002; Lee et al., 2002; Chapter II). This suggests that although Bmp activates a number of transcription factors in the nonneural ectoderm, the requirement for *tfap2a*, *tfap2c, foxi1* and *gata3* during placodal development is relatively specific.

Tfap2a and Tfap2c were first described to have a role in initial induction of neural crest and epidermal development in different chordates (Luo et al., 2003; Knight et al., 2003; Hoffman et al., 2007; Li and Cornell, 2007; Nikitina et al., 2008; de Crozé et al., 2011; Wang et al., 2011; Van Otterloo et al., 2012). Recently, Tfap2a and Tfap2c have been implicated in placodal development in zebrafish with combinatorial

knockdown of these two genes leading to reduction of mature placodal structures (Li and Cornell, 2007; Hoffman et al., 2007). Using both loss and gain of function studies we investigated the role of *tfapa2a/tfap2c* in placode induction in Chapter IV.

Foxi1, a winged helix transcription factor, has been implicated in the development of otic and epibranchial placodes in zebrafish. In the absence of *foxi1,* key otic markers such as *pax8* and *pax2a* are completely eliminated or significantly downregulated. *foxi1* has also been shown to be necessary for the induction of epibranchial placode development in zebrafish (Lee et al., 2003; Solomon et al., 2003; Nissen et al., 2003; Sun et al., 2007; Nechiporuk et al., 2007). Although activated by Bmp initially throughout the ventral ectoderm, *foxi1* gets upregulated at the neural-non neural interface in response to Fgf signaling at the end of gastrulation (Philips et al., 2004; Padanad et al., 2012). Gata3, the zinc finger transcription factor, is coexpressed in the ventral ectoderm along with *tfap2a*, *tfap2c* and *foxi1*. *gata3* mutants develop with severe otic defects in mice (Karis et al., 2001; Sheng and Stern, 1999; Neave et al., 1995). The regulatory and epistatic interactions between the four transcription factors during specification of individual placodes will be discussed in Chapter IV.

SPECIFICATION OF INDIVIDUAL PLACODES FROM PPE

PPE resolves into a number of distinct placodes along the anterior-posterior axis of the embryo in response to local inductive cues (Baker and Bronner-Fraser, 2000; Schlosser, 2006; Streit, 2007; Figure1.1). Below is a brief description of six placodes that get induced from this domain along the rostro-caudal axis of the embryo. Out of all the

placodes, otic placode induction has been most extensively studied among all the sensory placodes and hence is discuused in relatively more detail below.

Anterior pituitary

The adenohypophysis/anterior pituitary placode forms at the anterior most portion of the PPE in the midline. This thickened portion of the anterior neural ridge will subsequently get internalized by extensive growth of forebrain and contact the neurohypophysis (posterior pituitary) of the forebrain which together will form the mature pituitary gland. Anterior pituitary secretes hormones such as gonadotropins, prolactin, thyroid-stimulating hormone, melanophore-stimulating hormones (Baker and Bronner-Fraser, 2001; Kawamura, 2002) which are important for homeostasis and reproduction. The earliest markers expressed in this placode include *pitx3, lim3*. Sonic Hedgehog signals from the notochord and Fgf3 from the forebrain activate *pitx3* in prospective anterior pituitary cells (Dutta et al., 2005; Pogoda and Hammerschmidt, 2007; Herzog et al., 2004; Toro and Varga, 2007).

Olfactory and lens placode

The precursors of lens and olfactory placodes are intermingled initially but sort out by directed cell migration in such a way that olfactory precursors move medially and anteriorly while lens precursors remain localized laterally (Bhattacharyya et al., 2004; Whitlock and Westerfied, , 2000; Dutta et al., 2005). Olfactory placodes give rise to olfactory epithelium containing odorant sensing (olfactory) and pheromone sensing

(vomeronasal) neurons, support cells and glial cells. The lens placodal cells instead form the lens of the vertebrate eye. Lens placodal cells eventually cavitate to form the vesicle and accumulate crystallin proteins to form the mature lens of the eye (Baker and Bronner-Fraser, 2001). *otx-2*, *pax-6* and *sox3* are the earliest genes coexpressed in olfactory and lens placodes during specification (Zygar et al., 1998; Jin et al., 2012). Additionally, both Bmp and Fgf signaling are required for development of both lens and olfactory placodes during somitogenesis stages (Pandit et al., 2011; Garcia et al., 2011). In response to inducing factors, distinct genes are upregulated in olfactory and lens placodal domains: *pitx3*, *foxe3*, *crystallin, L-maf* in the lens placode and *cxcr4b*, *foxg1, dlx3b*, *emx2* in the olfactory placodes (Duggan et al., 2008; Baker and Bronner-Fraser, 2001). Recent explant studies in chick suggest that continued Fgf and transient Bmp signaling is required to promote olfactory fates while continued Bmp exposure and no Fgf signaling was required for proper lens differentiation (Bailey et al., 2006; Sjödal et al., 2008). However, these findings have yet to be confirmed in vivo. These reports also contradict other findings that show that Fgf is necessary for specification of both lens and olfactory placodes (Faber et al., 2001; Garcia et al., 2011). Therefore, the exact signaling requirements that distinguish olfactory and lens placodal fates *in-vivo* are yet to be completely resolved.

Trigeminal placode

Cranial nerve V is the largest cranial nerve and receives major contributions from trigeminal placodal precursors and neural crest precursors. These ganglia mediate touch,

pain, temperature, proprioception from skin of head, eyes and jaws. Trigeminal placodal precursors delaminate below the surface ectoderm where they are joined by neural crest cells which together make up the trigeminal ganglion (Baker and Bronner-Fraser, 2001; Lee et al., 2003; Artinger et al., 1998; Baker et al., 2002). While NC accumulates proximally and primarily gives rise to glia and some sensory neurons, the placode derived cells aggregate distally and give rise solely to sensory neurons (Artinger et al., 1998). It has recently been suggested that Wnt and Robo-Slit pathways promote the coalescence of neural crest and placodal cells (Shigetani et al., 2008; Shiau et al., 2008). *pax3* and *ngn1* are the earliest markers expressed in trigeminal placode. Receptors for Fgf, Shh, Pdgf, Igf, Tgfbeta and Wnt signaling pathways are expressed in trigeminal placodes (McCabe et al., 2007). However, only Wnt, Fgf and Pdgf ligands have so far been implicated in trigeminal placode induction (McCabe and Bronner-Fraser, 2008; Lassiter et al., 2007; Canning et al., 2008).

Otic placode

The otic placode gives rise to the complete inner ear, which is the most structurally and functionally complex organ among the placodal derivatives. It is also one of the most extensively studied placodes. The prospective otic domain is initially a single layered ectoderm which eventually forms a multilayered otic placode as morphogenesis proceeds. In zebrafish, this multilayered otic placode undergoes cavitation to form the otic vesicle. In response to localized signals and transcription factors, the otic vesicle subsequently undergoes complex morphogenesis to give rise to an interconnected set of

chambers along with mechanosensory hair cells and statoacoustic ganglion. These ganglion cells make appropriate connections in the brain to mediate hearing and balance across all vertebrates (Ladher et al., 2010; Riley and Philips, 2003; Whitfield et al., 2002).

Fgf is one of the primary secreted ligands implicated in otic development across all vertebrates. In vertebrate model systems such as zebrafish, mouse and chick Fgf ligands have been shown to be necessary and sufficient for otic induction, although the tissues that secrete Fgf differs among them (Ladher et al., 2000; Vendrell et al., 2000; Wright and Mansour, 2003; Alvarez et al., 2003; Zelarayan et al., 2007; Ladher et al., 2005). In zebrafish, Fgf3 and Fgf8 are implicated in otic induction (Philips et al., 2001; Philips et al., 2003; Maroon et al., 2002; Leger and Brand, 2002; Liu et al., 2003). These ligands are coexpressed at higher levels in hindbrain than the subjacent mesoderm at the time of otic induction in zebrafish while in other model systems such as chick, mesoderm is the main inducer. Therefore, the primary inducing source might be different among vertebrates; Fgf remains the main evolutionarily conserved ligand for otic induction.

In response to Fgf signals, *pax8* gets expressed in the pre-otic domain just before the end of gastrulation in zebrafish and mice. Subsequently, prolonged Fgf exposure leads to activation of *pax2a* at the beginning of somitogenesis (Leger and Brand, 2002; Philips et al., 2004; Philips et al., 2001; Pfeffer et al., 1998). Mackereth et al., 2005 showed that in the absence of *pax8,* otic domain is reduced by half. However, when *pax8*, *pax2a and pax2b* are downregulated simultaneously, the otic domain is severely

compromised and the remaining otic cells are unable to maintain their fate. This indicates that *pax8* is critical for the induction of otic fate and cooperates with *pax2a-2b* to maintain the otic fate (Hans et al., 2004; Mackereth et al., 2005).

foxi1 and *dlx3b* are the other earliest known transcription factors shown to play distinct roles in otic development. While knockdown of *foxi1* leads to complete abrogation of *pax8* expression, knockdown of *dlx3b* does not affect *pax8* expression while *pax2a* expression is delayed (Solomon and Fritz, 2002; Solomon et al., 2003; 2004; Liu et al., 2003; Hans et al., 2004; Hans et al., 2007). Therefore, *foxi1* and *dlx3b* operate at temporally distinct phases to mediate otic development through two parallel pathways: *foxi1-pax8* and *dlx3b-pax2a*. As mentioned above, *foxi1* and *dlx3b* are activated by Bmp during gastrulation. However, around the time of otic induction at the end of gastrulation, *foxi1* and *dlx3b* are positively regulated by Fgf signaling (Solomon et al., 2004; Hans et al., 2007; Padanad et al., 2012; Chapter II). Altogether, these studies indicate that Fgf orchestrates otic induction and activates several downstream targets which are together necessary for otic placode induction.

Epibranchial placode

Epibranchial neurons provide viscero-sensory and gustatory information to central nervous system. These neurons are derived from both neural crest and epibranchial placodes where the latter develop as focal thickenings ventro-lateral and dorsoanterior to pharyngeal clefts. These placodal cells delaminate from the surface and combine with the neural crest cells derived from specific segments of the hindbrain to give rise to

epibranchial ganglia. Although neural crest does not play any role in specification of epibranchial placode derived neurons, it is implicated in the proper delamination and assembly of epibranchial ganglia (Begbie and Graham, 2001; Culbertson et al., 2011).

One of the first genes to be induced in the epibranchial domain is *sox3*. *sox3* is initially induced in the otic domain in response to Fgf3/Fgf8 ligands from the hindbrain. As mentioned above, Fgf3/8 also induces *pax8* in the otic domain. *pax8* subsequently activates *fgf24* expression in the otic domain which induces *sox3* expression in the adjacent epibranchial domain and downregulates *sox3* from the otic domain. After induction, further epibranchial neurogenesis occurs in response to Bmp7 and Fgf3 from pharyngeal endoderm (Padanad and Riley, 2011; Begbie et al., 1999; Nechiporuk et al., 2005; Sun et al., 2007).

CELL MIGRATION AND THE RESOLUTION OF PPE

As mentioned above, placode specific upregulation of genes within PPE occurs in response to local inductive cues. Examples include *pax6* in lens, *pax3* in trigeminal and *pax8/2a* in otic domain. Temporal analysis of otic marker*, pax2a*, revealed that otic cells are more tightly packed at the time of morphological placode formation (mid-somitogenesis) as compared to more loose arrangement of pre-otic cells in PPE (Philips et al., 2006). This suggested that preotic cells might actively migrate to condense into a placodal structure. Detailed studies in more anterior placodal domain indicated that segregation of anterior placodal precursors into medially located olfactory and laterally located lens precursor domain correlates with differential expression of Dlx and Pax6

respectively in these placodes (Bhattacharyya et al., 2004; Dutta et. al 2005). Eventually, olfactory precursors located more medially undergo directed cell migration in response to Cxcr4b mediated chemokine signaling towards the anterior while more laterally located cells would eventually form lens placodes (Bhattacharyya et al., 2004; Whitlock and Westerfield, 2000). Similarly, Cxcr4b mediated chemokine signaling is shown to be involved in directed migration of trigeminal placode precursors (Knaut et al., 2005). In addition to chemokines, extracellular matrix binding transmembrane receptors, integrins, are also implicated in cell migration in different developmental contexts (Bokel and Brown, 2002). We were interested in examining the role of *integrin alpha5* during placodal morphogenesis because it was the only integrin molecule that showed relatively specific and robust expression throughout the PPE (Koshida et al., 2005; Crump et al., 2004). Below is a general description of integrins and a more specific function of *integrin alpha5* during posterior placodal morphogenesis will be described in Chapter IV.

INTEGRINS AS CANDIDATES FOR MEDIATING CELL MIGRATION

Integrins are transmembrane protein receptors composed of two non-covalently linked subunits alpha and beta and they bind to the fibrous extracellular matrix (ECM). Upon binding to the fibrous extracellular matrix on the outside, integrins undergo conformational change that results in the binding of several cytoskeltal proteins to the beta cytoplasmic domains. These proteins include several actin-binding proteins such as talin, filamin, vinculin and alpha-actinin which eventually will lead to polymerization or rearrangement of actin cytoskeleton. Binding to ECM also triggers clustering of

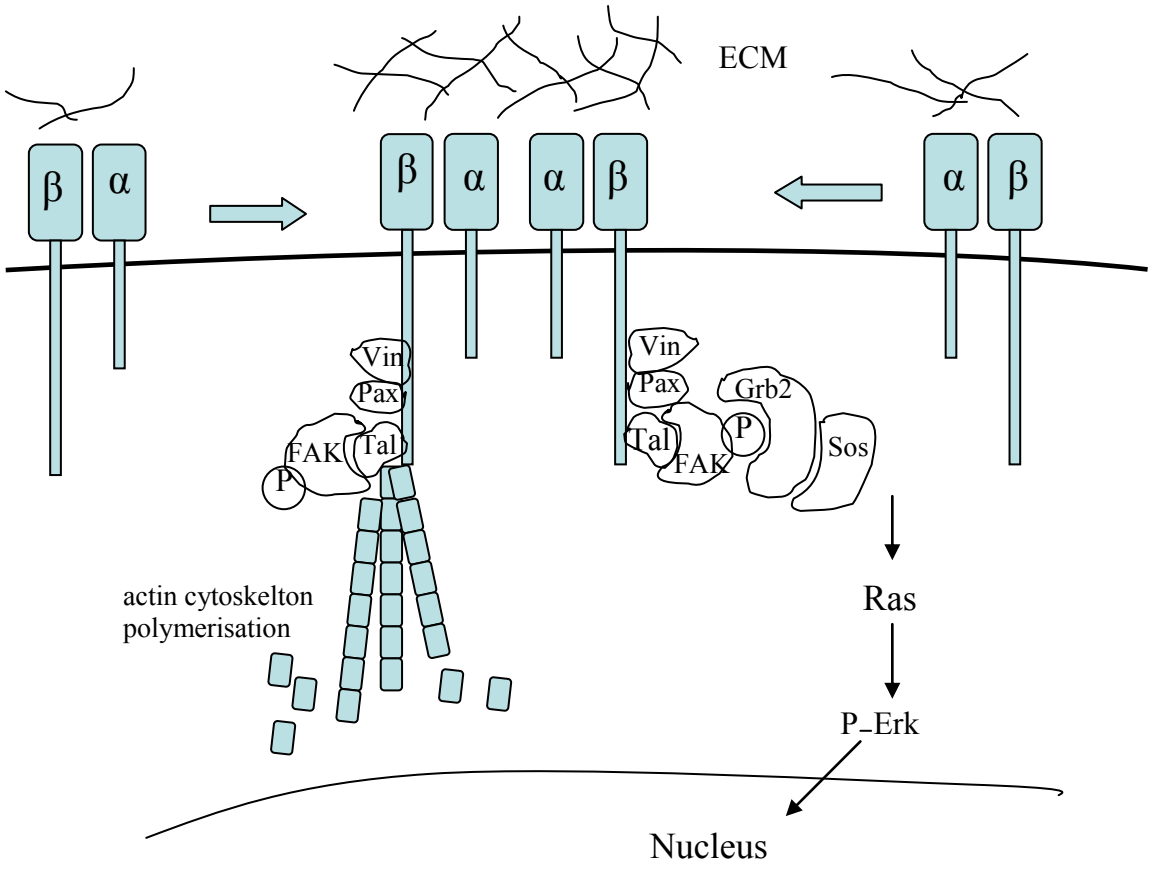

Figure 1.3: Integrins as convergence points for mediating both cell signaling and morphogenesis. After binding to extracellular matrix, integrin molecules cluster on the cell membrane and bind a number of proteins intracellularly such as Vinculin (Vin), Paxilin (Pax), Talin (Tal), Focal Adhesion Kinase (FAK). FAK autophosphorylates itself and also phosphorylates a number of other proteins leading to polymerization of actin cytoskeleton and hence changes in cell shape, migration and adhesion (Left side of the pathway). Additionally, integrins can also recruit a number of proteins belonging to Fgf signal transduction pathway that can lead to activation of series of kinases which could enter the nucleus and cause changes in gene expression (right side of the pathway). Thus, integrins can modulate both morphogenesis and signaling (Figure adapted from Giancotti and Ruoslahti 1999).

integrins in the cell membrane allowing cells to bind ECM with more affinity and avidity. This complex of several aggregated integrin molecules along with the bound cytoplasmic proteins is referred to as focal adhesion complex. The localized clustering of integrin molecules ensures the targeted accumulation of actin cytoskeleton in the membrane which can cause controlled changes in cell-shape, directed cell-migration and cell adhesion (Liu et al., 2000; Hynes, 2002; Schwatz and Ginsberg, 2002). Additionally , integrins are also implicated in signaling processes that control differentiation, survival and gene expression. In the absence of any enzymatic activity, these critical developmental events are mediated by other enzymes that bind to its cytoplasmic domain such as Focal Adhesion Kinase (FAK) and Src kinases. Other signaling molecules such as Rho GTPases can also get activated by integrins. These G-proteins could mediate changes in gene expression by activating downstream effectors (Katz and Yamada 1997; Bokel and Brown, 2002). Therefore, integrins provide convergence points for mediating both cell morphogenesis and cell signaling (Figure1.3).

DIVERSITY OF INTEGRIN MOLECULES IN METAZOANS

Integrins are responsible for morphogenetic events across all metazoans including sponges. The number of integrin molecules increased with more structural complexity of animals. The *C. elegans* genome encodes 1 beta and 2 alpha subunits; *Drosophila* genome encodes 2beta and 5 alpha integrin molecules. Mammals have 18alpha and 8 beta subunits and together form about 24 integrin combinations (Bokel and Brown, 2002). In zebrafish 12 alpha and 8 beta subunits have been described so far. The

increased redundancy between integrin molecules in vertebrates makes it harder to decipher their roles during development. On the other hand, effects of knocking down integrins are devastating in *C. elegans* and *Drosophila* because they are few in number and are implicated in several developmental processes. Integrins are classified broadly into two categories: those that bind Arginine-Glycine-Aspartic acid (RGD) containing ECM ligands and those that bind trimeric ECM molecules, laminins. Integrin alpha5, which will be described in Chapter IV, belongs to RGD containing class while the latter is more prevalent in basement membranes of epithelia lining visceral organs such as gut and otic vesicle.

ROLE OF INTEGRINS IN DEVELOPMENT

Integrins are implicated in a diverse array of developmental processes that include cell migration, cell adhesion and cell signaling. These developmental processes ensure proper morphogenesis and differentiation in metazoans. It is illustrated below by three different sections where integrin misregulation leads to defective morphogenesis.

Cell migration

One of the earliest and very essential biological processes where integrins are involved is gastrulation. In *Xenopus* embryos, absence of fibronectin (ECM for many integrins) or integrin beta1 causes gastrulation defects where mesodermal cells show reduced rates of involution and failure of ectodermal cells to intercalate properly resulting in a deformed embryo (Marsden and DeSimone, 2001). These defects were shown to result from

mesodermal cells extending actin-rich protrusions in random directions causing intercalation defects (Davidson et al., 2006). The other two major developmental events where extensive cell migration is involved during development are neural crest migration and neuronal organization of the central nervous system. In zebrafish and mice *integrin alpha5* is implicated in neural crest migration and survival (Crump et al., 2004; Goh et al., 1997) while in chick absence of *integrin alpha4* leads to delayed delamination of NC cells from the neural plate, defective cellular trajectories and increased NC cell death (Testaz and Duband, 2001). In *alpha3* mutant mice, the laminar organization of neurons in the cerebral cortex is disrupted due to compromised cell adhesion of neurons to radial glia (Anton et al., 1999). Additionally, integrins are also implicated in axon pathfinding in *Drosophila* and *C. elegans*. These axons eventually reach their targets but through different routes (Hoang and Chiba, 1998; Baum and Gariga, 1997).

Cell adhesion

Stable adhesion of cells to their ECM environment is critical for maintaining the integrity and functionality of adult organs. I will briefly illustrate this in the context of two tissues: epidermis and muscle. In *Drosophila* wings, clones of cells mutant for, otherwise embryonic lethal, integrin subunits alpha PS1 and PS2 causes blistering in the wings. This results from insufficient adhesion of dorsal and ventral wing epithelial cell layers to bind the extracellular matrix between them causing wing blistering (Brower and Jaffe, 1989). A similar skin-blistering phenotype is evident in mammals where

epidermal cells deficient in *integrin alpha 6* or *beta 4* fail to attach to the underlying basement membrane. This leads to in skin blistering phenotype also called epidermolysis bullosa (Vidal et. al, 1995; Pulkkinen et. al, 1997). Additionally, integrins have been implicated in muscle formation in several animal model systems: *C. elegans*, *Drosophila*, zebrafish and mammals. In *Drosophila beta1* mutant the attachment of muscles to the tendon-matrix is compromised resulting in rounding up of muscles (Newman and Wright, 1981). Zebrafish, *itga5* mutants show defective epithelialization at somite boundaries which eventually form muscle, bone etc. (Julich et al., 2005; Koshida et. al 2005). Mice mutant for *alpha5/ alpha7* display severe muscle dystrophy causing muscle cells to undergo apoptosis due to insufficient binding to the extracellular matrix at the tendons (Mayer et al., 1997; Taverna et al., 1998).

Cell signaling

There is no dedicated signal transduction pathway for integrins as compared to many other signaling molecules. However, recent reports indicate that integrins can significantly modulate the Fgf pathway. Integrins have been shown to interact with the Fgf pathway at different levels depending on the cell type and developmental context. Upon binding to ECM, one of the cytoplasmic proteins, Focal adhesion kinase (FAK) gets recruited to the beta tail of integrin cytoplasmic domain where it gets phosphorylated at several residues including Tyr 935. pFAK can recruit adaptor proteins Grb2 and SoS, which are components of Fgf pathway, leading to the activation of a series of kinases elevating the overall levels of pMAPK in the cells resulting in changes

in gene expression (Giancotti and Ruoslahti, 1998; Bokel and Brown, 2000; Hynes, 2002; Schwartz and Ginsberg, 2002; Katz and Yamada, 1997; Liu et al., 2000; Figure3). Rusnati et al., 1997 showed using immuno-histochemical approaches that integrin *alphaVbeta3* interacts with Fgf receptors at focal adhesion contacts in endothelial cell cultures suggesting cross talk among Integrins and Fgf receptors. In NIH3T3 cells and also in murine fibroblasts, loss of anchorage leads to inefficient accumulation of phosphorylated Elk-1 (target of MAP kinase) in the nucleus due to ineffective Rac activation (Aplin et al., 2001; Hirsch et al., 2002). One of the most striking roles for integrin signaling in-vivo has been described for *integrin beta1* subunit in *Drosophila* midgut morphogenesis. In the absence of *itgab1;* the midgut cells of *Drosophila* ectopically expresses genes normally repressed in these domains and these defects could get rescued by overexpression of a chimeric construct that lacks the extracellular domain but retains only the cytoplasmic domain of integrin beta subunit which mediates signaling functions (Martin-Bermudo and Brown, 1999). Martin-Bermudo 2000 further elucidated that absence of *itgab1* leads to disorganized ECM at the tendons that compromises the proper accumulation of Vein (EGF) ligand in the ECM indirectly leading to reduced expression of differentiation markers in muscles.

CONVERGENCE OF INTEGRINS AND CELL DEATH PATHWAYS DURING DEVELOPMENT AND HOMEOSTASIS

Apoptosis is an evolutionary conserved mechanism to clear unwanted cells and also to prevent growth of cells in unwanted places. Unrestrained growth of cells in foreign

environments can lead to many physiological conditions such as cancer. One way the cells can sense their extracellular environment is with the help of integrins. Therefore, apoptotic pathway and integrin pathway are intimately linked at the molecular level in nearly every cell in the animal. This form of apoptosis displayed by cells which are not bound to the extracellular matrix is also called 'anoikis'. There is no dedicated apoptotic pathway triggered by integrins and the exact biochemical pathway triggered by integrins is highly context dependent. Nevertheless, the apoptotic pathway culminates in the activation of caspases, DNA fragmentation and cell death (Chiarugi and Giannoni, 2008; Fan et al., 2005; Brenner and Mak, 2009).

DISSERTATION OBJECTIVES

This dissertation focusses on the elucidation of genetic mechanisms that regulate specification of PPE and its morphogenesis into individual sensory placodes. In Chapter II we show evidence in support of a two-step model for PPE specification: In the first step, Bmp is positively required to activate four competence factors, *tfap2a*, *tfap2c*, *foxi1* and *gata3* throughout the ventral ectoderm. These transcription factors render ventral ectoderm competent to respond to inductive factors which act in the second step. In the second step, inductive factors Fgf and Bmp antagonists act to completely block all Bmp signaling to specify PPE at neural-non neural interface. These data do not support a traditional Bmp gradient model where a discerete threshold of Bmp signal is required for PPE specification. This work was done in collaboration with a former post-doc Dr. Hye-Joo Kwon. Individual author contributions are listed in the beginning of Chapter II.

In Chapter III, I showed that the above mentioned Bmp-activated competence factors do not need Bmp for subsequent maintenance of expression. These transcription factors positively cross-regulate and autoregulate each other's expression forming a gene regulatory network. This genetic network is sufficient to rescue PPE, subset of specific placodes and NC in the complete absence of Bmp. Even though these transcription factors are redundantly required for PPE specification, they perform distinct non-redundant functions during the development of individual placodes. Hye-Joo Kwon contributed to the generation of transgenic *hs:tfap2a* line and some panels in Figure1. These are also listed in the beginning of Chapter III.

In Chapter IV, I showed a necessary requirement for *itga5* during the assembly of posterior placodal progenitors. When *itga5* is knocked down, trigeminal and epibranchial precursors are dispersed while the otic placode is significantly smaller. These defects are in part due to failure of cells to migrate directionally. In addition, we show that *itga5* and Fgf pathways coordinate to regulate patterning and survival of otic and epibranchial precursors. All together, this dissertation reveals novel genetic and molecular mechanisms responsible for early development of placodes from late-blastula to mid-somitogenesis stages.

CHAPTER II

IDENTIFICATION OF EARLY REQUIREMENTS FOR PREPLACODAL ECTODERM AND SENSORY ORGAN DEVELOPMENT*

AUTHOR CONTRIBUTIONS

This work was done in collaboration with Dr. Hye-Joo Kwon who was a former post-doc in the lab. She was the co-first author and I was the second co-first author on this paper. She performed the work shown in the following figures: Figure 2.4A-F, K-L, Figure 2.8, Figure 2.9A-H and I performed the work shown in Table1; Figure 2; Figure 3G-J, M and N, Figure 4, Figure 5, Figure 6D-H, Figure 7 I-S. I generated the data for Table 1 based on pilot studies done by Hye-Joo Kwon. The model figures 1 and 8 were generated by Dr. Bruce Riley and Dr. Hye-Joo Kwon. Elly Sweet generated the *Tg (hs:fgf8)* and *Tg (hs:fgf3)* lines.

INTRODUCTION

Cranial placodes provide major contributions to the paired sensory organs of the head. Examples include the anterior pituitary, the lens of the eye, the olfactory epithelium, the inner ear, and clusters of sensory neurons in the trigeminal and epibranchial ganglia (Baker and Bronner-Fraser, 2000; Schlosser, 2006; Streit, 2007; Brugmann and Moody,

---

*Reprinted from open access article "Identification of Early Requirements for Preplacodal Ectoderm and Sensory Organ Development" by **Kwon, H-J [#]., Bhat., N[#]., Sweet., E**., **Cornell, E**., **Riley B. B**., PLoS Genetics 6, e1001133. [#] These authors contributed equally to this work.

2005). Though diverse in fate, all placodes are thought to arise from a zone of pluripotent progenitors termed the preplacodal ectoderm. Preplacodal cells arise from the nonneural ectoderm immediately adjacent to neural crest. Neural crest cells originate in the lateral edges of the neural plate and later migrate to placodal regions to contribute to the corresponding sensory structures (Baker and Bronner-Fraser, 2000; Schlosser, 2006). However, while neural crest has been analyzed extensively, little is known about the early requirements for preplacodal development. Various preplacodal markers, including members of the *eya*, *six* and *dlx* gene families, are expressed at high levels along the neural-nonneural interface around the anterior neural plate near the end of gastrulation (Baker and Bronner-Fraser, 2000; Schlosser et al., 2006; Brugmann and Moody, 2005; Streit, 2007; Akimenko et al., 1994; Sahly et al., 1999; Kobayashi et al., 2000). How these genes are regulated is still unclear, but modulation of Bmp signaling appears to be critical. In a classical model (Fig. 2.1A), ectoderm is patterned during gastrulation by readout of a Bmp morphogen gradient. Such a gradient could coordinate specification of preplacodal ectoderm and neural crest in juxtaposed domains, with preplacodal ectoderm requiring slightly higher levels of Bmp than neural crest (Kishimoto et al., 1997; Neave et al., 1997; Wilson et al., 1997; Marchant et al., 1998; Nguyen et al., 1998; Barth et al., 1998; Reversade et al., 2005; Tucker et al., 2008).

Numerous studies provide strong support for the notion that neural crest requires a specific low threshold of Bmp signaling. In zebrafish mutations or inducible transgenes that weaken overall Bmp signaling can expand neural crest throughout the ventral domain (Nguyen et al. 1998; Barth et al., 1999; Tucker et al., 2008). Similarly,

development of neural crest in *Xenopus* is stimulated by misexpression of moderate but not high levels of Bmp-antagonists (Marchant et al., 1998).

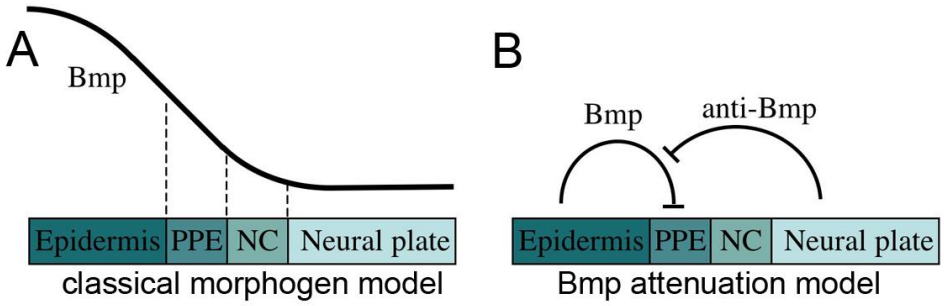

Figure 2.1. Models for the role of Bmp in preplacodal specification. (A) Classical model in which a Bmp morphogen gradient directly specifies multiple fates, including epidermal ectoderm, preplacodal ectoderm (PPE), neural crest (NC) and neural plate, at discrete threshold concentrations. (B) Bmp-attenuation model in which Bmp-antagonists, secreted from the dorsal tissue of the embryo, promotes preplacodal fate in nonneural ectoderm abutting the anterior neural plate. In this model, Bmp must be fully blocked to permit preplacodal specification.

In contrast, available data are ambiguous with regard to Bmp's role in preplacodal specification. A number of Bmp-antagonists expressed near the neural-nonneural interface late in gastrulation are required for normal preplacodal development (Esterberg and Fritz, 2008; Kwon and Riley, 2009). Similarly, high-level misexpression of Bmp antagonists expands preplacodal gene expression partway into the nonneural ectoderm (Brugmann et al., 2004; Glavic et al., 2004; Ahrens and Schlosser, 2005;

Litsiou et al., 2005). These findings have been alternately interpreted as support for either of two competing models: Some investigators have argued that Bmp-antagonists titrate Bmp signaling to a specific level appropriate for preplacodal specification, consistent with the Bmp morphogen model (Brugmann et al., 2004; Glavic et al., 2004) (Fig. 2.1A). Others counter that these misexpression conditions are likely to fully block Bmp signaling (Ahrens and Schlosser, 2005; Litsiou et al., 2005), leading to an alternative model in which preplacodal specification requires attenuation of Bmp (Fig. 2.1B). These opposing models invoke fundamentally different mechanisms: In the morphogen model Bmp is a positive requirement whereas in the attenuation model Bmp is an inhibitor that must be fully blocked to permit preplacodal development. Notably, none of these studies has measured changes in the level of Bmp signaling associated with their experimental manipulations, making it impossible to distinguish between the opposing models. A similar uncertainty applies to genetic studies in zebrafish, which suggest that neither of the models in Fig. 2.1 is fully adequate. Mutations that strongly impair Bmp signaling eliminate preplacodal development (Nguyen et al., 1998; Barth et al., 1999), revealing a definite requirement for Bmp. However, none of the mutations that impair Bmp to a lesser degree expand preplacodal fate throughout the ventral ectoderm, in sharp contrast to neural crest (Nguyen et al., 1998; Barth et al., 1999). Although these data fail to support predictions of the Bmp morphogen model for preplacodal specification, it is possible that available mutations do not expand the appropriate range of Bmp signaling required for preplacodal ectoderm, if one exists.

Thus the status of Bmp signaling during preplacodal specification remains an important unresolved question.

In addition to differing requirements for Bmp, preplacodal ectoderm and neural crest appear to be specified at different times. Recent studies in chick and zebrafish suggest that neural crest is specified by the beginning of gastrulation (Tucker et al., 2008; Basch et al., 2006). In contrast, preplacodal ectoderm appears to be specified during late gastrula or early neurula stages, as suggested by studies in chick and *Xenopus* (Ahrens and Schlosser, 2005; Litsiou et al., 2005). This difference in timing is especially relevant for the Bmp-attenuation model (Fig. 2.1B). Specifically, the lag in preplacodal specification allows time to reshape the Bmp gradient without jeopardizing the earlier requirement of neural crest for Bmp. There are currently no data to show when preplacodal specification occurs in zebrafish.

Other signals from dorsal tissues also appear critical for preplacodal development. In chick and *Xenopus*, grafting neurectoderm into more ventral regions induces expression of preplacodal markers in surrounding host tissue (Ahrens and Schlosser, 2005; Litsiou et al., 2005; Woda et al., 2003). Moreover, combining misexpression of Bmp antagonists with Fgf8, a relevant dorsal signal, is sufficient to induce at least some preplacodal markers; neither Fgf8 nor Bmp-antagonism is sufficient (Ahrens and Schlosser, 2005; Litsiou et al., 2005). Various transcription factors have also been implicated in preplacodal development, but most appear to act after preplacodal specification to influence fates of cells in different regions of this domain (Schlosser, 2006; Streit, 2007).

Here we provide the first direct evidence for a 2-step model in which Bmp is required only transiently during blastula/early gastrula stage to directly or indirectly induce ventral expression of four transcription factors, Tfap2a, Tfap2c, Gata3 and Foxi1 which establish preplacodal competence throughout the nonneural ectoderm. In this context, Bmp does not act as a morphogen because it does not distinguish between preplacodal and epidermal ectoderm within the nonneural domain. We initially focused on *foxi1*, *gata3*, *tfap2a* and *tfap2c* as potential competence factors because they show similar early expression patterns throughout the nonneural ectoderm and all have been implicated in later development of various subsets of cranial placodes (Schlosser, 2006; Streit, 2007; Neave et al., 1995; Sheng et al., 1999; Karis et al., 2001; Solomon et al., 2003; Lee et al., 2003; Li and Cornell, 2007). Once expressed, preplacodal competence factors no longer require Bmp for their maintenance. Near the end of gastrulation, Bmp must be fully blocked by dorsally expressed Bmp-antagonists, which combined with Fgf, are necessary and sufficient to induce preplacodal development within the zone of competence.

MATERIALS AND METHODS

Standard development, staging and pharmacological inhibitor treatment

Embryos were developed under standard conditions at 28.5°C except where noted and staged according to standard protocols (Kimmel et al., 1995). To block Bmp, dorsomorphin (DM) (Calbiochem, 171260) was added to the fish water from a 10mM stock in DMSO. Embryos were treated without removing their chorions. Treatment was

carried out in 24-well plates, with 40 embryos in 0.5 ml of solution per well. Relevant controls were incubated in fish water containing an equal concentration of DMSO to that of treated embryos. DM solutions should be exposed to as little light as possible as the drug is photo-unstable. Stock solution of DM may be stored in small aliquots at -80°C for several months, but storage at warmer temperatures and repeated freeze-thaw significantly reduces activity. To Block Fgf, SU5402 (Calbiochem) was diluted from a 10 mM stock in DMSO. To block Pdgf, AG1295 (Calbiochem) was diluted from a 20mM stock in DMSO.

In situ hybridization and immunostaining

Fixation and *in situ* hybridization were performed as previously described [Philips et al., 2006; Philips et al., 2001). Immunostaining for phosphorylated Smads was carried out as described (Tucker et al., 2008) with minor modifications. The primary antibody was used at a concentration 1:150 (anti-pSmad1/5/8 antibody; Cell Signaling Technology). Secondary antibody was HRP-conjugated anti-rabbit IgG at 1:200 (Santa Cruz Biotechnology).

Morpholino injection

For gene knockdown experiments, embryos were injected with 5ng per morpholino as indicated. Morpholino sequences for *foxi1, tfap2a*, *tfap2c* and *p63* have been previously published (Solomon et al., 2003; Li et al., 2007; Sidi et al., 2008). To knockdown *gata3*, either of two morpholinos was used: For blocking translation, *gata3*-MO1

TCCGGACTTACTTCCATCGTTTATT; for blocking mRNA splicing at the exon1-intron1 junction, *gata3*-MO2 AGAACTGGTTTACTTACTGTGAGGT. Neither *gata3*-MO1 nor *gata3*-MO2 produced discernable phenotypes on their own, but both showed identical interactions with morpholinos for other competence factors. The ability of *gata3*-MO2 to diminish production of mature *gata3* mRNA was confirmed with RT-PCR (data not shown). The MO-generated phenotypes described in this study were 100% penetrant, except where noted in the text. At least 10 specimens were examined or each experimental time point, unless stated otherwise.

Gene misexpression

Full length cDNAs of *foxi1*, *gata3*, *tfap2a*, *fgf3* and *fgf8* were ligated to *hsp70* heat shock promoter (Shoji et al., 1998) with flanking *I-SceI* meganuclease sites (Thermes et al., 2002; Rembold et al., 2006). Recombinant plasmid (10-40 pg/nl) was coinjected with *I-SceI* meganuclease (NEB, 0.5 U/µl) into 1-cell stage embryos. For transient ectopic expression, injected embryos were heat-shocked in a recirculating water bath. Stable transgenic lines *Tg(hsp70:fgf8a)*^{x17}, *Tg(hsp70:fgf3)*^{x18} and *Tg(hsp70:foxi1)*^{x19} were generated by raising injected embryos to adult and screening by PCR for germline transmission. Heterozygous transgene-carriers were easily distinguished based on the phenotype following heat shock at 30% epiboly: Activation of *Tg(hsp70:fgf8a)*^{x17} or *Tg(hsp70:fgf3)*^{x18} caused dorsalization of the embryo, whereas activation of *Tg(hsp70:foxi1)*^{x19} caused anterior truncations with defects in forebrain and eyes (data not shown). The *Tg(hsp70l:dnBmpr-GFP)* transgenic line (Pyati et al., 2005) was

provided by ZIRC. *Tg(hsp70:chordin)* (Tucker et al., 2008) was generously provided by Mary Mullins.

In most experiments, transgenic embryos were heterozygous for the transgenes in question, with the exception that homozygous *Tg*(*hsp70:chordin*)/Tg(hsp70*:chordin*) embryos were used to misexpress *chd*. To misexpress *foxi1*, *tfap2a* and *gata3*, embryos were heat shocked at 39°C for 30 min at various times as indicated in the text. *Tg(hsp70l:dnBmpr-GFP)* and *Tg(hsp70:chordin)* embryos were heat shocked at 39 °C for 30 min at 7.5 hpf; *Tg(hsp70:fgf8a)*and *Tg(hsp70:fgf3)* embryos at 35 °C for 3 hr from 7.5 hpf. After heat shock, the plate containing the embryos was transferred into a 28.5°C incubator until fixation or observation.

Cell transplantation

Donor embryos were injected with lineage tracer (mix of lysine fixable rhodamine dextran, 10000 MW, and 5 % biotin dextran, 10000 MW, in the ratio of 1:9 in 0.2 M KCl) at the one-cell stage. Cells were transplanted either from blastula stage donors into blastula stage hosts or from blastula stage donors into gastrula stage (~6 hpf) hosts. Mosaic embryos were then heat-shocked at 39°C for 30 min at 7 hpf and subsequently maintained at 33°C until fixed. Transplanted cells were identified in the hosts by streptavidin-FITC antibody staining.

Cell death assays

Embryos were dechorinated and incubated for 1 hour on agarose-coated plates

containing fish water with acridine orange (AO) (1μg/ml), as modified from (Philips et al., 2006). The embryos were then briefly washed and immediately examined under a fluorescence microscope.

RESULTS

Requirements for Bmp

To monitor early preplacodal development, we followed expression of *dlx3b*, *eya1* and *six4.1,*. *dlx3b* is the earliest marker, initially showing a low level of expression throughout the nonneural ectoderm at 8 hpf, with strong upregulation in preplacodal ectoderm and downregulation in ventral ectoderm by 9 hpf (late gastrulation) (Akimenko et al., 1995). Expression of *six4.1,* and *eya1* first appear in preplacodal ectoderm by 10 hpf (the close of gastrulation), and a low level of *six4.1,* is also seen in scattered mesendodermal cells in the head (Sahly et al., 1999; Kobayashi et al., 2000). For comparison, we also monitored the neural crest marker *foxd3*, which is expressed specifically in premigratory neural crest by 10 hpf (Kelsh et al., 2000; Montero-Balaguer et al., 2006).

To assess the role of Bmp in preplacodal specification, we treated embryos at various times with dorsomorphin (DM), a pharmacological inhibitor of Bmp signaling (Yu et al., 2003). Although we used DM at higher concentrations than previously reported (Yu et al., 2003), it did not appear to cause defects beyond the phenotypes associated with Bmp pathway mutants (see below). Thus, unintended non-specific

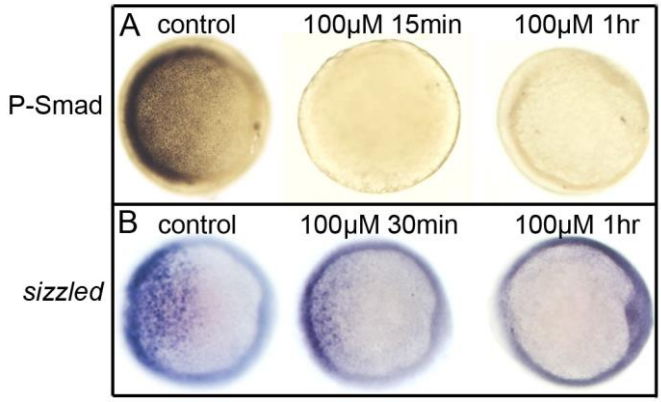

Figure 2.2: Dorsomorphin acts quickly to block Bmp signaling. Embryos were treated with either 1% DMSO (controls) or 100 µM DM beginning at 5 hpf. (A) Phospho-Smad staining in a control after 1 hour, or in DM-treated embryos after 15 minutes or 1 hour. (B) Expression of *sizzled* in a control embryo after 1 hour, or in DM-treated embryos after 30 minutes or 1 hour. All images show animal pole views with dorsal to the right.

effects of the drug, if present, are apparently mild and do not interfere with the ability to block Bmp signaling. We initially performed a dose-response to assess the effects of DM when added at 5, 6 or 7 hpf (Table 1). As expected, embryos were increasingly dorsalized after exposure to increasing concentrations of DM, and earlier exposure caused greater dorsalization than later exposure. Exposing embryos to 50 or 100 µM DM beginning at 5 hpf mimicked strong loss of function mutations in the Bmp pathway (Kishimoto et al., 1997; Nguyen et al., 1998; Barth et al., 1999; Mullins et al., 1996) and resulted in complete dorsalization (Table 1). In confirmation, exposure to 100 µM DM at 5 hpf eliminated phospho-Smad1/5/8 staining within 15 minutes (Fig. 2.2A), indicating rapid and complete cessation of Bmp signaling. Additionally, mRNA for *sizzled*, a

Table 1: Stage- and dose-dependent dorsalization caused by dorsomorphin (DM).

		100μM	50μM	25μM	12.5μM	6.25μM
	n	19	18	20	25	30
DM@5hpf	%C5	100	100	45	0	0
	%C4	0	0	55	0	0
	%C3	0	0	0	0	0
	%C2	0	0	0	52	0
	%C1	0	0	0	48	13
	n	25	23	19	18	18
	%C5	72	22	0	0	0
DM@6hpf	%C4	28	43	21	0	0
	%C3	0	35	79	0	0
	%C2	0	0	0	28	0
	%C1	0	0	0	72	0
	n	19	19	19	19	23
DM@7hpf	%C5	0	0	0	0	0
	%C4	11	0	0	0	0
	%C3	89	100	0	0	0
	%C2	0	0	26	0	0
	%C1	0	0	74	63	0
	n	10	7	7	7	7
hs:fgf8/+	%ectopic	100	100	0	0	0
+DM@7.5hpf	*six4.1*,					

%C1-C5, degree of dorsalization as previously defined (Mullins et al., 1996); Class 1 (C1) is the mildest and class 5 (C5) is the most severe strongest.

feedback inhibitor of Bmp (Yabe et al., 2003), decayed rapidly under these conditions, with only weak staining after 30 minutes and none after 1 hour (Fig. 2.2B).

Because the role of Bmp in neural crest specification has been well characterized (Marchant et al., 1998; Nguyen et al., 1998; Barth et al., 1999; Tucker et al., 2008), we tested whether DM could affect this tissue as predicted by these previous studies. Adding 100 or 200 μM DM beginning at 4 hpf totally ablated neural crest formation (Fig. 2.3A and data not shown). However, adding 50 μM DM at 4 hpf led to ventral expansion of cranial neural crest to fully displace the nonneural ectoderm, similar to the effects of mutations that weaken overall Bmp signaling in zebrafish (Nguyen et al., 1998; Barth et al., 1999).

These conditions are thought to create a broad plateau of low Bmp signaling appropriate for neural crest specification, providing strong support for the role of Bmp as a morphogen in specifying neural crest. Interestingly, after initially treating embryos with 50 μM DM at 4 hpf, fully blocking Bmp with a super-saturating dose of DM at 5, 6, or 7 hpf does not prevent formation of cranial neural crest, though the domain is somewhat reduced when Bmp is blocked earlier. These data are consistent with the effects of timed misexpression of Chordin (Tucker et al., 2008), showing that Bmp acts very early in cranial neural crest specification and is no longer needed after late blastula/early gastrula stage.

Analysis of preplacodal markers revealed a different pattern of Bmp-dependence. First, preplacodal ectoderm (Fig. 2.3B) and epidermal ectoderm (not shown) are totally ablated by exposure to 50 μM DM, reflecting loss of all nonneural ectoderm.

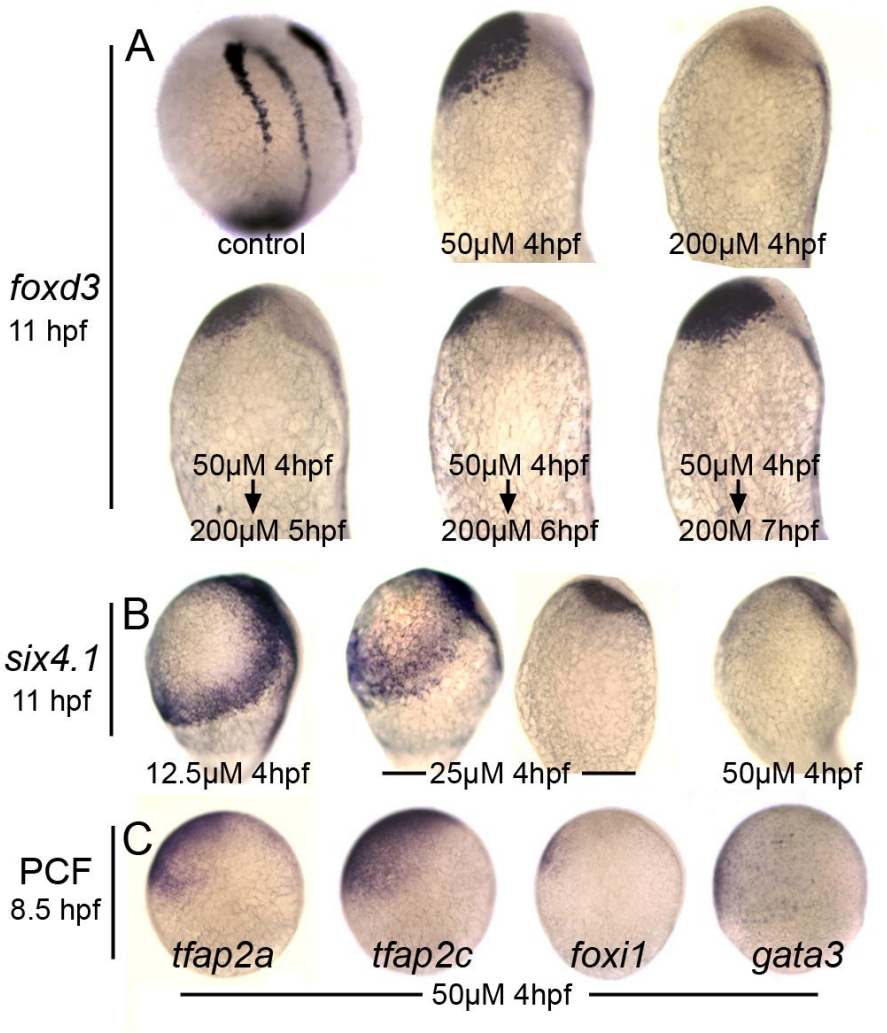

Figure 2.3: Distinct responses of neural crest and preplacodal ectoderm to graded impairment of Bmp. (A) Lateral views of *foxd3* expression at 11 hpf with anterior up and dorsal to the right. Embryos were treated with indicated concentrations of DM added at 4 hpf. Where indicated the DM concentration was increased to 200 μM (complete Bmp-inhibition) at 5 hpf, 6 hpf or 7 hpf. (B) Lateral views of *six4.1*, expression at 11 hpf in embryos treated with indicated concentrations of DM beginning at 4 hpf. Treatment with 25 μM DM yields two discrete responses, one in which *six4.1*, remains confined to two bilateral stripes flanking the neural plate and the other in which *six4.1*, expression is lost. (C) Lateral views showing expression of preplacodal competence factors *tfap2a*, *tfap2c*, *foxi1* and *gata3* in embryos were treated with 50 μM DM beginning at 4 hpf. Note that *tfap2a/c* remain broadly expressed in ventral ectoderm whereas *foxi1* and *gata3* are nearly eliminated.

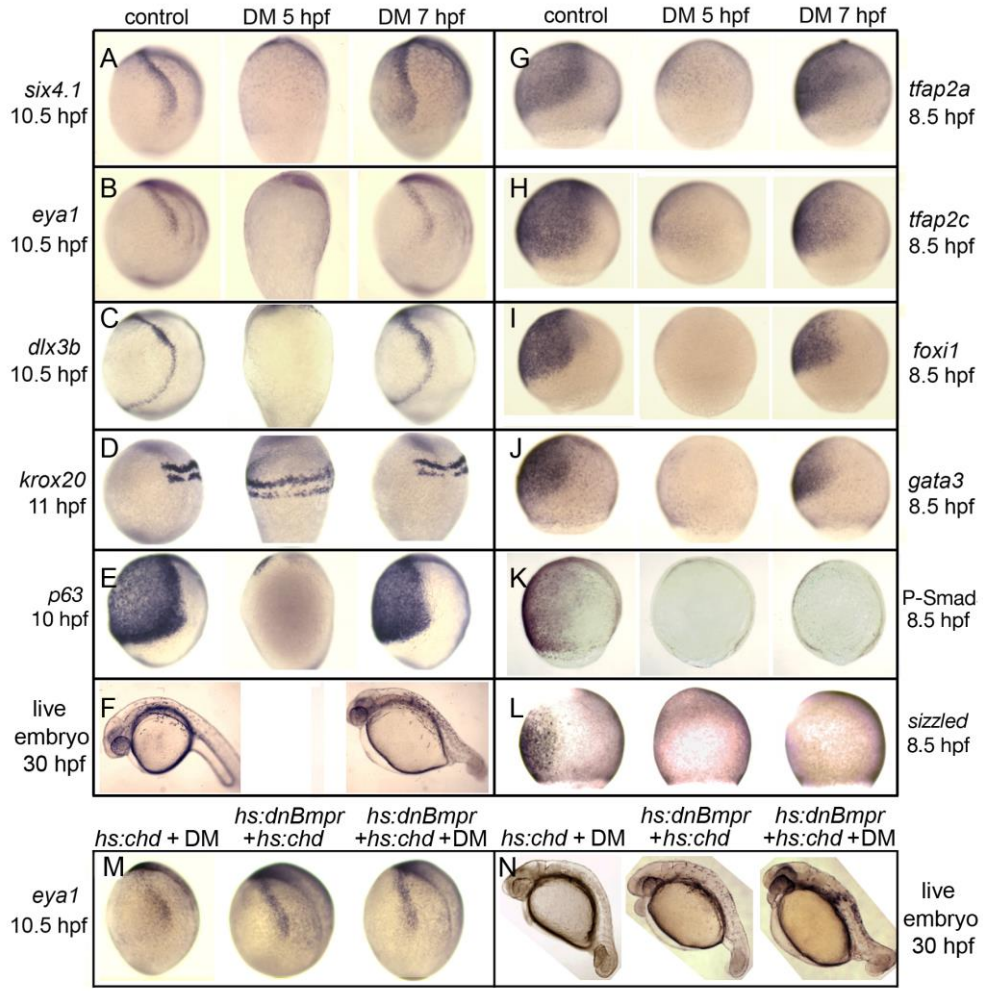

Figure 2.4: Stage-dependent requirements for Bmp. (A-E, G-L) Analysis of indicated gene expression patterns in control embryos and embryos treated with 100 µM dorsomorphin (DM) at 5 hpf or 7 hpf. Lateral views with dorsal to the right and anterior up. Expression of *six4.1, eya1* and *dlx3b* (A-C) in PPE, *krox20* in hindbrain(D) and *p63* in epidermal ectoderm (E). Expression of competence factor genes *tfap2a*, *tfap2c*, *foxi1* and *gata3* (G-J). Reporters of Bmp-signaling, Phospho-Smad1/5/8 antibody staining (K) and *sizzled* in situ hybridization (L). Note the complete loss of Bmp signaling by 100 µM DM-treatment either at 5 hpf or 7 hpf. (F) Lateral views of live embryos at 30 hpf. Embryos treated with DM at 7 hpf show a partially dorsalized C3 phenotype [33]. (M, N) *Tg(hs:chd)* and/or *Tg(hs:dnBmpr)* embryos heat-shocked and treated with 100 µM DM at 7.5 hpf. *eya1* expression (M) and C3 phenotypes (N) are comparable to embryos treated with 100 µM DM alone.

Accordingly, this treatment eliminated expression of putative preplacodal competence factors *foxi1* and *gata3*, though *tfap2a* and *tfap2*c continue to be expressed (Fig. 2.3C). The latter two genes are also required in the lateral edges of the neural plate for neural crest development (Li et al., 2007; Hoffman et al., 2007). Second, we found no dose of DM that caused expansion of preplacodal markers throughout the ventral ectoderm. Instead, exposure to 25 μM at 4 hpf yielded two distinct responses; either preplacodal markers were lost entirely or preplacodal ectoderm was shifted ventrally but was still confined to two bilateral stripes bordering the neural plate (Fig. 2.3B and data not shown). Thus, there does not appear to be a specific level of Bmp that can expand the preplacodal ectoderm at the expense of more ventral (epidermal) ectoderm.

To characterize the temporal requirements for Bmp, embryos were treated with 100 μM DM at different times during late blastula and early gastrula stages and subsequently analyzed for expression patterns of various ectodermal markers. As expected from the severe dorsalization caused by administering this dose at 5 hpf (Table 1), neural markers were expanded throughout the ectoderm and all nonneural markers were lost, including putative preplacodal competence factors (Fig. 2.4D, E, G-J). Additionally, definitive preplacodal markers *dlx3b*, *eya1* and *six4.1,* were not expressed in these embryos (Fig. 2.4A-C). In contrast, exposure to 100 μM DM from 7 hpf resulted in only partial dorsalization (Table 1; Fig. 2.4D, F) and all embryos expressed nonneural markers, albeit in diminished ventral domains (Fig. 2.4E, G-J). Preplacodal markers *dlx3b*, *eya1* and *six4.1,* were expressed on time by 10.5 hpf (Fig. 2.4A-C). Moreover, all placodal derivatives were produced on time in embryos treated with 100

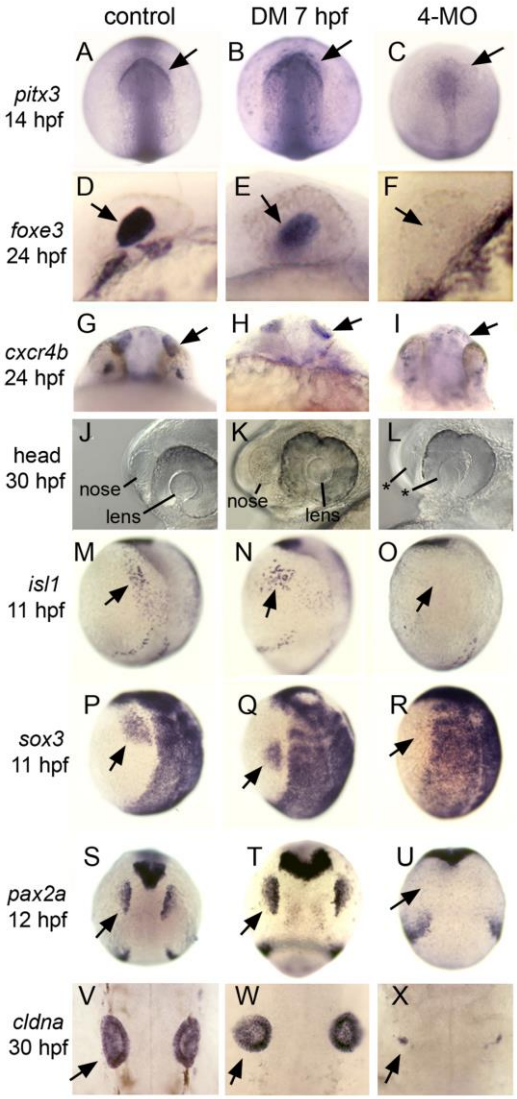

Figure 2.5: Formation of cranial placodes requires competence factors but not Bmp during gastrulation. Analysis of various cranial placode markers in control embryos, embryos treated with 100 µM DM at 7 hpf, or *foxi1/gata3/tfap2a/c* quadruple morphants (4-MO). Arrows indicate relevant expression domains in placodal tissues. (A-C) Dorsal views (anterior up) of *pitx3* expression in anterior pituitary and lens placode. (D-F) Lateral views (anterior to left) of *foxe3* expression in the lens placode. (G-I) Frontal views of *cxcr4b* expression in olfactory placode. (J-L) Lateral views (anterior to left) showing the lens and nasal pits in live specimens at 30 hpf. Asterisks in (L) depict the absence of morphologically discernable structures. (M-O) Lateral views (anterior up) of *isl1* expression in the trigeminal placode. (P-R) Lateral views (anterior up) of *sox3* expression in the epibranchial placode. (S-U) Dorsal views (anterior up) of *pax2a* expression in the otic placode. (V-X) Dorsal views (anterior up) of *cldna* expression in the otic vesicle. All placodal markers are expressed normally in DM-treated embryos. Expression of *cldna* is severely deficient in quadruple morphants (X, n = 13/21) or ablated altogether (8/21, not shown). All other placodal markers are ablated in quadruple morphants ($n \geq 10$ for each marker).

μM DM from 7 hpf, including the anterior pituitary, olfactory, lens, trigeminal, epibranchial and otic placodes (Fig. 2.5B, E, H, K, N, Q, T, W) (Krauss et al., 1991; Kollmar et al., 2001; Kaji and Artinger, 2004; Dutta et al., 2005; Knaut et al., 2005; Swindell et al., 2008; Miyasaka et al., 2007; Nikiado et al., 2007; Sun et al., 2007; Pyati et al., 2005; Bakkers et al., 2002). Adding 100 μM DM at 6 hpf yielded two classes of embryos, with roughly half being fully dorsalized and the rest resembling the partially dorsalized embryos obtained with 100 μM DM at 7 hpf (data not shown, Table 1). Adding 100 μM DM at 5.5 hpf eliminated *eya1* and *six4.1,* expression in all embryos, though some embryos still expressed *dlx3b* in bilateral stripes (data not shown). These data indicate that embryos make a transition around 5.5-6 hpf after which Bmp is no longer required for preplacodal development. As with treatment during blastula stage, treatment with 100 μM DM during gastrulation eliminated phospho-Smad1/5/8 accumulation and *sizzled* expression, confirming loss of Bmp signaling (Tucker et al., 2008; Yabe et al., 2003; Fig. 2.4K, L). Additionally, the effects of adding 100 μM DM at 7 hpf were identical to the effects of 500 μM DM, the highest dose tested (data not shown), arguing that the block to Bmp signaling was saturated at these doses. Nevertheless, to ensure that Bmp was fully blocked, we combined addition of 100 μM DM at 7 hpf with activation of heat shock-inducible transgenes encoding Chordin and/or dominant-negative Bmp receptor (Tucker et al., 2008; Pyati et al., 2005) (Fig. 2.4M, N). The effects on preplacodal specification and morphological development were identical to treatment with 100 μM DM alone. These data show that Bmp is not directly required after the onset of gastrulation for preplacodal specification. The data further show that

Bmp signaling is required to induce expression of putative competence factors *foxi1, gata3*, *tfap2a* and *tfap2c* during blastula stage, but is not required to maintain them thereafter (Fig. 2.4G-J).

Requirement for ventrally expressed competence factors

We hypothesized that *foxi1, gata3*, *tfap2a* and *tfap2c* encode preplacodal competence factors because they are expressed early throughout the nonneural ectoderm yet are specifically required for later development of various subsets of placodes (Neave et al., 1995; Sheng et al., 2009; Karis et al., 2009; Solomon et al., 2004; Lee et al., 2003; Li et al., 2007). To test the functions of these genes, we injected morpholino oligomers (MOs) to knockdown their functions. Knockdown of any one gene had no discernable effect on preplacodal gene expression (data not shown), though loss of *foxi1* specifically impairs development of the otic and epibranchial placodes (Solomon et al., 2003; Lee et al., 2003). Knockdown of both *foxi1* and *gata3* enhanced the otic placode deficiency (data not shown), and caused a slight reduction in expression levels of *dlx3b*, *eya1* and *six4.1,* (Fig. 2.6, data not shown). Knockdown of both *tfap2a* and *tfap2c* caused a stronger reduction in expression levels of preplacodal markers (Fig. 2.6B). Co-injecting either *gata3*-MO or *foxi1*-MO with *tfap2a/c*-MOs further reduced preplacodal gene expression (data not shown) whereas simultaneous knockdown of *foxi1, gata3*, *tfap2a* and *tfap2c* (quadruple morphants) resulted in complete loss of preplacodal gene expression (Fig. 2.6C). Moreover, development of all cranial placodes (pituitary, olfactory, lens, trigeminal, otic and epibranchial) was severely deficient or totally ablated in all

quadruple morphants examined (Fig. 2.5 C, F, I, L, O, R, U, X). Disruption of preplacodal development in quadruple morphants did not reflect general impairment of nonneural ectoderm, as the epidermal marker *p63* (Bakkers et al., 2002; Lee et al., 2002) was appropriately expressed in the ventral ectoderm (Fig. 2.6D). Additionally, quadruple morphants did not exhibit elevated cell death, as indicated by relatively normal levels of staining with the vital dye acridine orange (Philips et al., 2006) (data not shown). These data show that *foxi1, gata3*, *tfap2a* and *tfap2c* are specifically required for formation of preplacodal ectoderm and all placodal derivatives, and are partially redundant in this function.

Importantly, quadruple morphants retained a neural-nonneural interface (Figs. 2.5R and 2.6D), the region normally associated with preplacodal specification. Moreover, Bmp signaling also persisted in quadruple morphants as shown by continued ventral accumulation of phospho-Smad1/5/8 and expression of *sizzled* (Fig. 2.6D). Expression of *fgf3*, *fgf8* and the Fgf-target gene *erm* were also appropriately localized in quadruple morphants (data not shown). Thus, neither Bmp signaling, Fgf signaling, nor neural-nonneural interactions are sufficient for preplacodal specification in this background. These data support the hypothesis that *foxi1, gata3*, *tfap2a* and *tfap2c* are required for preplacodal competence or early differentiation. Although *p63* is normally co-expressed with preplacodal competence factors and is only known to regulate epidermal development (Bakkers et al., 2002; Lee et al., 2002), we examined whether it is required for preplacodal development. Knockdown of *p63* did not detectably alter preplacodal development, nor did it enhance the deficits in preplacodal gene expression

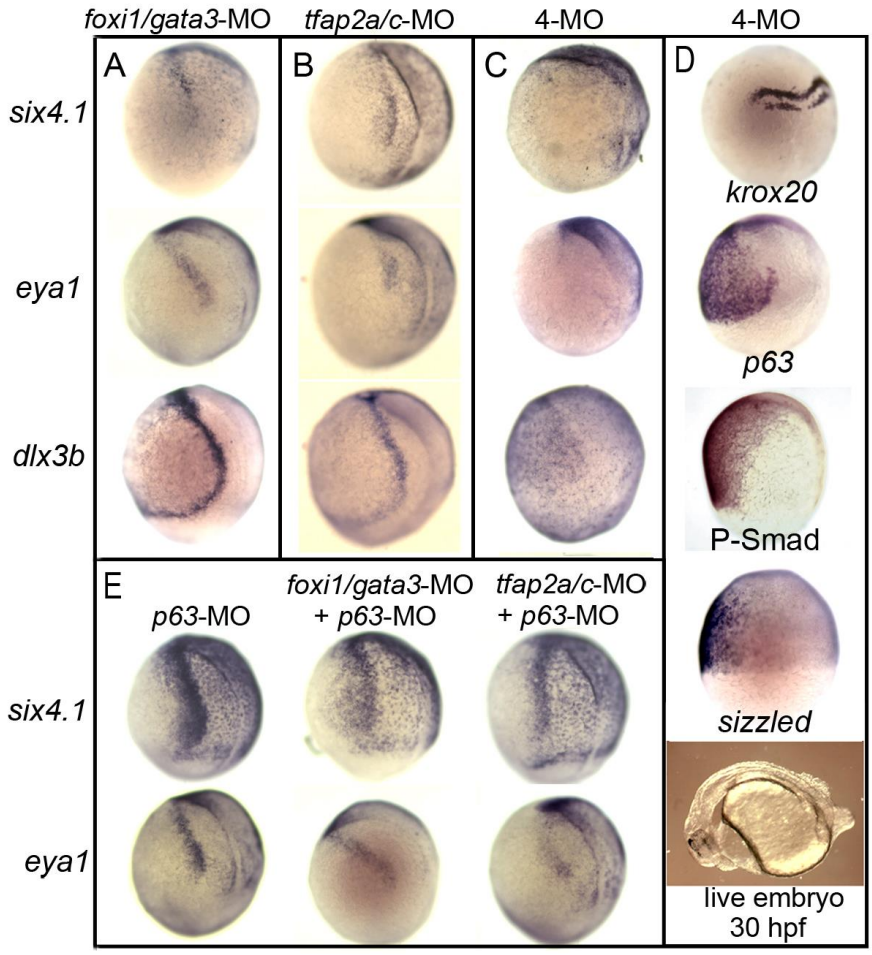

Figure 2.6: Knockdown of competence factors impairs preplacodal specification. (A-C) Expression of preplacodal markers at 10.5 hpf in (A) *foxi1/gata3* double morphants, (B) *tfap2a/c* double morphants, (C) *foxi1/gata3/tfap2a/c* quadruple morphants (4-MO). Note the complete loss of preplacodal markers in C. (D) Expression of *krox20*, *p63*, P-smad and *sizzled* during gastrulation in *foxi1/gata3/tfap2a/c* quadruple morphants. Morphology of a live quadruple morphant at 30 hpf is also shown. (E) Expression of *six4.1,* and *eya1* in *p63* morphants alone or in combination with *tfap2a*/*c*-MO or *foxi1*/*gata3*-MO. All images show lateral views with dorsal to the right and anterior up, except for the live specimen in (D), which shows a lateral view with anterior to the left.

or morphological development seen in *foxi1-gata3* or *tfap2a/c* double morphants (Fig. 2.6E, and data not shown). This further shows that not all early Bmp-target genes are required for preplacodal development and that the requirement for *foxi1, gata3*, *tfap2a* and *tfap2c* is relatively specific.

We also investigated the requirements for *foxi1, gata3*, *tfap2a* and *tfap2c* in neural crest formation. Knockdown of both *foxi1* and *gata3* did not alter expression of *foxd3* (data not shown), whereas knockdown of *tfap2a/c* completely eliminated expression of *foxd3* as reported previously (Li and Cornell, 2007; Hoffman et al., 2007). Not surprisingly, *foxd3* expression is also ablated in *foxi1-gata3-tfap2a/c*-quadruple morphants (data not shown). This likely reflects a cell-autonomous requirement for *tfap2a/c* in neural crest specification (Li and Cornell, 2007; Hoffman et al., 2007).

Dorsal misexpression of preplacodal competence factors

To further test the functions of preplacodal competence factors, we generated constructs to misexpress *foxi1, gata3* and *tfap2a* under the control of the *hsp70* heat shock promoter (Shoji et al., 1998). We reasoned that if these genes provide preplacodal competence, then misexpressing them in dorsal ectoderm, where preplacodal inducing factors are normally expressed, should be sufficient to induce ectopic expression of preplacodal genes. We performed transient transfections to introduce *hs:tfap2a* and *hs:gata3* whereas a stable transgenic line was used for *hs:foxi1* (see Materials & Methods). Global heat shock-activation of any one of these genes at 4.5 hpf (late blastula) or 5.5

hpf (early gastrula) resulted in scattered ectopic expression of preplacodal markers within the neural plate by 11 hpf (Fig. 2.7A-C, and data not shown). In most experiments, over half of embryos showed ectopic expression of preplacodal genes. Co-activation of any two heat shock genes yielded more robust and widespread expression of preplacodal genes in the neural plate, with nearly complete penetrance in most experiments. For reasons that are unclear, misexpression of competence factors at these stages caused widening of the neural plate and narrowing of the ventral Bmp signaling domain (data not shown). Nevertheless, Bmp signaling and general DV patterning are still evident following activation of *hs:foxi1, hs:gata3* and/or *hs:tfap2a* (data not shown). Importantly, we never observed ectopic expression of the epidermal marker *p63* in the neural plate following misexpression of competence factors, indicating that preplacodal competence factors do not induce all nonneural fates in this domain. Co-activation of all three transgenes at 4.5 hpf led to widespread expression of preplacodal genes, but also caused severe axial patterning defects during gastrulation, making results difficult to interpret (data not shown). However, mosaic misexpression of all three competence factors at 4.5 hpf avoided defects in axial patterning yet still led to dorsal expression of *dlx3b* and *six4.1,* in a subset of misexpressing cells (Fig. 2.7D). These data are consistent with the hypothesis that *foxi1, gata3* and *tfap2a* are sufficient to render dorsal ectoderm competent to express preplacodal genes in response to dorsally expressed inducing factors. In addition to their role in preplacodal development, Tfap2a and Tfap2c are required for neural crest (Li and Cornell, 2007; Hoffman et al., 2007), whereas Foxi1 and Gata3 are required for preplacodal ectoderm but not neural crest. We

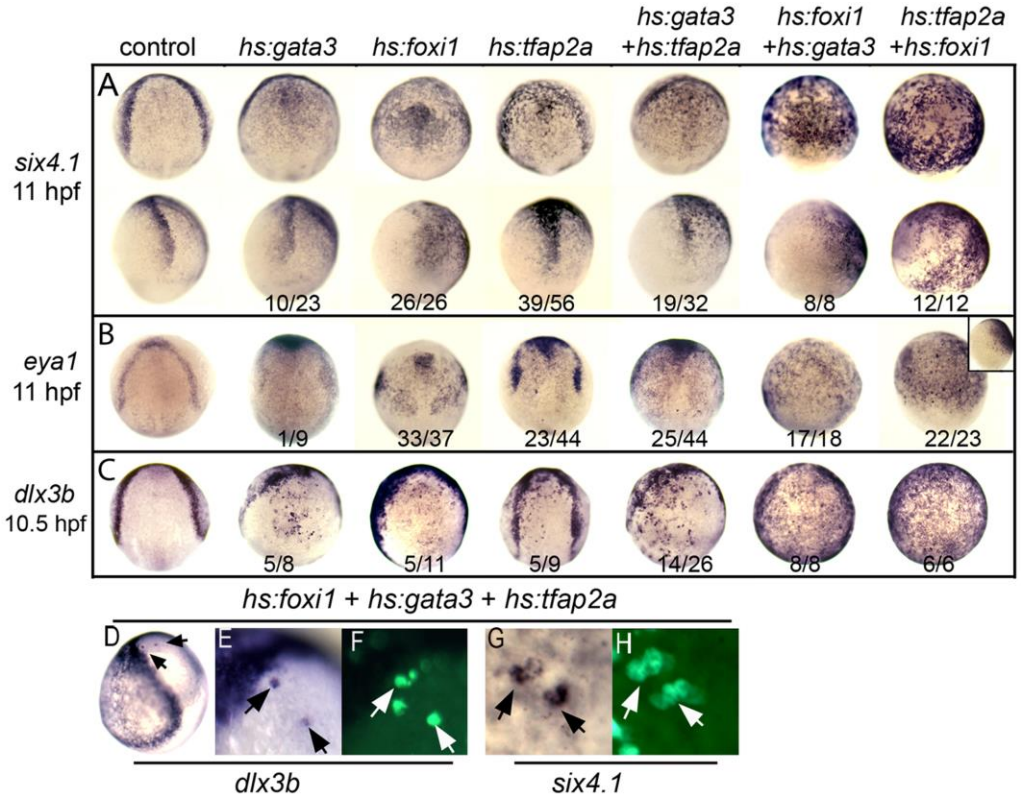

Figure 2.7: Misexpression of competence factors induces ectopic expression of preplacodal markers. (A-C) Analysis of indicated gene expression patterns in control embryos and embryos carrying *hs:gata3, hs:foxi1* and/or *hs:tfap2a* heat-shocked at 30 % epiboly (4.5 hpf). Dorsal views with anterior up except bottom row in A, inset in B, which are lateral views with dorsal to the right. Note the ectopic expression of PPE markers, *six4.1,* (A), *eya1* (B) and *dlx3b* (C) in neuroectoderm of embryos misexpressing one or more competence factors. (D-H) Dorsolateral views (anterior up) of mosaic embryos showing ectopic expression of *dlx3b* and *six4.1,* at 10.5 hpf. Donor cells obtained from *Tg(hs:foxi1)* injected with *hs:gata3* and *hs:tfap2a* plasmid were transplanted into wild type hosts and heat shocked at 4.5 hpf at 39°C. Transplanted cells were identified with Strepavidin-FITC (arrows F, H). Mosaic embryos shows cell autonomous expression of *dlx3b* and *six4.1,* in the neural plate (compare E, F and G, H).

asked whether these differing roles in neural crest could also be distinguished in misexpression experiments. Similar to the effects of injecting *tfap2a* mRNA (Li and Cornell, 2007), we found that misexpression of *hs:tfap2a*, either alone or in combination with other competence factors, resulted in ectopic *foxd3* expression in the neural plate (data not shown). In contrast, activation of *hs:foxi1* and/or *hs:gata3* did not induce ectopic *foxd3* expression (data not shown), but instead reduced expression of *foxd3* in the endogenous neural crest domain (data not shown). Importantly, these findings show that formation of ectopic preplacodal tissue is not always associated with neural crest, further arguing that preplacodal competence can be regulated independently from other ectodermal fates.

Ventral misexpression of preplacodal-inducing factors

We next attempted to induce preplacodal development throughout the zone of competence in the nonneural ectoderm by providing appropriate inductive signals normally limited to dorsal tissue. Previous studies have implicated dorsally expressed Bmp-antagonists and Fgfs as preplacodal inducers (Esterberg and Fritz, 2008; Kwon and Riley, 2008; Brugmann et al., 2004; Glavic et al., 2004; Ahrens and Schlosser, 2005; Litsiou et al., 2005). To mimic such signals throughout the nonneural ectoderm, we used heat shock-inducible transgenic lines to misexpress Fgf3 or Fgf8 (*hs:fgf3* and *hs:fgf8*) while blocking Bmp with DM. Using standard heat shock conditions (39°C for 30 minutes) to activate *hs:fgf8* combined with DM treatment at 7.5 hpf fully dorsalized the embryo and was not informative. However, full dorsalization was avoided by

prolonged incubation at more moderate temperatures, achieving a weaker level of transgene activation. Incubating *hs:fgf8/+* transgenic embryos at 35°C with 100 μM DM from 7.5-10.5 hpf resulted in expression of *eya1* and *six4.1,* throughout the nonneural ectoderm in all embryos (Fig. 2.8B, F). Diffuse ectopic expression of *erm* confirmed that this heat shock regimen elevated Fgf signaling within nonneural ectoderm (Fig. 2.8I-K). Similar results were obtained with *hs:fgf3/+* transgenic embryos incubated at 36°C with 100 μM DM from 7-10.5 hpf (Fig. 2.8D, H). Activation of *hs:fgf3* or *hs:fgf8* alone was not sufficient to activate ectopic preplacodal gene expression (Fig. 2.8A, C, E, G). These data show that the entire nonneural ectoderm is competent to express preplacodal genes in response to Fgf plus inhibition of Bmp.

We next titrated the dose of DM required for ectopic induction of preplacodal genes. Incubating *hs:fgf8/+* embryos at 35°C with 50 μM DM at 7 hpf led to ventral expression of preplacodal genes, but lower concentrations of DM were not sufficient (Table 1). The finding that 25 μM DM is not sufficient indicates that even very low levels of Bmp signaling can block preplacodal gene activation.

To express inductive signals with greater spatial control, we generated mosaic embryos to locally co-misexpress Fgf8 and Chordin. Donor cells carrying both *hs:fgf8* and *hs:chd* transgenes were transplanted into non-transgenic host embryos at the mid-blastula stage to obtain a random distribution of misexpressing cells. To achieve

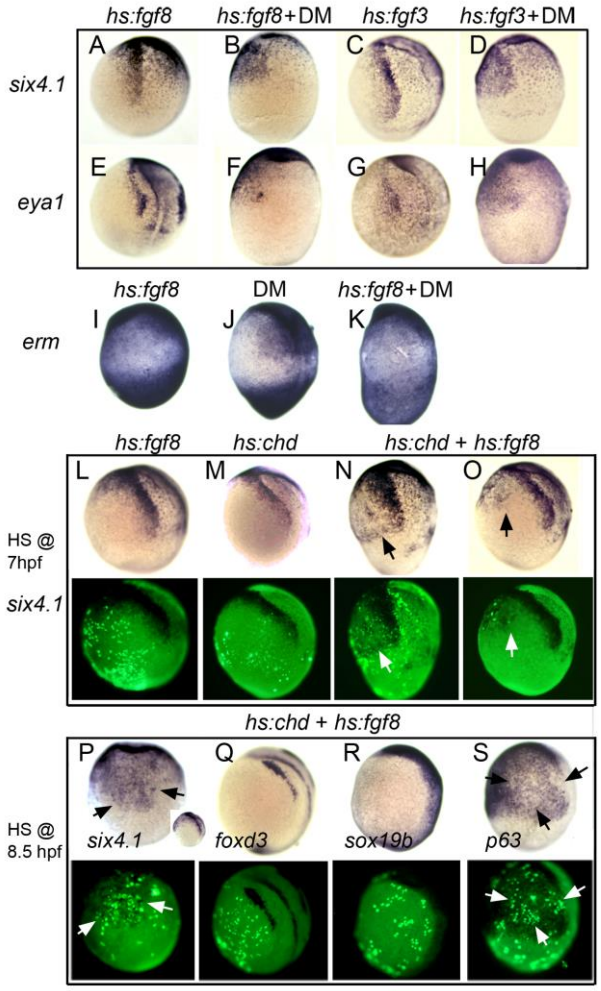

Figure 2.8: The entire nonneural ectoderm is competent to form preplacodal tissue. (A-H) Expression of preplacodal markers in (A, B, E, F) *Tg(hs:fgf8)* embryos incubated at 35°C from 7.5-10.5 hpf, or (C, D, G, H) *Tg(hs:fgf3)* embryos incubated at 36°C from 7-10.5 hpf. 100 μM DM was added as indicated. (I-K) Expression of *erm* in (I) *Tg(hs:fgf8)* embryo incubated at 35°C without DM, (J) a non-transgenic embryos incubated at 35°C with 100 μM DM, and (K) a *Tg(hs:fgf8)* embryo incubated at 35°C with 100 μM DM. (L-S) Mosaic misexpression of Fgf8 and/or Chordin. (L-O) Brightfield images (top row) and fluorescent images (bottom row) of host embryos with cells transplanted from *Tg(hs:fgf8)* (L), *Tg(hs:chd)* (M) or *Tg(hs:fgf8); Tg(hs:chd)* donor embryos (N, O). Donor embryos were injected with lineage tracer (biotin-dextran) and transplanted at mid-blastula (L, M, N) or early gastrula stage (O) into unlabeled host embryos. Embryos were heat-shocked at 39°C for 30 minutes at 7 hpf and examined for *six4.1,* expression at 10.5 hpf. Transplanted transgenic cells were identified by Strepavidin-FITC staining after in situ hybridization. All panels show lateral views of host embryos with anterior up. Mosaic embryos with *Tg(hs:fgf8)*;*Tg(hs:chd)* double transgenic cells showed ectopic *six4.1,* expression in surrounding ventral ectoderm (N, O), whereas no ectopic *six4.1,* expression was detected following activation of *hs:fgf8* alone (L) or *hs:chd* alone (M). (P-S) Brightfield images (top row) and fluorescent images (bottom row) of host embryos with cells transplanted during early gastrula stage from double heterozygous *Tg(hs:fgf8)*; *Tg(hs:chd)* embryos. Embryos were heat shocked for 30 minutes at 39°C beginning at 8.5 hpf and examined for expression of *six4.1,* (preplacodal ectoderm), *foxd3* (neural crest), *sox19b* (neural plate) or *p63*(epidermal ectoderm) at 10.5 hpf. All panels show lateral views except (P) which shows a ventral view (lateral view in inset) and (S) which shows ventro-lateral view. Heat shock activation at 8.5 hpf (P) leads to stronger ectopic expression of *six4.1,* than heat shock at 7 hpf (O). No ectopic expression of *foxd3* or *sox19b* is detected (Q, R) whereas *p63* expression appears downregulated in and around transgenic cells (arrows in S).

maximal transgene activation, mosaics were heat-shocked at 39°C for 30 minutes beginning at 7 hpf and then maintained at 33°C until tailbud stage (10 hpf). Of 4 mosaic embryos harboring transgenic donor cells on the ventral side, all showed significant ventral expression of *six4.1,* in surrounding host cells (Fig. 2.8N). In another experiment, transgenic donor cells were transplanted directly to the ventral side at the early gastrula stage (6 hpf). Following heat shock at 7 hpf, all mosaic embryos (n = 4) showed ectopic *six4.1,* expression in surrounding host cells (Fig. 2.8O). In contrast, no ectopic *six4.1,* expression was seen following mosaic misexpression of *hs:fgf8* alone (n = 13) or *hs:chd* alone (n = 10) (Fig. 2.8L, M). This confirms that both Fgf and Bmp-antagonists are required to induce expression of preplacodal genes.

Because preplacodal specification has been reported to occur near the end of gastrulation in frog and chick embryos (Ahrens and Schlosser, 2005; Litsiou et al., 2005), we tested whether activation of *hs:fgf8*; *hs:chd* cells at later stages could also stimulate ectopic preplacodal gene expression. Heat shock activation of ventrally transplanted transgenic cells at 8.5 hpf (yielding peak transgene expression at 9 hpf) led to robust ectopic expression of *six4.1,* in surrounding host ectoderm by 11 hpf (Fig. 2.8P). This suggests that in zebrafish, too, preplacodal specification occurs near the end of gastrulation.

Importantly, activation of *hs:fgf8* and *hs:chd* did not lead to ectopic expression of the general neural plate marker *sox19b* nor the neural crest marker *foxd3* (Fig. 2.8Q, R). Thus, induction of ectopic *six4.1,* expression did not result indirectly from ectopic formation of neural plate. On the other hand, activating transgenic cells at 8.5 hpf

caused downregulation of *p63*, suggesting that nearby host cells lose epidermal identity in response to preplacodal specifying signals.

Finally, we reassessed the requirement for Fgf during normal preplacodal specification. Previous studies have reported that expression of preplacodal markers does not require Fgf in zebrafish (Hans et al., 2007; Solomon et al., 2004; Leger and Brand, 2002; Liu et al., 2003). We find that blocking Fgf by adding the pharmacological inhibitor SU5402 at 8.5 hpf did not block expression of preplacodal markers, but levels of expression were reduced (Fig. 2.9). We speculated that Pdgf, which is also dorsally expressed near the end of gastrulation (Liu et al., 2002) and activates a similar signal transduction pathway, might provide redundancy with Fgf. We tested this by applying another inhibitor, AG1295, which blocks Pdgf activity in zebrafish (Montera et al., 2003). Treatment with AG1295 alone had little effect on preplacodal gene expression, but co-incubation with AG1295 and SU5402 from 8.5 hpf led to further reduction of preplacodal gene expression (Fig. 2.9). Indeed, expression of *eya1* was almost totally eliminated in the preplacodal domain, though robust expression continues in the cranial mesoderm. These data support the hypothesis that Fgf and Pdgf are partially redundant dorsal factors required for preplacodal specification.

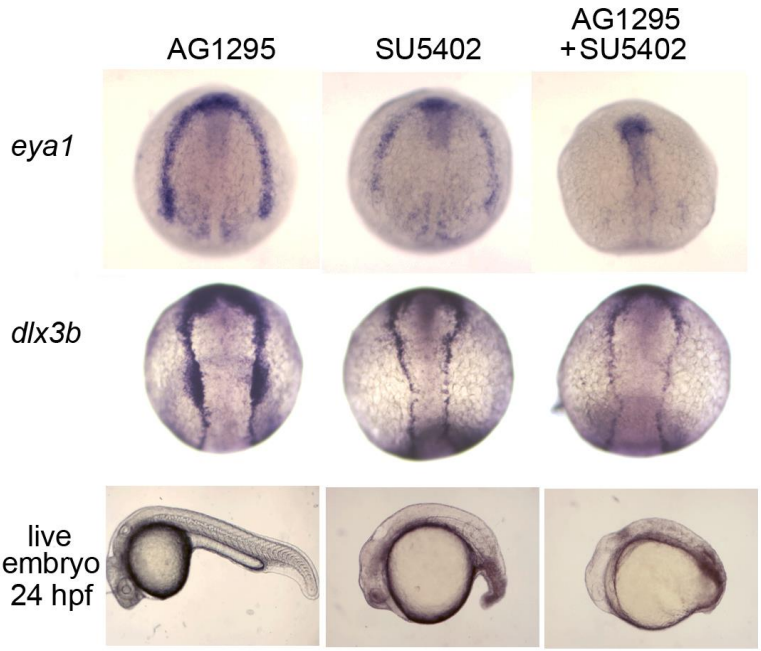

Figure 2.9: Blocking Fgf and Pdgf signaling leads to downregulation of preplacodal markers. (Upper two rows) Dorsal views showing expression of *eya1* and *dlx3b* at 1l hpf in wild-type embryos that were treated beginning at 8.5 hpf with 15μM AG1295, 25μM SU5402, or both. AG1295 did not cause any significant changes in the expression. SU5402 reduced expression of both genes. Addition of both inhibitors caused loss of *eya1* within the preplacodal domain and significant downregulation of *dlx3b*. (Lower row) Images of live embryos at 24 hpf. Treatment with SU5402 or both SU5402 and AG1295 severely perturbed caudal development and blocked formation of the otic vesicle.

DISCUSSION

We have presented data supporting a relatively simple two-step model of preplacodal development (Fig. 2.10). First, during late blastula/early gastrula stage Bmp establishes a broad zone of preplacodal competence throughout the nonneural ectoderm. Second, near the end of gastrulation signals from dorsal tissue locally specify preplacodal

ectoderm bordering the anterior neural plate. Interestingly, Nguyen et al., proposed a broadly similar two-step model based on analysis of Bmp-pathway mutants in zebrafish (Nguyen et al., 1998). However, at that time neither the molecular basis of preplacodal competence nor the signals required for preplacodal specification were known. Additionally, more recent studies have led to disagreement as to whether Bmp is required at a specific low level or must be blocked entirely for preplacodal specification (Brugmann et al., 2004; Glavic et al., 2004; Ahrens and Schlosser, 2005, Litsiou et al., 2005). Our model resolves the role of Bmp, confirms that Fgf plus Bmp-antagonists are sufficient for preplacodal specification, shows for the first time that Fgf and Pdgf cooperate as redundant preplacodal inducing factors, and highlights the importance of Foxi1, Gata3, Tfap2a and Tfap2c as preplacodal competence factors. We also readdress mechanisms of neural crest specification, which show a number of crucial differences from preplacodal ectoderm.

Distinct roles for Bmp in specification of neural crest and preplacodal ectoderm

Using DM to finely control Bmp signaling, we show that Bmp regulates neural crest and preplacodal ectoderm by markedly different mechanisms. In agreement with earlier genetic studies in zebrafish (Nguyen et al., 1998; Barth et al., 1999; Tucker et al., 2008), our data indicate that neural crest is specified by a discrete low level of Bmp signaling as predicted by the classical morphogen model (Fig. 2.1A). Adding DM at 4 hpf at a dose sufficient to fully block Bmp signaling ablates neural crest formation, whereas a slightly lower dose causes a dramatic ventrolateral expansion of neural crest to fully displace

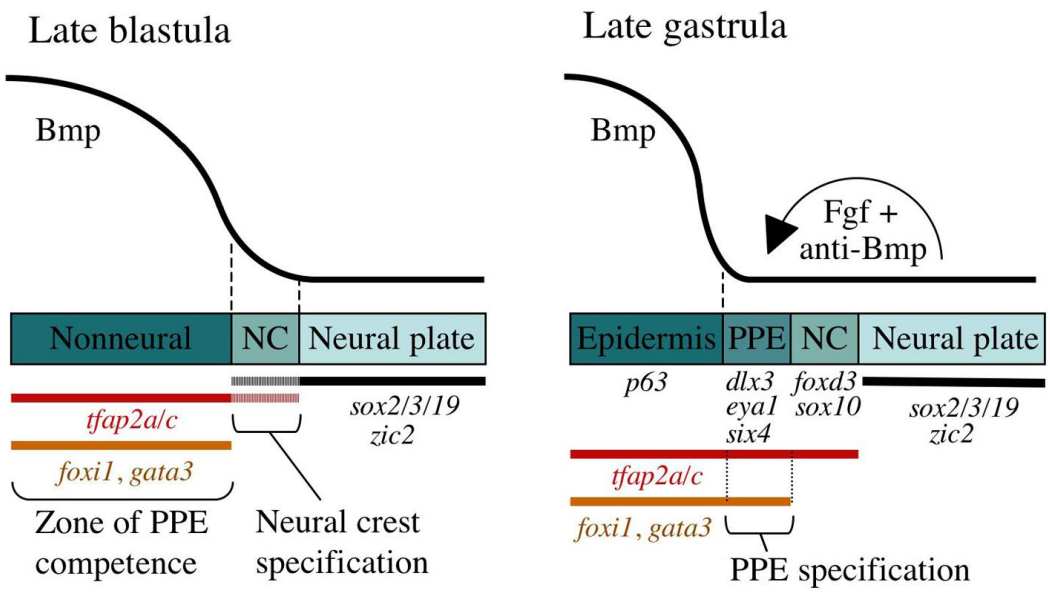

Figure 2.10: A model for sequential phases of preplacodal development. During late blastula stage, Bmp acts as a morphogen that specifies neural crest (NC) within a narrow but low range of signaling, whereas higher levels of Bmp signaling establish the nonneural ectoderm as a broad zone of uncommitted cells with potential to form epidermal or preplacodal ectoderm (PPE). Within the nonneural ectoderm, changing levels of Bmp do not distinguish preplacodal from epidermal potential, and preplacodal competence factors are uniformly induced throughout this domain. However, expression of *tfap2a/c* overlaps with the lateral edges of the neural plate where, perhaps in combination with neural markers, they cell-autonomously specify NC fate. During late gastrula stage (9-10 hpf), PPE fate is specified in competent cells near the neural-nonneural border by dorsally expressed Bmp antagonists, Fgf and Pdgf. Complete attenuation of Bmp is required for PPE specification. Relevant markers for each ectodermal domain are shown.

nonneural ectoderm (Fig. 2.3A). Fully blocking Bmp after the onset of gastrulation does not block neural crest, in agreement with studies involving timed misexpression of

Chordin (Tucker et al., 2008). These data suggest that cranial neural crest is already specified by early gastrula stage, after which it no longer requires Bmp. In chick, too, neural crest is specified by early gastrula stage (Basch et al., 2006).

Preplacodal ectoderm, marked by expression of *dlx3b*, *eya1* and *six4.1,* develops in two distinct phases with distinct signaling requirements, neither of which resemble the pattern shown by neural crest. Preplacodal ectoderm requires a robust Bmp signal during late blastula/early gastrula, but unlike neural crest, there does not appear to be a specific range of Bmp signaling that uniquely specifies preplacodal fate. We found no dose of DM that could expand the preplacodal ectoderm in a manner similar to neural crest. Instead, increasing the concentration of DM (lowering Bmp signaling) either shifted discrete bilateral stripes of preplacodal ectoderm to a more ventral position or eliminated them altogether, depending on the degree of neural plate expansion. Indeed, treatment with a single dose (25μM DM beginning at 4 hpf) yielded both classes of embryo, with nothing in between. Thus, DM cannot expand preplacodal ectoderm at the expense of epidermal ectoderm, indicating that changing Bmp levels do not distinguish between these fates.

The requirement for Bmp changes during the second phase of preplacodal development beginning soon after the onset of gastrulation. Adding a full blocking dose of DM at 7 hpf does not block preplacodal specification, even if transgenic Chordin and dominant-negative Bmp receptor are also activated during this period. Thus, Bmp is not required during gastrulation for preplacodal specification. By extension, the requirement of preplacodal ectoderm for locally secreted Bmp-antagonists (Esterberg and Fritz, 2008;

Kwon and Riley, 2008; Brugmann et al., 2004; Glavic et al., 2004; Ahrens and Schlosser, 2005; Litsiou et al., 2004) cannot reflect a requirement for a specific low threshold of Bmp; instead Bmp-antagonists are presumably needed to fully attenuate Bmp. This conclusion is further supported by our experiments showing that a full blocking dose of DM is required to induce ectopic preplacodal markers throughout the ventral ectoderm (Fig. 2.9, Table 1; and see below).

Other essential signals

We have found that Fgf combined with Bmp attenuation is sufficient to induce preplacodal markers in ventral ectoderm, as has been shown in chick and frog (Ahrens and Schlosser, 2005; Litsiou et al., 2005), suggesting that this mechanism is broadly conserved. Thus, using heat shock-inducible transgenes, we show that misexpression of Fgf combined with DM treatment is sufficient to induce ectopic preplacodal markers anywhere within the nonneural ectoderm. This supports two important conclusions. First, it demonstrates that the entire nonneural ectoderm is competent to form preplacodal ectoderm, even at the ventral midline far from the neural plate. This is consistent with the expression domains of preplacodal competence factors (see below). Second, although Fgf and Bmp-antagonists likely constitute a small subset of signals associated with the neural-nonneural border, no other signals are needed to trigger preplacodal development. Fgf and Bmp-attenuation induces ectopic expression of preplacodal markers in chick and *Xenopus*(Ahrens and Schlosser, 2005; Litsiou et al., 2005), though this combination of signals also induces expression of general neural plate

markers in those species. By contrast, our experimental conditions do not induce formation of ectopic neural plate or neural crest, tissues that could themselves have induced ectopic preplacodal markers (Ahrens and Schlosser, 2005; Litsiou et al., 2005; Woda et al., 2003). Thus induction of ectopic preplacodal ectoderm appears to be a direct and specific response to Fgf combined with Bmp attenuation, at least in zebrafish.

In addition to being able to induce ectopic preplacodal markers, we have found that Fgf is required in zebrafish for normal preplacodal development, and furthermore that Pdgf acts partially redundantly in this process. Fgf and Pdgf have been shown to regulate distinct aspects of gastrulation, with Fgf promoting dorsal fate specification and Pdgf promoting convergence towards the dorsal midline (Kudoh et al., 2004; Montera et al., 2003). Although Fgf is not absolutely required for expression of general preplacodal markers (Hans et al., 2007; Solomon et al., 2003; Leger and Brand, 2002), we find that treating embryos with the Fgf inhibitor SU5402 during the latter half of gastrulation reduces the level of expression of preplacodal markers. Treating embryos with the Pdgf inhibitor AG1295 alone has no effect on preplacodal specification, but blocking both Fgf and Pdgf further reduces preplacodal gene expression, nearly eliminating *eya1* expression. Homologs of Fgf and Pdgf are preferentially expressed in dorsal tissues near the end of gastrulation (Liu et al., 2002; Kudoh et al., 2004; Philips et al., 2001) and likely activate the same signal transduction pathways required for preplacodal specification. It is not known whether Pdgf regulates preplacodal development in other species, but Pdgf and Fgf are specifically required for induction of the trigeminal placode in chick (McCabe et al., 2008).

In this study we have not addressed the role of Wnt inhibitors, which are also required for preplacodal development (Brugmann et al., 2004; Litsiou et al., 2005). Numerous Wnt inhibitors are abundantly expressed in the head and are vital for cranial development in general, including preplacodal ectoderm. Otherwise, preplacodal fate is restricted from the trunk and tail by posteriorizing Wnt signals (Patthey et al., 2008; Patthey et al., 2009).

The role of competence factors

We show that Tfap2a, Tfap2c, Foxi1 and Gata3 act as partially redundant competence factors required specifically for preplacodal development. These genes are expressed uniformly within the nonneural ectoderm beginning in late blastula stage. Knockdown of individual competence factors can impair development of discrete subsets of cranial placodes but formation of preplacodal ectoderm is not detectably altered (Neave et al., 1995; Sheng et al., 1999; Karis et al., 2001; Solomon et al., 2003; Lee et al., 2003; Li and Cornell, 2007). In contrast, knockdown all four competence factors specifically blocks formation of preplacodal ectoderm and all placodal derivatives (Figs. 2.5, 2.6). Importantly, formation of a ventral Bmp gradient and the neural-nonneural interface still occurs. Formation of this region reflects a signaling environment that normally promotes preplacodal development yet, without the four competence factors, cells in the nonneural ectoderm cannot respond to such signals. Conversely, misexpression of one or more competence factors in the neural plate, where preplacodal inducing signals are expressed, leads to ectopic expression of preplacodal markers (Fig. 2.8). Although

global misexpression of competence factors causes various developmental defects, localized mosaic misexpression avoids global perturbation yet still results in cell-autonomous expression of preplacodal markers in the neural plate. Thus, these genes are necessary and sufficient to render cells competent to form preplacodal ectoderm, while additional dorsal signals are required for overt specification of preplacodal fate.

Though *tfap2a/c*, *foxi1* and *gata3* are required for preplacodal ectoderm; they are neither necessary nor sufficient for epidermal fate: Expression of the epidermal marker *p63* remains appropriately localized following either knockdown or misexpression of preplacodal competence factors (Figs. 2.5, 2.6). Conversely, knockdown of *p63* does not detectably impair preplacodal development nor enhance the effects of knocking down subsets of preplacodal competence factors (Fig. 2.6). The simplest interpretation is that Bmp initially co-induces epidermal and preplacodal potential throughout the nonneural ectoderm, with fate specification occurring later according to differences in local signaling.

Differential regulation of preplacodal competence factors by Bmp explains the differing Bmp-requirements of preplacodal ectoderm vs. neural crest. *tfap2a*, *tfap2c*, *foxi1* and *gata3* all require Bmp for ventral expression during blastula stage. Because these genes are expressed uniformly throughout the nonneural ectoderm, it is now clear why no dose of DM is capable of expanding preplacodal ectoderm at the expense of epidermal ectoderm, though both fates can be eliminated together at sufficiently high concentrations. However, *tfap2a* and *tfap2c* are expressed in a broader domain that includes the lateral edges of the neural plate where they are required for neural crest

specification (Li and Cornell, 2007; Hoffman et al., 2007). The broader domain of expression suggests that *tfap2a* and *tfap2c* can be induced by a lower level of Bmp than *foxi1* and *gata3*. Indeed, we identified a dose of DM that permits continued broad expression of *tfap2a/c* but eliminates expression of *foxi1* and *gata3* (Fig. 2). Thus the greater sensitivity of *tfap2a/c* to Bmp explains the ability of a low threshold of Bmp to expand neural crest at the expense of nonneural ectoderm. After the onset of gastrulation, expression of all four genes becomes independent of Bmp. This is an important regulatory feature because it allows maintenance of preplacodal competence as Bmp signaling is attenuated along the neural-nonneural border during preplacodal specification. Likewise, stability of *tfap2a/c* in the neural plate safeguards neural crest fate after Bmp signaling abates.

It is still unclear how *tfap2a/c* can alternately promote either neural crest or preplacodal development. We speculate that the overlap of *tfap2a/c* with early markers of neural plate such as *sox2/3/19* favors neural crest, whereas overlap with *foxi1* and *gata3* in the nonneural ectoderm favors preplacodal development (Fig. 2.11). However, misexpression of *tfap2a* in the neural plate can induce both neural crest and preplacodal markers, albeit in non-overlapping clusters of cells (data not shown). It is possible that the level of *tfap2a* and *tfpa2c* also influences its developmental function. Both genes show diminishing expression near the edges of the neural plate, which might facilitate their neural crest functions. Similarly, cell-to-cell variation in the level of *hs:tfap2a* transgene expression might explain the ability to activate ectopic preplacodal and neural crest markers in dorsal ectoderm.

The long lag between expression of competence factors and expression of preplacodal markers remains unexplained. That is, why are preplacodal competence factors expressed prior to gastrulation yet preplacodal markers are not induced until the end of gastrulation? We cannot accelerate expression of preplacodal markers by changing the time of activation of *hs:fgf8* and *hs:chd*. Regardless of whether we activated these transgenes at 7 hpf or 8.5 hpf, we only detected ectopic expression of preplacodal markers at 10.5-11 hpf, the same time these genes are induced within the endogenous preplacodal domain. It is possible that competence factors require sufficient time to "condition" ectoderm, for example through chromatin remodeling (Yam et al., 2006), or by activating other essential co-factors. These are important issues that require further investigation.

CHAPTER III

A GENE NETWORK THAT COORDINATES PREPLACODAL COMPETENCE AND NEURAL CREST SPECIFICATION IN ZEBRAFISH*

AUTHOR CONTRIBUTIONS

I performed the experiments in the following figures: Fig 3.1 A- G and K-M, Fig 3.2, Fig 3.3, Fig 3.4, Fig 3.5, Fig 3.6, Fig 3.7 and Fig 3.8. Dr. Hye-Joo Kwon generated the *Tg (hs:tfap2a)* line and perfomed the work shown in Figure 3.1 H, I, J.

INTRODUCTION

Preplacodal ectoderm (PPE) and neural crest (NC) form along neural-nonneural interface near the end of gastrulation and together contribute to the peripheral nervous system. PPE later resolves into a number of sensory placodes that give rise to diverse structures such as the inner ear, olfactory epithelium, lens, anterior pituitary, and parts of trigeminal and epibranchial ganglia (reviewed by Baker and Bronner-Fraser, 2001; Streit, 2007; Schlosser et al., 2010). Transcription factors encoded by Six, Eya and Dlx gene families are specifically induced or upregulated in the PPE in response to signals from the dorsal tissue, including Fgf, Wnt antagonists and Bmp antagonists (Brugmann et al., 2004; Glavic et al., 2004; Ahrens and Schlosser, 2005; Litsiou et al., 2005; Esterberg and Fritz, 2009; Kwon and Riley, 2009; Kwon et al., 2010). Although PPE

---

*Reprinted with permission from "A gene network that coordinates preplacodal competence and neural crest specification in zebrafish"; by **Bhat, N, Kwon, H-J, Riley B.B,** *Developmental Biology*, 2012, Epub ahead of print.

formation is restricted to a relatively narrow band abutting the neural plate, the competence or potential to form PPE is present throughout the ventral ectoderm from the beginning of gastrulation (Mancilla and Mayor, 1996; Woda et al., 2003; Glavic et al., 2004; Ahrens and Schlosser, 2005; Kwon et al., 2010). Localized misexpression of Fgf plus Chordin during gastrula stages can induce PPE markers ectopically anywhere within the nonneural ectoderm (Ahrens and Schlosser, 2005; Kwon et al., 2010). We showed previously that competence to form PPE is mediated by a set of four Bmp-activated transcription factor genes, *tfap2a*, *tfap2c*, *foxi1* and *gata3* (Kwon et al., 2010). Knockdown of pairs of competence factors, such as *tfap2a* plus *tfap2c* or *foxi1* plus *gata3*, does not block PPE gene expression, although expression levels are reduced. Knockdown of all four competence factors leads to complete and specific loss of all PPE markers without disrupting the neural plate or epidermal development (Kwon et al., 2010). Thus, these genes are partially redundant and are together necessary for PPE specification.

Although these competence factors are redundant with respect to PPE specification, they appear to play unique roles during later development of various tissues. For example, *foxi1* and *gata3* show dramatic upregulation in the otic/epibranchial placodal region towards the end of gastrulation (Neave et al., 1995; Solomon et al., 2003), due in part to rising levels of Fgf (Padanad et al., 2012). Loss of *foxi1* causes severe deficiency of both otic and epibranchial placodes in zebrafish (Lee et al., 2003; Solomon et al., 2003; Nissen et al., 2003; Sun et al., 2007) whereas loss of *gata3* leads to a severe otic phenotype in mice (Karis et al., 2001). Likewise, *tfap2a/c*

genes have several unique functions: *Tfap2a* has been extensively studied for its essential early role in neural crest development (Luo et al., 2003; Knight et al., 2003; Hoffman et al., 2007; Li and Cornell, 2007; Nikitina et al., 2008; Arduini et al, 2009; de Crozé et al., 2011; Wang et al., 2011; Van Otterloo et al., 2012). In zebrafish, disruption of both *tfap2a* and *tfap2c* ablates neural crest and also causes significant deficiencies in all placodal derivatives (Hoffman et al., 2007; Li and Cornell, 2007; Kwon et al., 2010). However, it is not known whether the latter defects reflect disruption of placode formation or faulty regulation of subsequent growth, maintenance and differentiation of placodal derivatives. More generally, the degree to which *tfap2a/c*, *foxi1* and *gata3* can compensate for each other in regulating placodal development remains unexplored.

We showed previously that Bmp is required for the activation but not subsequent maintenance of PPE competence factors at late-blastula stage. Expression of competence factors continues at near normal levels even if Bmp signaling is totally blocked from the beginning of gastrulation (Kwon et al., 2010). We speculated then that auto-regulation and cross-regulation amongst competence factors help maintain proper expression levels during PPE specification when Bmp must be attenuated, though this idea has not been tested directly. Similarly, the sufficiency of competence factors to foster PPE development in the complete absence of Bmp remains an open question.

Here we show through gain and loss of function that, despite the partial redundancy of competence factors for PPE specification, competence factors also have unique placode-specific functions. Additionally, during gastrulation these competence factors form a self-sustaining gene regulatory network that maintains proper expression

levels even after attenuation of Bmp. In the absence of Bmp, misexpression of *tfap2a* alone cannot activate other competence factors but nevertheless supports both PPE and NC development. Misexpression of any two competence factors in the absence of Bmp signaling not only restores PPE and NC markers but also restores the larger network of competence factors and rescues development of some specific placodes. Thus, we have identified a gene regulatory network that is sufficient, together with appropriate inductive signals, for the formation of sensory organs in zebrafish.

MATERIALS AND METHODS

Developmental conditions

Embryos were incubated in embryo medium (Kimmel et al., 1995) at 28.5°C, except for heat shock experiments as noted in the text. Wild-type embryos were derived from the AB line.

In-situ hybridization and immunostaining

In-situ hybridization and immunostaining were was performed as previously described (Phillips et al., 2001). Primary antibody for immunostaining against Isl-1 was obtained from Hybridoma bank (dilution 1:100) and anti-mouse HRP- conjugated secondary antibody was obtained from Vector labs (dilution 1:200).

Pharmacological treatment

Dorsomorphin (Sigma, P5499) was diluted in DMSO at a concentration of 10 mM. To fully block Bmp signaling, DM stock solution was diluted to a concentration of 200 µM in embryo media. Treatments were conducted in 24-well plates with a maximum of 40 embryos per well in 500 µl of DM solution. Aliquots of DM stock solution were stored frozen at -80°C indefinitely without detectable loss of activity. Repeated freeze-thaw cycles significantly reduce DM activity. Once thawed, aliquots can be stored for several days at 4°C. However, long-term storage at 4°C leads to degradation, with 10% loss of activity after 1 month and 85% loss of activity after 1 year. DM solution should also be shielded from light exposure.

Morpholino injection

For gene knockdown, embryos were injected at the one-cell stage with 5 ng morpholino (1 nl of 5 ng/nl solution), unless otherwise stated. The morpholino sequences used here have been previously tested and published and include *tfap2a* E2I2 splice blocker AGCTTTTCTTCTTACCTGAACATCT (O'Brien et al., 2004); *tfap2c* E3I3 splice blocker TCTGACATCAACTCACCTGAACATC (Li and Cornell, 2007); *foxi1* translation blocker TAATCCGCTCTCCCTCCAGAAACAT (Solomon et al., 2003); *gata3* translation blocker TCCGGACTTACTTCCATCGTTTATT (Kwon et al., 2010). To assess morphant phenotypes, at least 20 embryos were examined for each experiment unless otherwise stated. For RNA extractions, 100 morphant embryos were used per experiment (see below).

Gene misexpression

Transgenic line *Tg(hsp70:foxi1)*^{x19} was previously described (Kwon et al., 2010). For this study we also generated new lines *Tg(hsp70:tfap2a)*^{x24} and *Tg(hsp70:gata3)*^{x25}: *tfap2a* and *gata3* cDNAs were inserted into *hsp70* vector (Shoji et al., 1998) with I-SceI meganuclease sites (Thermes et al., 2002). 10-40 pg of recombinant plasmid was co-injected with meganuclease (NEB, 0.5 U/µl) into wild-type embryos at the one-cell stage (Rembold et al., 2006). Injected embryos were raised to adulthood and screened for germline transmission by PCR. For simplicity, transgenic lines are referred to in the text as *hs:foxi1*, *hs:tfap2a* and *hs:gata3*, respectively. For misexpression, heterozygous transgenic carriers were heat shocked at 37°C for 30 minutes, after which embryos were maintained at 33°C until fixation. The effects of transgene activation were fully penetrant, except where noted. Phenotypes for double-transgenic carriers were readily distinguishable from single transgene carriers. At least 20 embryos were analyzed for each experiment, except for experiments involving RNA extraction for which 100 embryos were used for each experiment (see below).

RNA extraction and cDNA synthesis

For each sample, RNA was extracted from 100 embryos using Trizol, followed by phenol-chloroform extraction. DNA was digested by treating samples with DNAase and RNA was re-extracted by Trizol-phenol-chloroform. cDNA was synthesized from 1 µg of total RNA using an Invitrogen kit. Samples were collected at the end of gastrulation. For misexpression studies, embryos obtained from outcrossing *hs:foxi1/+*, *hs:gata3/+*,

and *hs:tfap2a/+* heterozygotes were heat shocked at 7hpf at 37ºC for 30 minutes and RNA was collected at 10 hpf. Corresponding wild-type embryos were also heat shocked to serve as controls.

Real time PCR

For each set of gene-specific primers, cDNA samples were diluted appropriately to generate a linear range of PCR product. For most genes, PCR was performed on template-dilutions of 1:8 and 1:64. For *b-actin* (a constitutive control), template-dilutions were 1:512 and 1:2048. For each independent experiment, two dilutions were repeated in triplicate, and each experiment was repeated three times. 2X Sybr green master mix was prepared by combining the following reagents: Taq buffer, $MgCl_2$, ROX reference dye, Sybr Green, dNTPs, DEPC H_2O. The 2X sybr green was mixed with primers and cDNA in the ratio of 5:2:3 in a 10µl reaction volume. Reactions were performed in 96-well plates (Thermo Scientific, AB-1100) with optical adhesive covers (Applied Biosystems, P/N: 4360954) in an Applied Biosystems 7300 real time PCR system using the default protocol. The fold change was calculated using $2^{-\Delta\Delta C}{}_T$ method. Extrapolation of transcript levels gave similar values for each dilution, confirming that PCR conditions were held within the linear range. Data from both dilutions from independent experiments were averaged to obtain an overall mean and standard deviation for the sample in question. Data are expressed in fold-change relative to wild-type control levels measured. P-values were calculated using t-tests. For misexpression

experiments, only half of embryos were expected to carry the transgene in question, hence the fold change in mRNA level was doubled to compensate.

RESULTS

Requirement for Tfap2a and Tfap2c in formation of cranial placodes

Tfap2a and Tfap2c are best known for their essential roles in neural crest specification (Luo et al., 2003; Knight et al., 2003; Knight et al., 2005; Hoffman et al., 2007; Li and Cornell, 2007; Nikitina et al., 2008; de Crozé et al., 2011; Wang et al., 2011). In addition, embryos knocked down for both genes (*tfap2a/c* morphants) show severe deficiencies at 24 hpf in the otic vesicle, olfactory pit and various cranial ganglia (Li and Cornell, 2007), all of which are derived from cranial placodes. However, it was not determined whether defects in placodal derivatives arose from misregulation of initial formation or subsequent growth and maintenance of placodes. By examining early markers, we found *tfap2a/c* morphants are severely deficient in initial formation of all cranial placodes. This includes the anterior pituitary, olfactory and lens placodes (*pitx3*) and subsequent olfactory pit (*cxcr4b*) and developing lens (*foxe3*), the trigeminal placode (*neuroD*), otic placode (*pax8* and *pax2a*), and epibranchial placodes and ganglia (*sox3* and *phox2a*) (Fig. 3.1A-G, and data not shown). We showed previously that *tfap2a* and *tfap2c* act redundantly with coexpressed genes *foxi1* and *gata3* to establish preplacodal competence in the ventral ectoderm (Kwon et al., 2010). Despite this redundancy, we hypothesized that placodal defects might result from reduced expression levels of competence factors in *tfap2a/c* morphants. In support, knockdown of *tfap2a*

and *tfap2c* substantially reduced the level of expression of competence factors *gata3* and *foxi1* (Fig. 3.1H, I). Expression of *dlx3b*, the earliest known marker of PPE specification,

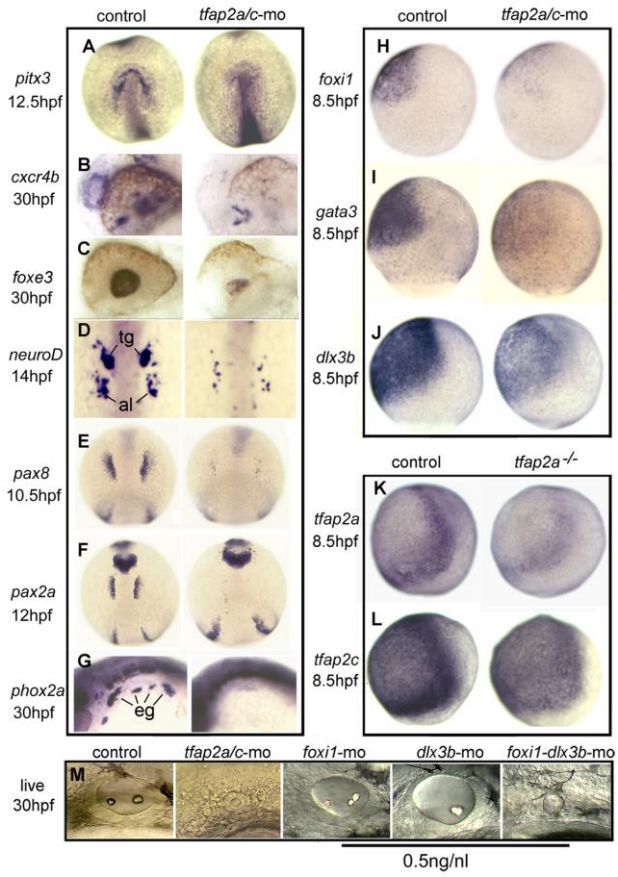

Figure 3.1: Knockdown of *tfap2a/c* impairs early placode development. **A-G**, Expression of early placodal markers in control embryos and *tfap2a/c* morphants. Expression of *pitx3* at 12.5 hpf marks pituitary/olfactory/lens precursors (A); *cxcr4b* marks the olfactory pit at 30 hpf (B); *foxe3* marks the lens at 30 hpf (C); *neuroD* marks the trigeminal (tg) and anterior lateral line (al) at 14 hpf (D); *pax8* at 10 hpf (E) and *pax2a* at 12 hpf (F) mark otic/epibranchial precursors; *phox2a* marks epibranchial ganglia (eg) at 30 hpf (G). **H-J**, Expression of competence factors *foxi1* (H) and *gata3* (I), and PPE marker *dlx3b* (J), at 8.5 hpf in control embryos and *tfap2a/c* morphants. **K, L**, Expression of *tfap2a* (K) and *tfap2c* (L) at 8.5 hpf in control embryos and *tfap2a*$^{-/-}$ (*lockjaw*) mutants. **M**, Otic vesicle at 30 hpf in a control embryo, *tfap2a/c* morphant, and embryos injected with sub-effective doses (0.5 ng) of *foxi1*-MO, *dlx3b*-MO or both *foxi1*-MO and *dlx3b*-MO. Sub-effective doses of these MO have little or no effect by themselves, but when combined have synergistic effects that phenocopy the *tfap2a/c* morphant. Images show dorsal views with anterior up (A, D-F), lateral views with anterior to the left (B, C, G, M) or lateral views with dorsal to the right (H-L).

was also reduced in *tfap2a/c* morphants (Fig. 3.1J). Because the morpholinos for knocking down *tfap2a/c* are splice blockers that destabilize target transcripts, we could not address whether these morpholinos affected feedback regulation of *tfap2a* and *tfap2c* expression. However, *lockjaw* (*low*) mutants, which are disrupted in *tfap2a* function (Knight et al., 2003), were found to express substantially reduced levels of *tfap2a* and *tfap2c* in prospective PPE cells (Fig. 3.1K, L). Thus, Tfap2a and Tfap2c are required for achieving a proper level of expression of a number of genes acting upstream of PPE specification. We next tested whether weak impairment of several upstream regulators is sufficient to perturb later placode formation. As a specific example, we tested the effects of injecting sub-effective doses of morpholinos targeting *foxi1* and *dlx3b*, which are critical for proper development of the otic placode (Solomon and Fritz, 2002; Nissen et al., 2003; Liu et al., 3003; Solomon et al., 2003; Solomon et al., 2004). Injecting either morpholino alone at 0.5 ng per embryo (10% of the level required to fully knock down gene function) had little effect on early otic gene expression or formation of the otic vesicle (Fig. 3.1M). However, co-injecting 0.5 ng each of *foxi1*-MO and *dlx3b*-MO caused a severe synergistic deficiency of otic tissue, phenocopying the *tfap2a/c* morphant phenotype (Fig. 3.1M). Thus, mild impairment of a few upstream regulators is sufficient to explain the deficiencies in otic placode formation seen in *tfap2a/c* morphants. Similar combinatorial reduction seems likely to account for impairment of other placodes as well.

Overexpression of *tfap2a* expands placodal development

To further investigate the role of *tfap2a* in placodal development, we generated a heat shock inducible transgenic line to misexpress *tfap2a* (*hs:tfap2a*). Full activation of *hs:tfap2a* during gastrulation by heat shocking embryos at 39°C caused elevated cell death, confounding clear interpretation. However, activation of the transgene at 37°C did not detectably elevate cell death, so all results reported here are based on heat shocking embryos for 30 minutes at 37°C. Activation of *hs:tfap2a* at any time during gastrulation had similar stimulatory effects on placodal development, though optimal effects as reported here were obtained by heat shocking embryos at 7 hpf. Under these conditions, misexpression of *tfap2a* led to subsequent enlargement of nearly all placodes and their derivatives, including anterior pituitary, olfactory, trigeminal and otic tissues (Fig. 3.2A-L). Only the lens was relatively unaffected (Fig. 3.2A, B, and data not shown). Misexpression of *tfap2a* did not detectably increase proliferation based on immunostaining for phosphohistone H3 (not shown). Thus, misexpression of *tfap2a* during gastrulation is sufficient to expand initial domains of most cranial placodes. Activation of *hs:tfap2a* also led to elevated expression of competence factors *tfap2c*, *foxi1, gata3* and preplacodal marker *dlx3b* during gastrulation (see below), and significant upregulation of these genes persisted through early- to mid-somitogenesis stages (Fig. 3.2M-T). Together, these findings suggest that *hs:tfap2a* upregulates expression of upstream regulators of PPE formation, resulting in overproduction of placodal tissue.

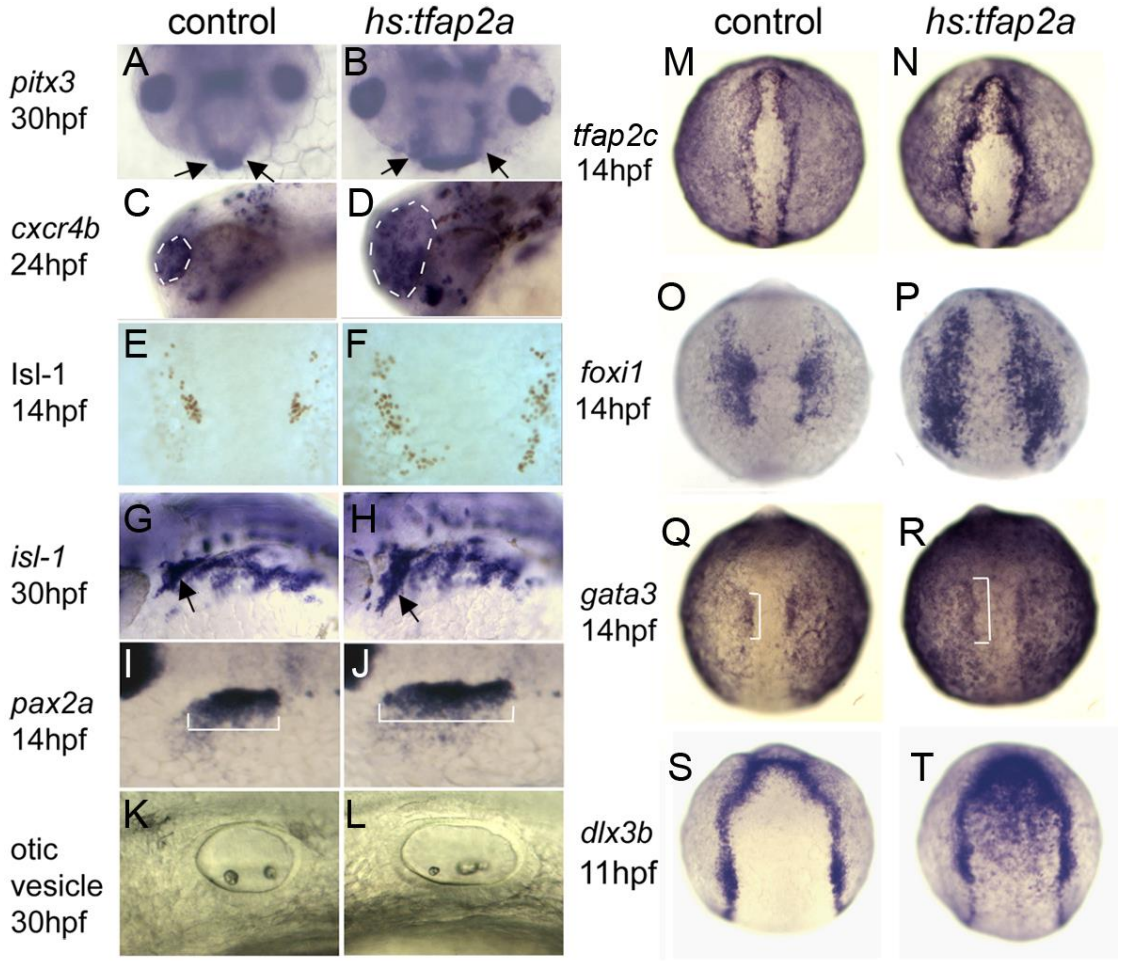

Figure 3.2: Misexpression of *tfap2a* promotes overproduction of placodes. A-L, Markers of placodal derivatives, including *pitx3* in the anterior pituitary at 30 hpf (A, B, arrows), *cxcr4b* in the olfactory pit at 24 hpf (C, D, circled), Isl1 in trigeminal placode at 14 hpf (E, F), *isl1* in cranial ganglia at 30 hpf (G, H, trigeminal ganglion indicated by arrows), *pax2a* in the otic/epibranchial placodes at 14 hpf (I, J, brackets indicate otic domain), and the otic vesicle at 30 hpf (K, L) in control embryos and *hs:tfap2a/+* transgenic embryos. All indicated placodal derivatives are enlarged following activation of *hs:tfap2a* at 7 hpf. **M-T**, expression of competence factors *tfap2c* (M, N), *foxi1* (O, P) and *gata3* (Q, R, otic domain indicated by brackets) at 14 hpf, and the general PPE marker *dlx3b* at 11 hpf (S, T) in control embryos and *hs:tfap2a* embryos. Activation of *hs:tfap2a* at 7 hpf results in upregulated and expanded expression of all of these genes in placodal tissues. Images show lateral views with anterior to the left (C, D, G-L), dorsal views with anterior up (E, F, M-T), or facial views of the front of the head (A, B).

Temporal requirement for *tfap2a*

To establish when *tfap2a* is required for PPE and NC development, we knocked down *tfap2a/c* using splice-blocking morpholinos and then activated *hs:tfap2a* at various times and examined expression of *foxd3* (neural crest) and *pax2a* (otic placode). Note, we focuesd on *pax2a* because it is the most sensitive indicator for mild impairment of PPE development. As expected, neither marker was expressed in *tfap2a/c* morphants (Fig. 3.3B, H). Activation of *hs:tfap2a* at late blastula stage (4 hpf) in *tfap2a/c* morphants led to abundant expression of *foxd3* but did not rescue placodal expression of *pax2a* (Fig. 3.3C, I) or *fgf24* (not shown). In contrast, activation of *hs:tfap2a* in *tfap2ac* morphants at any time during gastrulation (between 6 hpf and 10 hpf) rescued both NC and placodal markers to near wild type expression patterns (Fig. 3.3D, E, J, K). Heatshock activation at 12 hpf (6 somites stage) led to weak expression of *foxd3* in cranial neural crest but did not rescue otic expression of *pax2a* (Fig. 3.3F, L). Thus, the requirement for *tfap2a* by NC can be met at any time between late blastula to early somitogenesis stages whereas the requirement for placodal development occurs during a more restricted interval spanning gastrulation.

The role of *foxi1* and *gata3* in placodal development

To further investigate unique and redundant functions of PPE competence factors, we examined the effects of knocking down *foxi1, gata3* or both *foxi1* and *gata3* (*foxi1-gata3* morphants). Disruption of *foxi1* alone ablates epibranchial placodes and strongly reduces otic placodes (Lee et al., 2003; Nissen et al., 2003; Solomon et al., 2003), and

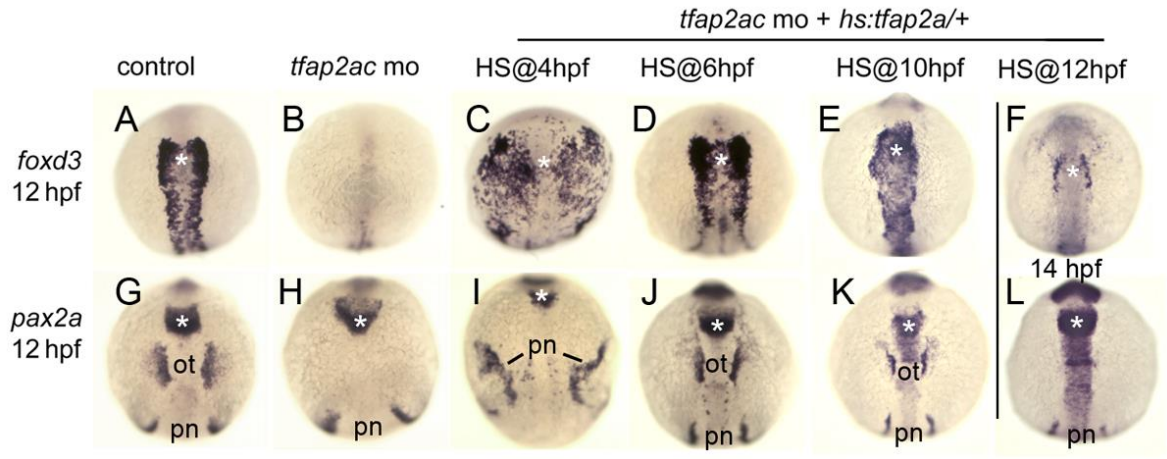

Figure 3.3: Temporal requirements for *tfap2a/c*. Expression of neural crest marker *foxd3* at 12 hpf (A-E) and 14 hpf (F), and otic marker *pax2a* at 12 hpf (G-K) and 14 hpf (L) in control embryos (A, G), *tfap2a/c* morphants (B, H), and *tfap2a/c* morphants in which *hs:tfap2a* was activated (HS) at the indicated times (C-F, I-L). Expression domains of *pax2a* in the otic placode (ot) and pronephros (pn) are indicated, and the midbrain-hindbrain border region is marked with an asterisk. Cranial neural crest was rescued by activating *hs:tfap2a* at any time between late blastula stage (4 hpf) and 6 somite-stage (12 hpf), whereas rescue of the otic domain of *pax2a* required activation of the transgene during gastrulation (6-10 hpf). All images show dorsal views with anterior to the top.

we reported previously that injecting *gata3*-MO alone has no discernable effect on embryonic development (Kwon et al., 2010). In contrast, *foxi1-gata3* morphants show a substantial phenotypic enhancement such that the otic placode is quite small at 13 hpf (Fig. 3.4D, E) and a morphologically visible otic vesicle fails to form in most specimens (Fig. 3.4G, H). In addition, the trigeminal placode is reduced by nearly half at 14 hpf (Fig. 3.4A, B). However, anterior placodes including anterior pituitary (Fig. 3.4J, K), olfactory pit (Fig. 3.4M, N) and lens (not shown) develop normally in *foxi1-gata3*

morphants, indicating that *foxi1* and *gata3* are specifically required for development of posterior placodes but not anterior placodes.

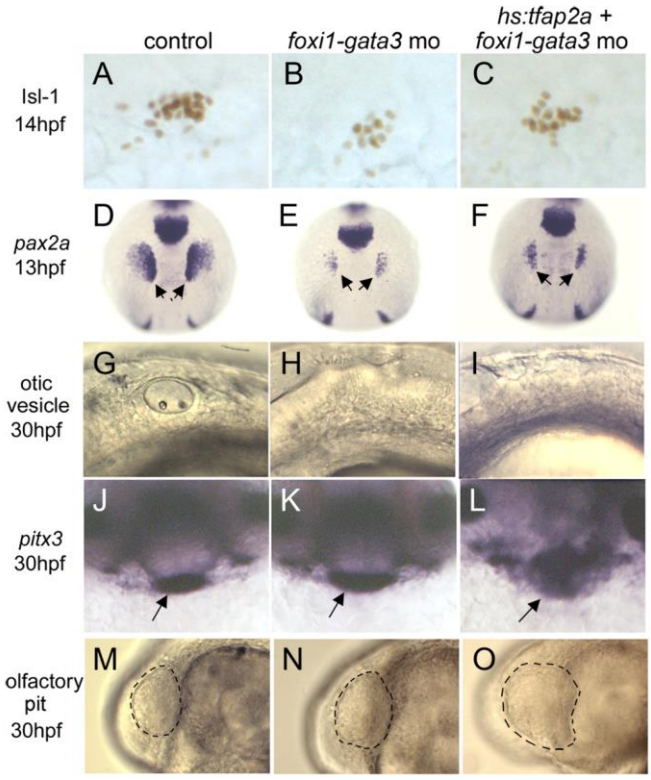

Figure 3.4: Unique requirements for *foxi1* and *gata3* in posterior placodes. Markers of cranial placodes and placodal derivatives, including Isl1 in the trigeminal placode at 14 hpf (A-C), *pax2a* in the otic/epibranchial placodes at 13 hpf (D-F, arrows), otic vesicle at 30 hpf (G-I), *pitx3* in the anterior pituitary at 30 hpf (J-L, arrows) and the olfactory pit at 30 hpf (M-O, outlined) in control embryos (A, D, G, J, M), *foxi1-gata3* morphants (B, E, H, K, N), and *foxi1-gata3* morphants in which *hs:tfap2a* was activated at 7 hpf (C, F, I, L, O). Knockdown of *foxi1* and *gata3* reduces the size of the trigeminal, otic and epibranchial placodes, but anterior placodes develop normally. Activation of *hs:tfap2a* does not rescue development of posterior placodes in *foxi1-gata3* morphants, and the transgene still enlarges anterior placodes despite knockdown of *foxi1* and *gata3*. Images show lateral views with anterior to the right (A-C, G-I, M-O), dorsal views with anterior up (D-F), and facial views of the front of the head (J-L).

We next tested whether misexpression of *tfap2a* can compensate for loss of *foxi1* and *gata3*. Anterior placodes were enlarged following activation of *hs:tfap2a* at 7 hpf in *foxi1-gata3* morphants (Fig. 3.4L, O), but *hs:tfap2a* activation did not improve development of trigeminal, anterior lateral line, otic or epibranchial placodes (Fig. 3.4C, F, I). Thus, whereas *tfap2a/c* are required for proper development of all cranial placodes, *foxi1* and *gata3* are required only for posterior placodes and their functions cannot be compensated for by elevating *tfap2a*.

To test the effects of misexpressing *foxi1* and *gata3*, we used heat shock inducible transgenic lines and used the same heat shock regimen (37°C, 30 minutes) as described above. Activating either *hs:foxi1* or *hs:gata3* alone during gastrulation caused slight enlargement of the otic placode but had no effect on other placodes (not shown). Co-activation of both *hs:foxi1* and *hs:gata3* at 7 hpf caused a more pronounced enlargement of the otic placode (Fig. 3.5B, F) and the otic vesicle was reproducibly enlarged at 24 hpf (Fig. 3.5N). Again, no other placodes were affected under these conditions. We next tested whether misexpressing *foxi1* and *gata3* could rescue the placodal defects seen in *tfap2a/c* morphants. Co-activation of *hs:foxi1* and *hs:gata3* restored early markers of the otic and epibranchial placodes to nearly wild-type levels (Fig. 3.5C, D, G, H, and data not shown) and the otic vesicle also showed substantial recovery (Fig. 3.5O, P). However, epibranchial ganglia did not form under these conditions, and no other placodes were rescued by *foxi1* and *gata3* (not shown). On the other hand, activation of *hs:foxi1* and *hs;gata3* led to elevated expression of *dlx3b* throughout the preplacodal ectoderm (Fig. 3.5J) and also restored *dlx3b* levels in

tfap2a/c morphants (Fig. 3.5K, L). Together, these data support the conclusion that *foxi1, gata3* and *tfap2a/c* genes are partially redundant for PPE specification, but also provide unique (non-redundant) functions during later development of individual placodes.

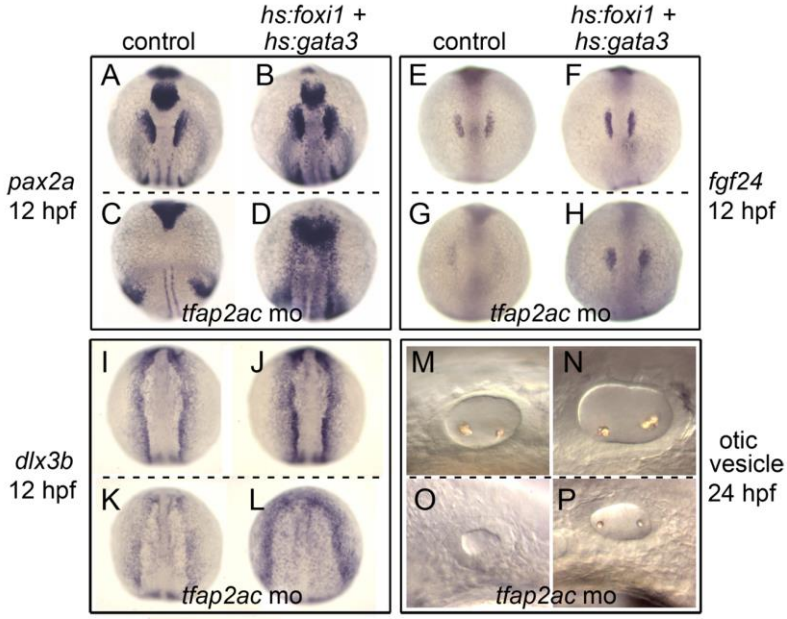

Figure 3.5: Co-misexpressing *foxi1* and *gata3* in *tfap2a/c* morphants. A-D, Expression of *pax2a* in the otic/epibranchial placodes at 12 hpf. **E-H**, Expression of *fgf24* in the otic placode at 12 hpf. **I-L**, Expression of *dlx3b* in placodal tissues at 12 hpf. **M-P**, Otic vesicle at 24 hpf. Non-transgenic controls and *hs:foxi1-hs:*gata3 double transgenic embryos are marked across the top, and and the lower half of each panel shows *tfap2a/c* morphants and double transgenic *tfap2a/c* morphants. Activation of the transgenes at 7 hpf partially rescued otic development in *tfap2a/c* morphants. Images show dorsal views with anterior to the top (A-L) or lateral views with anterior to the left (M-P).

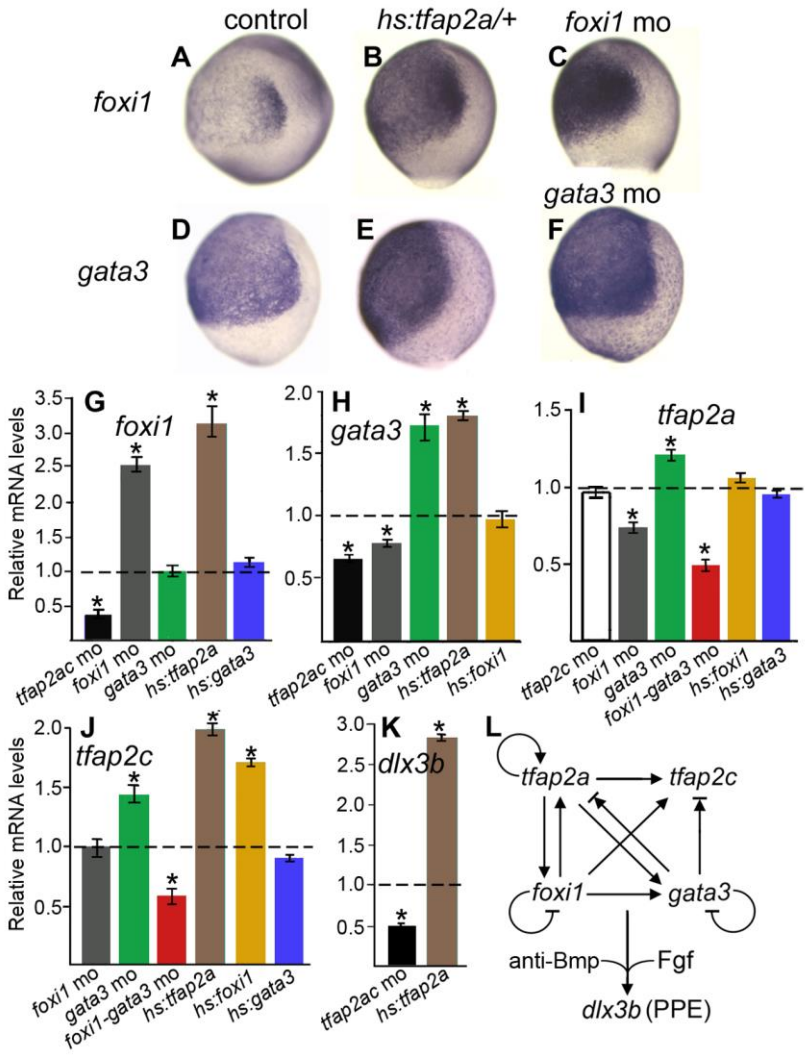

Figure 3.6: A network of auto- and cross-regulation amongst competence factors. Changes in expression levels of PPE regulatory genes near the end of gastrulation following misexpression or knockdown of the indicated genes. **A-F**, 10 hpf wholemount expression patterns of *foxi1* (A-C) and *gata3* (D-F) in control embryos (A, D), *hs:tfap2a* transgenic embryos (B, E), a *foxi1* morphant (D) and a *gata3* morphant (F). **G-K**, Quantitative real time PCR measurements of relative mRNA abundance for *foxi1* (G), *gata3* (H), *tfap2a* (I), *tfap2c* (J), and *dlx3b* (K) in the indicated backgrounds. Expression levels were normalized relative to wild-type controls, which are represented by dashed lines set at a value of 1.0. Genetic backgrounds are color coded to facilitate comparison between data sets: Black, *tfap2a/c* morphants; white, *tfap2c* morphants; gray, *foxi1* morphants; green, *gata3* morphants; red, *foxi1-gata3* morphants; brown, *hs:tfap2a*; yellow, *hs:foxi1*, blue, *hs:gata3*. Data represent means of three independent experiments, each performed at two different dilutions, each measured in triplicate. The effects of gene misexpression were assayed at 10 hpf following heat shock at 7 hpf, and corresponding wild-type controls were also heat shocked at 7 hpf. Error bars represent standard deviations. Asterisks indicate statistically significant differences from the controls, as measured by t-tests. **L**, Model and summary of functional relationships between PPE competence factors and the general PPE marker, *dlx3b*. Arrows indicate positive regulation, cross-bars indicate negative regulation, and arrows with cross-bars indicate ambiguity in the data. Specifically, *tfap2a* and *tfap2c* are slightly upregulated in *gata3* morphants but are strongly downregulated in *foxi1-gata3* morphants.

half (Fig. 3.6G, H, K, black bars), while activation of *hs:tfap2a* increased expression of these genes by 2- to 3-fold (Fig. 3.6G, H, K, brown bars). *hs:tfap2a* also doubled the level of *tfap2c* transcript (Fig. 3.6J, brown bar). Thus, *tfap2a* positively regulates its own expression and expression of other competence factors.

Although *lockjaw* (*tfap2a*$^{-/-}$) mutants appeared to express reduced levels of *tfap2c* (Fig 3.1L), knockdown of *tfap2c* did not signficantly affect *tfap2a* mRNA levels (Fig. 3.6I, white bar). Thus, despite the general similarity of *tfap2a* and *tfap2c* structure and function, only *tfap2a* plays an essential role in regulating expression levels of both genes (Fig. 3.6L).

We next measured the effects of manipulating *foxi1* and *gata3*. Injecting *foxi1*-MO caused a 20-30% decrease in *gata3* and *tfap2a* transcript levels (Fig. 3.6H, I, gray bars), whereas activation of *hs:foxi1* increased accumulation of *tfap2c* transcript by 70% (Fig. 3.6J, orange bar). These data suggest that *foxi1* positively regulates these genes. Surprisingly, injecting *gata3*-MO caused a 20-40% elevation of *tfap2a* and *tfap2c* transcript levels (Fig. 3.6I, J, green bars). However, co-injection of *gata3*-MO with *foxi1*-MO reduced *tfap2a* and *tfap2c* transcript levels by half (Fig. 3.6I, J, red bars), reversing the effects of *gata3*-MO alone and strongly enhancing the effects of *foxi1*-MO. Thus, *gata3* function appears highly context-dependent, with *gata3* and *foxi1* together being required to fully activate *tfap2a/c* expression. Activation of *hs:gata3* alone had little effect on any of these genes (Fig. 3.6G, I, J, blue bars) despite its ability to enhance the effects of *hs:foxi1* (Fig. 3.5, and see below).

We next investigated whether *foxi1* and *gata3* regulate their own expression. Injecting *foxi1*-MO increased the level of *foxi1* transcript by 2.5-fold (Fig. 3.6C, G, gray bar), suggesting an auto-inhibitory loop. Similarly, injecting *gata3*-MO nearly doubled the level of *gata3* transcript (Fig. 3.6F, H, green bar), suggesting that it, too, is auto-inhibitory. Together, these data suppport a model in which mutual cross-activation between competence factors, plus auto-activation of *tfap2a*, helps boost expression levels of all competence factors; and the degree of feedback amplification is held in-check by auto-inhibition by *foxi1* and *gata3* (Fig. 3.6L). Self-regulation of this network likely explains why expression can be maintained even after Bmp is attenuated by signals that specify PPE fate (Kwon et al., 2010). This model is further supported by data provided below.

Sufficiency of competence factors in the absence of Bmp signaling

During late blastula stage, Bmp signaling establishes PPE competence throughout the nonneural ectoderm and, at a lower level, Bmp specifies neural crest along the lateral edges of the neural plate (Nguyen et al., 1998; Tucker et al., 2007; Kwon et al., 2010). Tfap2a and Tfap2c help mediate both of these functions, but it is unknown whether Tfap2a/c are sufficient to mediate all aspects of early Bmp signaling. To test this, we used the pharmacological inhibitor dorsomorphin (DM) (Yu et al., 2008) to fully block Bmp from blastula stage onward and examined whether activating *hs:tfap2a* during gastrulation could rescue later development of PPE and neural crest. Incubation with DM alone (100-200 μM) blocks Bmp signaling immediately and completely, as shown

by complete loss phosph-Smad1/5 staining within 15 minutes (Kwon et al., 2010). Accordingly, treating embryos with 200μM DM treatment from 4 hpf (late blastula stage) caused complete dorsalization, such that neural plate markers such as *krox20* expanded throughout the DV axis (Fig. 3.7D) and markers of PPE (*six4.1,* and *dlx3b*), neural crest (*foxd3*), and epidermis (*p63*) were lost entirely (Fig. 3.7A-C, G). As expected, expression of *sizzled*, a direct feedback inhitor of Bmp signaling (Yabe et al., 2003), was also abolished by DM treatment (Fig. 3.7H). Activation of *hs:tfap2a* at 6 hpf in DM-treated embryos led to co-expression of *six4.1, dlx3b* and *foxd3* by the end of gastrulation (Fig. 3.7A-C) whereas expression of *p63* was not restored (Fig. 3.7G). Despite expression of general PPE markers *dlx3b* and *six4.1,* markers of discrete types of placodes (anterior placodes-*pitx3*, otic/epibranchial placodes-*pax8*, trigeminal and anterior lateral line placodes-*neurod*) were not expressed (Table 2). Additionally, activation of *hs:tfap2a* did not activate expression of *foxi1* or *gata3* in DM-treated embryos (Fig. 3.7E, F, Table 2). Thus, in the absence of Bmp signaling Tfap2a alone is sufficient to provide competence to form PPE and to specify neural crest but cannot activate the larger network of PPE competence factors nor support development of specific placodes.

Interestingly, PPE and neural crest markers induced by activation of *hs:tfap2a* were preferentially expressed on the ventral side of the embryo despite the complete abrogation of Bmp. This likely reflects the action of other factors known to regulate DV patterning. For example, *fgf3* and *fgf8* are still expressed in a DV gradient in DM-treated embryos (not shown), which could influence the ability to express PPE and NC markers.

It is also noteworthy that in *hs:tfap2a*-rescued embryos the domains of NC and PPE overlapped in the ventral ectoderm (compare Figs. 3.7A-C). However, under such conditions cells express one marker or the other, but not both (data not shown, and Kwon et al., 2010), indicating that cells with distinct fates are intermingled.

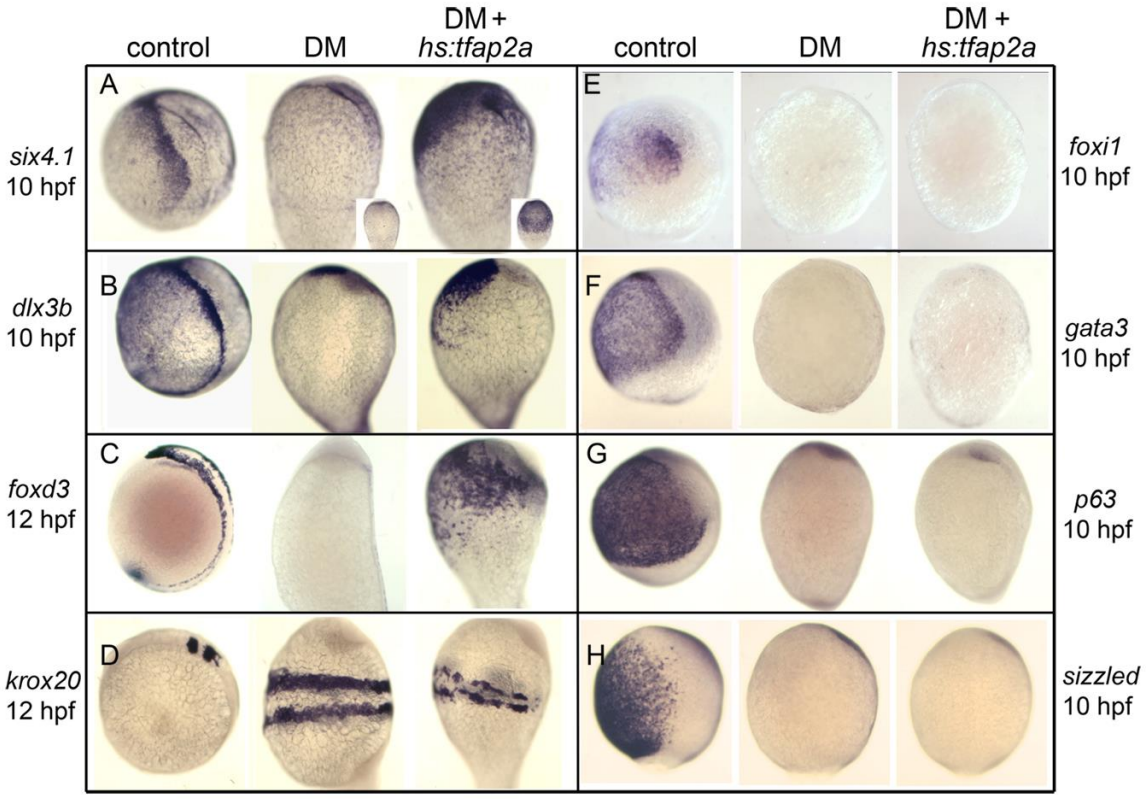

Figure 3.7: Misexpression of *tfap2a* rescues PPE and NC in Bmp-blocked embryos. Expression of PPE markers *six4.1,* (A) and *dlx3b* (B) at 10 hpf, NC marker *foxd3* at 12 hpf (C), neural plate marker *krox20* at 12 hpf (D), competence factors *foxi1* (E) and *gata3* (F) at 10 hpf, epidermal marker *p63* at 10 hpf (G) and Bmp-feedback inhibitor *sizzled* at 10 hpf (H) in control embryos, embryos treated with 200 µM DM from 4 hpf, or *hs:tfap2a*/+transgenic embryos treated with 200 µM DM from 4 hpf and heat shocked at 6 hpf. Images show lateral views with dorsal to the right and anterior up. Insets in (A) show ventral views of corresponding specimens. Misexpression of *tfap2a* in DM-treated embryos rescues PPE and NC markers while causing slight disruption in stripes of *krox20*, but does not restore expression of other competence factors, *p63* or *sizzled.*

Table 2: Effects of activating transgenes in DM-treated embryos.

	Transgenes activated at 6 hpf*					
Marker gene	*hs:foxi1*	*hs:gata3*	*hs:tfap2a*	*hs:foxi1*+ *hs:gata3*	*hs:foxi* + *hs:tfap2a*	*hs:gata3*+ *hs:tfap2a*
foxi1 10 hpf	n.d.	-	-	n.d.	n.d.	+
gata3 10 hpf	-	n.d.	-	n.d.	+	n.d.
tfap2a 10 hpf	+/-	+/-	n.d.	++	n.d.	n.d.
tfap2c 10 hpf	+/-	+/-	-	+	+	+
foxd3 11 hpf	+/-	+/-	+	++	++	++
dlx3b 11 hpf	+/-	+/-	+	++	++	++
six4.1, 11 hpf	-	-	+	+/-	++	++
pax8 11 hpf	+/-	-	-	+	+	+/-
neurod 14 hpf	-	-	-	+/-	+	+
pitx3 14 hpf	-	-	-	-	-	-

* Embryos were treated with 200 μM DM beginning at 4 hpf and the indicated transgenes were activated at 6 hpf. Data indicate very strong expression (++), moderate expression (+), weak scattered expression (+/-), or no expression detected (-). Observed patterns were fully penetrant ($n \geq 15$ embryos for each genotype). n.d., not determined.

We next tested whether other competence factors, alone or in combination, could restore the competence factor network or rescue placodal development in Bmp-blocked embryos. Activation of either *hs:foxi1* or *hs:gata3* in DM-treated embryos led to weak ventrally restricted expression of *tfap2a* and *tfap2c*, as well as *foxd3*, but induced little or no epxression of PPE or placodal markers (Table 2). Co-activation of *hs:foxi1* and *hs:gata3* had much stronger effects: This led to robust expression of *tfap2a*, *tfap2c*, and

foxd3, as well as *dlx3b* and *six4.1,* (Fig. 3.8A-D, Table 2) indicating activation of the competence factor network and support of both PPE and neural crest development. Under these conditions, cells expressing *dlx3b* or *foxd3* were observed in largely complementary clusters (Fig. 3.8E), again suggesting inermingled patterns of cells that adopt either PPE or neural crest fate. In addition to robust expression of general PPE markers, a band of strong *pax8* expression was also induced under these conditions (Fig. 3.8F), suggesting early stages of otic/epibranchial placode development. Weak expression of *neurod* expression (trigeminal and lateral line placodes) was also seen, although in a very sparse pattern (Fig. 3.8G, Table 2). Expression of *pitx3* (pituitary, olfactory, lens placodes) was not detected (Table 2).

Next, co-activation of *hs:foxi1* with *hs:tfap2a* led to moderate expression of *tfap2c* and *gata3* in the ventral ectoderm (Table 2), suggesting partial restoration of the competence factor network. Additionally, there was strong but scattered expression of *pax8* and *neurod* (Fig. 3.8F, G), indicating substantial rescue of posterior placodes. However, expression of *pitx3* (pituitary, olfacotry and lens placodes) was not detected. Co-activation of *hs:gata3* with *hs:tfap2a* led to moderate expression of *foxi1, tfap2c* and *neurod* (Fig. 3.8G and Table 2). In this case, however, *pax8* expression was observed in only a few cells in the ventral ectoderm (Fig. 3.8F). Together, these data indicate that although Bmp is normally required for inducing expression of competence factors,

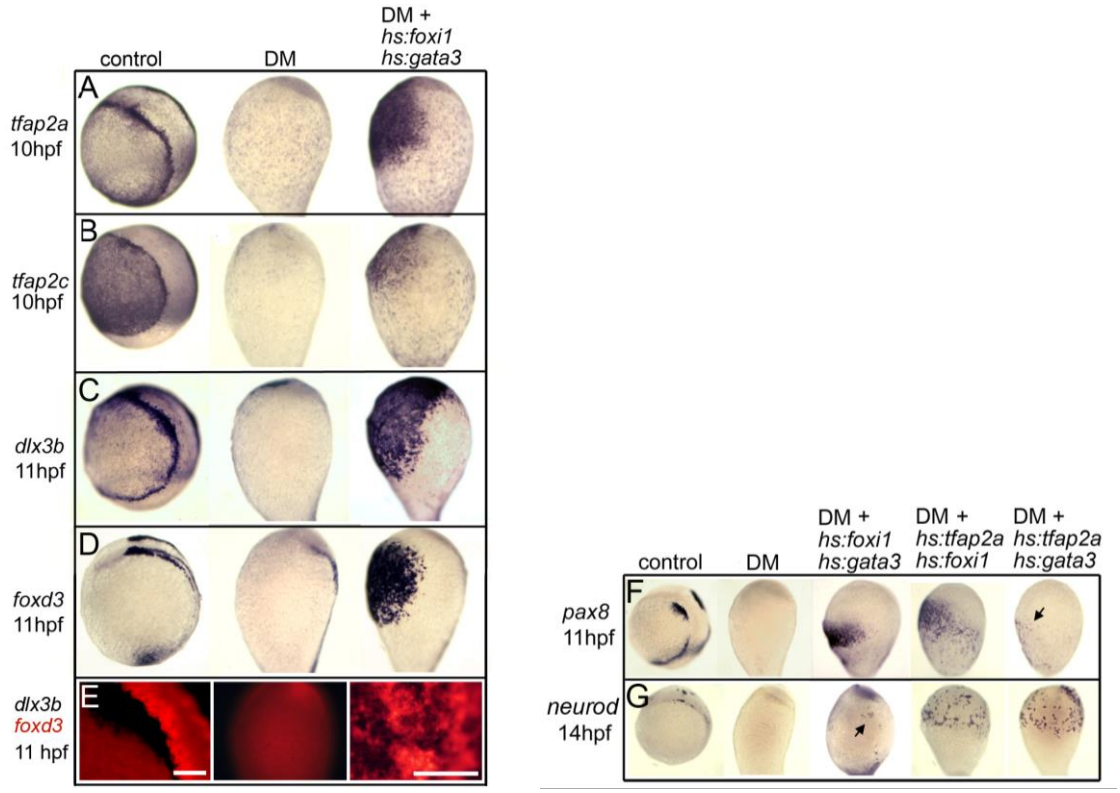

Figure 3.8: Effects of co-misexpressing pairs of competence factors in Bmp-blocked embryos. **A-E**, Expression of competence factors *tfap2a* (A) and *tfap2c* (B) at 10 hpf, PPE marker *dlx3b* at 11 hpf (C), NC marker *foxd3* at 11 hpf (D), and two-color in situ hybridization to visualize patterns of *dlx3b* and *foxd3* (E) in controls, embryos treated with 200 µM DM from 4 hpf, and *hs:foxi1/+; hs:gata3/+* transgenic embryos treated with 200 µM DM from 4 hpf and heat shocked at 6 hpf. All markers show rescue in DM-treated embryos following transgene activation. Two-color staining in (E) shows a dorsolateral view of the hindbrain area in a control embryo, a lateral view of a whole DM-treated embryo (dorsal to the right), and a close-up of the ventral midline of a rescued DM-treated transgenic embryo in which *dlx3b* and *foxd3* are expressed in intermingled, largely non-overlapping clumps of cells. Scale bars, 100 µm.

F, G, Expression of otic/epibranchial marker *pax8* at 11 hpf (F) and trigeminal/anterior lateral line marker *neurod* at 14 hpf (G) in control embryos, embryos treated with 200 µM DM from 4 hpf, or in embryos carrying the indicated combinations of transgenes treated with 200 µM DM from 4 hpf and heat shocked at 6 hpf. Arrows point to weak, scattered expression of *pax8* or *neuroD* in various backgrounds.

misexpressing any two factors in the absence of Bmp can cross-activate other components of the network and, to varying degrees, restore the expression of markers of specific placodes.

DISCUSSION

We have shown that Tfap2a, Tfap2c, Foxi1 and Gata3 together form a self-maintaining gene regulatory network during gastrulation that fosters competence to form PPE and, in addition, Tfap2a and Tfap2c simultaneously coordinate specification of neural crest along the edges of the neural plate. Robustness of the PPE network arises from mutual cross-activation between its members, and Tfap2a also activates its own expression. The network is also self-limiting because Foxi1 and Gata3 each show auto-repression, thereby preventing unrestrained feedback amplification and assuring maintenance of a proper level of expression in the face of changing signaling interactions that occur during gastrulation. Although competence factors are initially induced by Bmp the network later functions independently of Bmp. Moreover, misexpressing individual competence factors can bypass the need for Bmp. In embryos treated with DM to block all Bmp signaling, the neural plate expands around the entire circumference of the embryo, eliminating NC, PPE and epidermal ectoderm. Activation of *hs:tfap2a* in DM-treated embryos restores both PPE and NC markers but cannot activate the rest of the preplacodal competence network nor support formation of individual placodes. Misexpression of any two PPE competence factors restores the entire competence network and supports formation of NC, PPE and posterior placodes. Epidermal

ectoderm is not rescued, confirming that this fate is regulated independently (Kwon et al., 2010). After PPE formation, the full suite of competence factors must be maintained to support subsequent formation of individual placodes. Foxi1 and Gata3 play indispensible roles in development of posterior placodes whereas Tfap2a/c are required for achieving sufficient levels of Foxi1, Gata3, and general PPE markers needed for all cranial placodes. These findings extend our previous studies and have important implications for competing models of NC and PPE formation.

Models for coordinating NC and PPE formation

There are currently two competing models for specification of NC vs. PPE. In the "neural border" model, cells lining the neural-nonneural border are initially specified as a distinct zone of common progenitors through early interactions between dorsal and ventral tissues. The NB later subdivides to form NC and PPE in abutting domains depending on differential exposure to Bmp and Wnt (Streit and Stern, 1999; Baker and Bronner-Fraser, 2001; McLarren et al., 2003; Woda et al., 2003; Brugmann et al., 2004; Glavic et al., 2004; Litsiou et al., 2005; Patthey et al., 2008; Patthey et al., 2009; de Crozé et al., 2011; Steventon and Mayor, 2012). In the "binary competence" model, neural and nonneural ectoderm are specified early by a gradient of Bmp, with the former harboring neural and NC progenitors and the latter epidermal and PPE progenitors, respectively (Schlosser, 2010; Pieper et al., 2012). That is, PPE and NC potentials are separated quite early, with no intermediate state or stage common to both fates. The data presented here contain aspects consistent with both models, although many of our

overall findings are more generally compatible with the binary competence model. Most notably, we reported previously that PPE and NC are specified at different times by different mechanisms (Kwon et al., 2010). NC is specified during late blastula/early gastrula stage by a discrete low level of Bmp (Nguyen et al., 1998; Tucker et al., 2007; Kwon et al., 2010). Conditions that appropriately flatten the Bmp gradient can expand the NC domain to cover the entire ventral half of the ectoderm. In this context, Bmp serves only to induce expression of *tfap2a* and *tfap2c* along the edges of the neural plate; afterwards Bmp is no longer required (Kwon et al., 2010), in sharp contrast to predictions of the neural border model. Unlike NC, PPE is specified later and has two successive steps with opposing Bmp requirements such that no single dose of Bmp can expand PPE fates in a manner similar to NC. Initially, high Bmp levels act in late blastula stage to establish preplacodal competence throughout the nonneural ectoderm, mediated by the overlap of Tfap2a/c, Foxi1 and Gata3 (Kwon et al., 2010). Second, overt specification of PPE occurs near the end of gastrulation and requires stringent attenuation of Bmp by signals from dorsal tissue, including Fgf and Bmp-antagonists (Kwon et al., 2010). Misexpression of Fgf8 and Chordin can induce ectopic PPE anywhere within the nonneural ectoderm without co-inducing neural plate or NC (Ahrens and Schlosser, 2005; Kwon et al., 2010). Moreover, when Fgf8 and Chordin are co-misexpressed during late gastrulation, ectopic PPE markers appear quite rapidly thereafter (Kwon et al., 2010), suggesting that ventral ectoderm can develop directly into PPE without first passing through a discrete neural border stage. On the other hand, expression of *tfap2a* and *tfap2c* encompass both PPE and NC domains, providing a

mechanistic link between these fates. Accordingly, disruption of *tfap2a/c* ablates neural crest and diminishes, though does not eliminate, PPE (Hoffman et al., 2007; Li and Cornell, 2007; Kwon et al., 2010). This shared early requirement is more consistent with the neural border model. Additionally, misexpression of PPE competence factors in the neural plate (Kwon et al., 2010), or in embryos dorsalized by blocking Bmp (Figs. 7 and 8), result in overlapping domains of PPE and NC. Such patterns reflect intermixing of cells expressing one fate or the other, but not both (Fig. 8E, and Kwon et al., 2010). It is not clear how the two fates are diversified under these conditions since all cells likely experience similar global signals. However, these data do suggest a close kinship between PPE and NC, as predicted by the neural border model. How these data are viewed depends on the relative importance ascribed to initial expression patterns of various regulatory genes, the context in which they act, and whether they specify cell fate directly or merely confer potential.

CHAPTER IV

INTEGRIN-α5 COORDINATES ASSEMBLY OF POSTERIOR CRANIAL PLACODES IN ZEBRAFISH AND ENHANCES FGF-DEPENDENT PATTERNING AND SURVIVAL IN OTIC/EPIBRANCHIAL CELLS*

INTRODUCTION

Development of cranial sensory organs in vertebrates requires essential contributions from transient embryonic structures termed cranial placodes. Cranial placodes form during early segmentation stages as a series of epithelial thickenings adjacent to developing brain tissue (McCabe and Bronner-Fraser, 2009; Schlosser, 2010). The anterior-most placodes produce the anterior pituitary, olfactory epithelium, and the lens of the eye. Amongst more posterior placodes, the otic placode produces the entire inner ear, including the complex epithelial labyrinth, internal sensory epithelia, and all of its innervating neurons; and trigeminal and epibranchial placodes produce a segmental array of sensory ganglia that innervate much of the craniofacial and pharyngeal apparatus. Despite their morphological and functional diversity, all cranial placodes arise from a common domain of preplacodal ectoderm that forms earlier around the anterior neural plate (Schlosser, 2010; Streit, 2007). Specification of preplacodal ectoderm involves a sequence of signaling interactions that occur during blastula and gastrula stages, culminating in expression of a characteristic set of transcription factor

---

*Reprinted from open access article "Integrin-α5 Coordinates Assembly of Posterior Cranial Placodes in Zebrafish and Enhances Fgf-Dependent Regulation of Otic/Epibranchial **Cells"** by**, Bhat., N., Riley B. B**., PLoS One 6, e27778.

genes near the end of gastrulation (Ahrens and Schlosser, 2005; Brugmann et al., 2004; Glavic et al., 2004; Kwon et al., 2010; Litsiou et al., 2005). This contiguous domain of gene expression subsequently breaks into discrete clusters of cells that generate the various diverse placodes.

Lineage studies in zebrafish and chick indicate that resolution of preplacodal ectoderm into discrete placodes requires active cell migration and rearrangement. For example, precursors of the anterior pituitary, olfactory and lens placodes are initially intermixed but subsequently sort out to form their respective placodes (Bhattacharyya et al., 2004; Dutta et al., 2005; Toro and Varga, 207; Whitlock and Westerfield, 2000). In the case of the olfactory placode, precursors converge into a compact placode via chemotaxis mediated by the Sdf1-Cxcr4 chemokine signaling pathway (Miyasaka et al., 2007). Similarly, trigeminal precursors are initially widely scattered but then undergo Sdf1/Cxcr4-dependent chemotaxis to converge into a coherent placode (Knaut et al., 2005). Less is known about the otic and epibranchial placodes, which in zebrafish form in rapid succession from a broad field of contiguous gene expression that includes *pax8*, *pax2a* and *sox3* (Nikaido et al., 2007; Sun et al., 2007). The otic domain forms first and induces epibranchial development in more lateral cells (Padanad and Riley, 2011). The otic/epibranchial gene expression domain then undergoes marked contraction as the respective placodes coalesce, suggesting active cell migration and convergence. However, there have been no systematic studies of cell migration associated with formation of otic and epibranchial placodes. It is possible that directed cell migration is

a general feature common to all placodes, in which case it will be important to identify factors that coordinate these morphogenetic movements.

Directed cell migration often involves navigation along specific ECM domains, attachment to which requires cellular Integrins. Integrins comprise α/β transmembrane heterodimers that bind Fibronectin or Laminin in the ECM to coordinate cell attachment, migration, differentiation and survival (Chodniewicz and Klemke, 2004; Gilcrease, 2007; Hehlgans et al., 2007; Petrie et al., 2009). Integrin-ECM binding triggers several signal transduction pathways, including Ras-MAPK and PI3K signaling, to regulate rapid reorganization of the actin cytoskeleton as well as changes in gene expression. In zebrafish, *integrin-α5* (*itga5*) has been shown to regulate a number of early developmental processes, including formation of regular somite boundaries and proper differentiation of cranial neural crest (Crump et al., 2004; Jülich et al., 2005; Koshida et al., 2005). Expression is initially widespread, but near the end of gastrulation *itga5* is restricted primarily to preplacodal ectoderm (Crump et al., 2004). However, there have been no studies of the role of *itga5* in development of preplacodal ectoderm or its derivatives. Here we investigate the role of *itga5* in morphogenesis of cranial placodes in zebrafish. Both *itga5* morphants and *itga5* mutant, b926, which have a missense mutation in fibronectin binding domain, showed no discernable change in development of anterior placodes, but posterior placodes showed a number of developmental defects resulting in disorganization of trigeminal and epibranchial ganglia and significant reduction in the size of the otic placode/otic vesicle. To examine cell migration patterns, time lapse movies were taken of transgenic embryos expressing *pax2a:GFP*

(otic/epibranchial precursors) and *neuroD:EGFP* (trigeminal precursors). Analysis of control (non-morphant) embryos showed that the otic/epibranchial and trigeminal domains normally coalesce by highly focused convergence of cells from within their respective fields. Furthermore, new cells continued to enter the *pax2a:GFP* expression domain from more lateral regions in a process of ongoing recruitment. In *itga5* morphants, cell migration was erratic and unfocused, causing inefficient convergence, redistribution of distal pre-otic cells into epibranchial regions, and failure of recruitment of new cells. Additionally, cells in the otic/epibranchial domain showed a significantly elevated rate of apoptosis, limiting the increase in epibranchial cells and exacerbating the deficiency of otic cells. Further studies revealed strong genetic interactions between *itga5* and Fgf. For example, the cell death defect was rescued by misexpressing Fgf8. Furthermore, *itga5* morphants showed changes in gene expression that mimic the effects of reducing Fgf signaling; and knockdown of the Fgf-mediator *erm*, which normally causes no overt defects by itself, significantly enhanced the defects in *itga5* morphants. Finally, we showed that proper expression of *itga5* requires *dlx3b*, *dlx4b* and *pax8*, which are regulated by Fgf. These data support a model in which *itga5* coordinates directed cell migration into posterior placodes and also augments Fgf signaling to promote cell survival and tissue patterning within the otic/epibranchial domain.

MATERIALS AND METHODS

Strains

Control embryos were derived from the AB line (Eugene, OR). We used transgenic lines *Tg(pax2a:GFP)*^{e1} (Picker et al., 2002), *Tg(neuroD:EGFP)*^{nl1} (Obholzer et al., 2008) and *Tg(hsp70:fgf8)*^{x17} (Millimaki et al., 2010).

In-situ hybrization and immunostaining

In-situ hybridization was performed as described in (Phillips et al., 2001). Primary antibodies were used for Isl-1 (Hybridoma Bank, 1:100), Caspase3 (R&D Systems, 1:100) and GFP (Santa Cruz Biotechnology, 1:250). Secondary antibodies were HRP-conjugated anti-mouse (Vector Labs, 1:200) and Alexa-conjugated anti-mouse and anti-rabbit (Invitrogen, 1:50).

Morpholino injections

Morpholino sequences for *itga5*, *dlx3b*, *dlx4b* and *pax8* have been previously described and tested (Jülich et al., 2005; Mackereth et. al 2005; Solomon and Fritz 2002). For *erm* knockdown we used erm-MO 5'-CTTGCTGGTCATAAAACCCATCCAT-3', which is nearly identical to *etv5/erm*-MO described previously (Znosko et al., 2010). Embryos were injected at the one-cell stage with 5 ng each of the indicated MOs.

RFP misexpression

CMV:RFP plasmid was injected into one-cell stage embryos at a concentration of 75ng/ul to give mosaic expression of RFP.

Time lapse imaging

Embryos were mounted on glass slides in drops of 0.8% low-gel agarose surrounded by plastic frame. After mounting, embryos were hydrated and coverslips were affixed with petroleum jelly. Embryos were imaged for time-lapse using a Zeiss Axioimager2-ApoTome. Fluorescent images were taken every 3 minutes using Axiovision 4.6.3 software.

Cell tracking and vector maps

To correct for inadvertent movement of the embryo during recording, GFP expression in rhombomeres 3 and 5 was used to provide a fixed reference in each frame. ImageJ software was used to manually track individual cells. Tracks were then projected onto representational maps using Photoshop. Calculations for displacement, total distance and the angle for each vector were calculated using ImageJ software.

Cell transplantation

Tg(CMV:rfp) transgenic embryos were coinjected with 100ng/nl cmv:rfp plasmid DNA and *itga5* morpholino or just plasmid DNA and used as donors. pax2a:gfp transgenic animals were used as hosts to visualize the otic/epibranchial domain. After screening

through the hosts at around 10-11hpf, animals with cells in the otic/epibranchial domain were selected for time-lapse imaging.

RESULTS

itga5 is required for proper development of posterior placodes

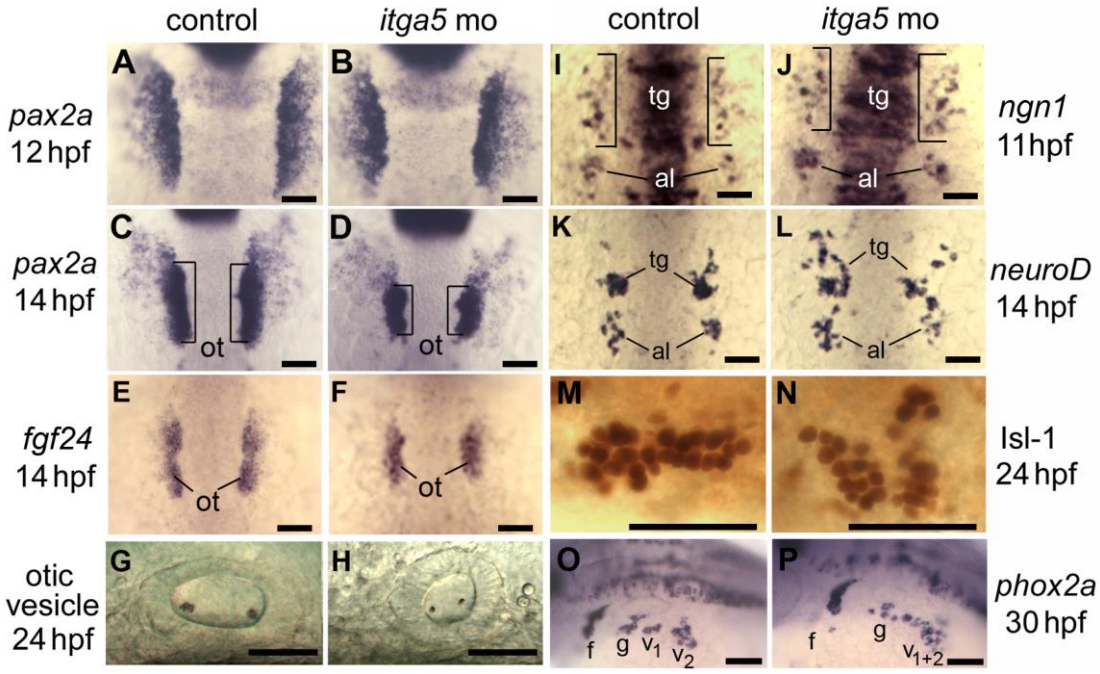

Figure 4.1: Knockdown of *itga5* impairs morphogenesis of posterior cranial placodes. (**A–D**) *pax2a* expression at 12 and 14 hpf in the otic/epibranchial domain in control embryos (A, C) and *itga5* morphants (B, D). Expression is normal at 12 hpf in *itga5* morphants but the otic placode (o, brackets) is smaller than normal by 14 hpf. (**E, F**) *fgf24* expression at 14 hpf in a control embryo (E) and *itga5* morphant (F). (**G, H**) Otic vesicles at 24hpf in a control embryo (G) and *itga5* morphant (H). (**I, J**) *ngn1* expression at 11 hpf in a control embryo (I) and *itga5* morphant (J). (**K, L**) *neuroD* expression at 14 hpf in a control embryo (K) and *itga5* morphant (L). Precursors of the trigeminal ganglion (tg) and anterior lateral line (al) are indicated. (**M, N**) Anti-Isl-1 immunostaining at 24 hpf in a control embryo (M) and *itga5* morphant (N). (**O, P**) *phox2a* expression in epibranchial ganglia at 30 hpf in a control embryo (O) and *itga5* morphant (P). Facial (f), glossopharyngeal (g), and vagal ganglia (v1+v2) are indicated. A–E, I–K are dorsal views with anterior to the top; G, H, M–P are lateral views with anterior to the left. Scale bar, 50 μm.

itga5 is required for proper development of posterior placodes. *itga5* is expressed in preplacodal ectoderm by 10 hpf (Crump et al., 2004). We hypothesized that *itga5* regulates morphogenetic movements associated with formation of discrete cranial placodes. To test this idea, we used *itga5* mutant, b926, and translation-blocking morpholino against *itga5* and monitored subsequent placodal development. We observed no changes in development of anterior placodes, including the anterior pituitary, olfactory, and lens placodes, judging by morphology and early expression of pitx3, cxcr4b and foxe3, respectively (data not shown). In sharp contrast, posterior placodes, including the trigeminal, otic and epibranchial placodes, showed a variety of developmental defects. In control embryos, *pax2a* is strongly expressed at 12 hpf in otic cells, with weaker expression in otic/epibranchial precursors just lateral to the otic domain (Fig. 4.1A). The otic cells then appear to undergo marked convergence by 14 hpf to form a morphologically visible otic placode and the weakly expressing non-otic *pax2a* cells get segregated from the otic precursors (Figs. 4.1C, See Fig. 4.3). In *itga5* morphants as well as in the mutants, the initial otic/epibranchial domain of pax2a was normal at 12 hpf (Fig 4.1B). However, the otic placode appeared smaller than normal by 14 hpf (Fig 4.1D), and the otic vesicle was similarly reduced in size at 24 hpf (Fig. 4.1F, 4.2A,B) in both *itga5* morphants and *b926* mutants. *b926* mutants have a point mutation in the critical residue responsible for ligand binding. Epibranchial ganglia, marked by expression of phox2a (Lee et al., 2003), were highly disorganized in *itga5* morphants and *b926* mutants, though it is unclear whether the amount of epibranchial tissue was altered (Compare Figs. 4.1G,F). Early development of trigeminal placodes

was monitored by expression of *ngn1*, which is initially seen in scattered cells by 11 hpf in control embryos (not shown). Subsequently, trigeminal cells converge to form

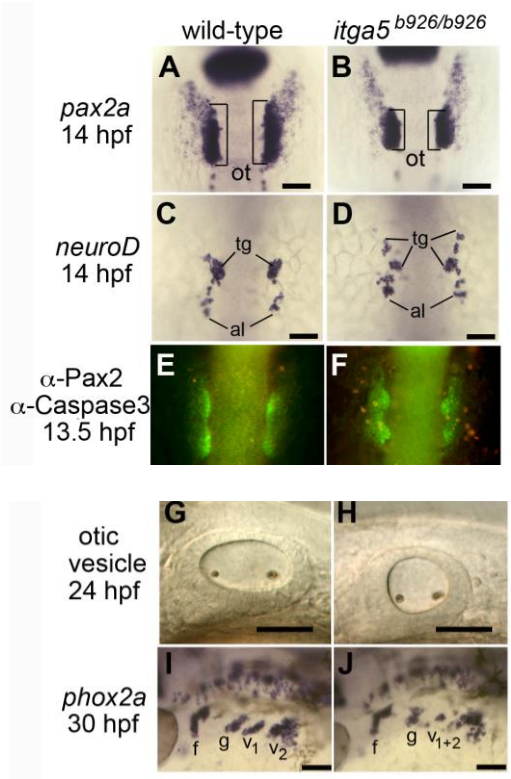

Figure 4.2: Abnormal development of posterior placodes in *itga5*$^{b926/b926}$ mutants. (**A, B**) *pax2a* expression at 14 hpf in the otic/epibranchial domain in a wild-type embryo (A) and *itga5* mutant (B). Otic placodes (o, brackets) are indicated. (**C, D**) *neuroD* expression at 14 hpf in a control embryo (C) and *itga5* morphant (D). Precursors of the trigeminal ganglion (tg) and anterior lateral line (al) are indicated. (**E, F**) Immunolocalization of Pax2 (green) and Caspase 3 (red) in a wild-type embryo (E) and *itga5* mutant (F). (**G, H**) Otic vesicles at 24hpf in a wild-type embryo (G) and *itga5* mutant (H). (**I, J**) *phox2a* expression in epibranchial ganglia at 30 hpf in a wild-type embryo (I) and *itga5* mutant (J). Facial (f), glossopharyngeal (g), and vagal ganglia (v1+v2) are indicated. A–E are dorsal views with anterior to the top; G–J are lateral views with anterior to the left. Scale bar, 50 μm.

compact ganglia by 14 hpf (Andermann et a., 2002; Knaut et al., 2005), as shown by neuroD expression (Fig. 4.1I). In *itga5* morphants and *b926* mutants, *ngn1* expression was normal at 11 hpf (data not shown) but neuroD staining at 14 hpf revealed that trigeminal cells were still scattered and disorganized (Fig. 4.1J, Fig 4.2). Anti-Islet1/2 staining at 24 hpf showed that trigeminal ganglia persisted as disorganized clusters in itga5 morphants (Fig. 4.1L). In summary, disruption of *itga5* does not alter initial placodal development but impairs assembly of trigeminal, otic and epibranchial placodes after their induction.

Morphogenesis of the otic/epibranchial domain

We hypothesized that the abnormal development of posterior placodes seen in *itga5* morphants arose in part through defective cell migration. To test this, we tracked cell movements in time-lapse movies using transgenic backgrounds in which precursor cells were labeled with GFP. To monitor otic/epibranchial morphogenesis, we used a *pax2a:GFP* transgenic line that recapitulates the expression of endogenous *pax2a* in the otic/epibranchial domain and midbrain-hindbrain border (Picker et al., 2002). Additionally, the *pax2a:GFP* line shows ectopic expression in rhombomeres 3 and 5 of hindbrain, providing a convenient spatial marker to help gauge positions of individual cells. In pilot studies we found it was often difficult to track individual cells for several hours within the multi-layered otic placode. To enhance cell-discrimination, we injected transgenic embryos with plasmid DNA to express RFP mosaically, permitting independent tracking of RFP and GFP in individual cells (see Materials and

Methods). Embryos were recorded in time-lapse from 11.5 hpf to14.5 hpf. An example of early and late frames of a movie of a control embryo (Movie1) is shown in Fig. 4.3A,B. Tracks of RFP-labeled cells in the same specimen are summarized in Fig . 4.3E. Most cells migrated in a relatively straight line to contribute to the otic placode, with little deviation in the angle of migration. Similar patterns were documented in a total of five control embryos. The net displacement of all RFP-positive cells (n=42) tracked in these five embryos is represented in Fig. 3F. To assess typical cell behaviors in different regions, we divided the *pax2a:GFP* domain into quadrants along the anteroposterior axis and calculated the mean net displacement and the range of the angle of displacement for cells in each quadrant (Fig. 4.3G). Several conclusions regarding patterns of migration emerged from this analysis. First, cells beginning near the medial edge of the *pax2a:GFP* domain usually migrated only short distances to build up this part of the otic placode, whereas cells in more lateral positions migrated much longer distances with a predominant medial vector. Second, in addition to a general medial migration, there was also a marked centripetal convergence into the otic placode from the broader field of GFP-positive cells. That is, many cells in the anterior end of the field showed a posterior trajectory while cells in the posterior showed an anterior trajectory. Third, a few labeled cells in the first and second quadrants did not contribute to the otic placode but instead migrated to the position just anterior of the otic placode. Similarly, not all cells in the posterior pax2a field contribute to the otic placode (See Figure 4.4). As compared to the otic cells in the first

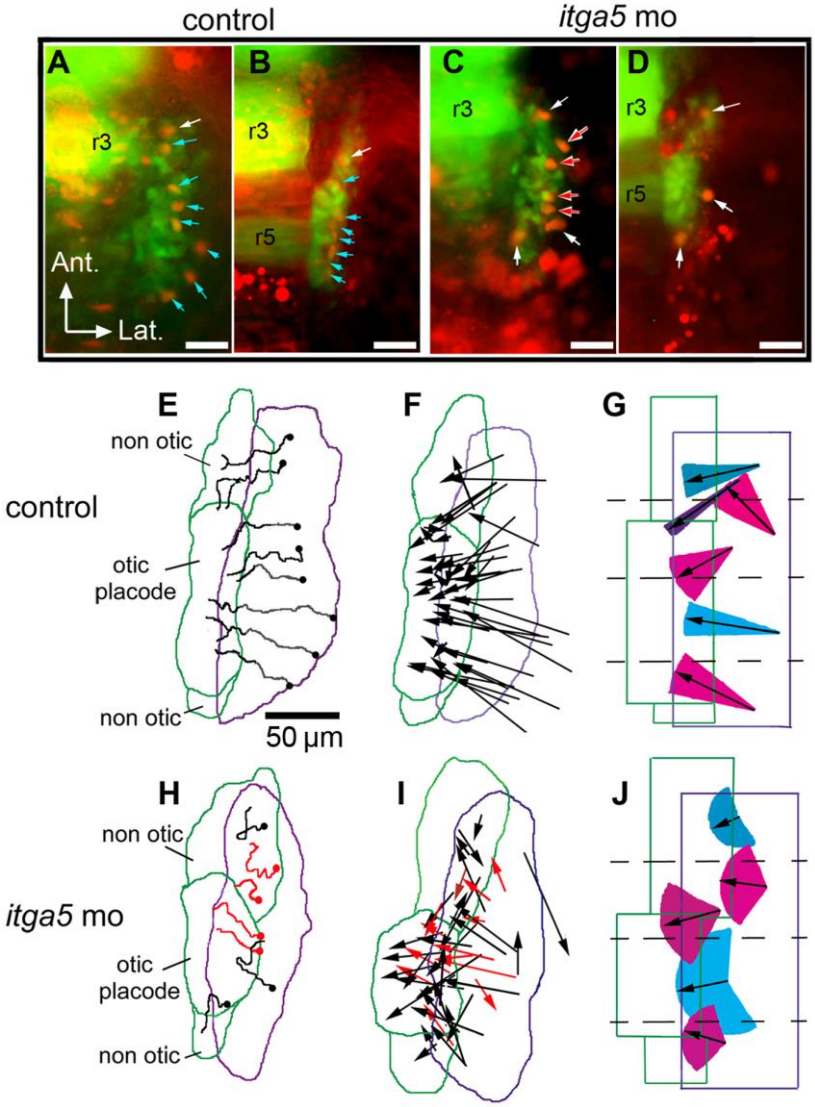

Figure 4.3: Otic/epibranchial precursors show aberrant migration in *itga5* morphants. (**A–D**) Images from time-lapse movies showing transgenic expression of *pax2a:GFP* (green) and mosaic expression of *cmv:RFP* (red). The first frame (11.5 hpf) and final frame (14.5 hpf) of a control movie (A, B) and *itga5* morphant movie (C, D) are shown. Arrows indicate cells that expressed both GFP and RFP. Blue arrows indicate cells that contributed to the otic domain, and white arrows indicate cells that contributed to non-otic domains. Red arrows indicate cells that lysed during the recording period (C, D). Positions of rhombomeres 3 and 5 (r3, r5) are indicated. (**E, H**) Maps showing the trajectories of all marked cells in the embryos recorded in A–D. Trajectories in red denote cells that lysed during recording (H). The origins of cell trajectories are marked with dots. The initial and final positions of the *pax2a:GFP* domain are indicated by purple and green boundaries, respectively. Final positions of the otic placode and non-otic domains are indicated. (**F, I**) Vector maps showing net displacement of all cells tracked in 5 control movies (F) and 4 *itga5* morphant movies (I). Red arrows indicate cells that died during recording (I). (**G, J**) Summaries of average migration patterns of cells in different quadrants of the *pax2a:GFP* domain in control embryos (G) and *itga5* morphants (J). Arrow length indicates the mean of the net displacement of cells in the indicated region, and colored cones represent the range of angle of net displacement. Quadrants 1 and 2 contained cells contributing to both otic and non-otic domains, which were grouped separately. All images depict the right half of the embryo with lateral to the right and anterior to the top. Scale bar, 50um.

and second quadrant which have the net angle of displacement vector directed more posteriorly, the non-otic have net angle of displacement directed more anteriorly. This suggests that they don't respond to the same cues as the otic cells. The anterior and posterior non-otic domains of *pax2a:GFP* contribute predominantly to epibranchial ganglia (unpublished observations). The anterior and posterior non-otic domains of *pax2a:GFP* contribute predominantly to epibranchial ganglia based on the loss of this domain in *pax8-sox3* double morphants and laser ablation studies (data not shown). Also, the overlap between *pax2a:GFP* and *neuroD:EGFP* suggests that anterior non-otic domain also contains precursors of the anterior lateral line (data not shown). Fourth, we observed numerous cases in which GFP-negative cells neighboring the *pax2a:GFP* domain subsequently entered the domain and became GFP-positive. Indeed, 29% of tracked cells (12/42 cells in five embryos) exhibited this pattern. Presumably these cells were induced to express *pax2a* once they migrated into range of inductive Fgf signaling, reflecting a process of ongoing recruitment (Figure 4.4).

Morphogenesis in *itga5* morphants

Recordings of *itga5* morphants revealed a number of striking differences from control embryos. First, cells in *itga5* morphants showed much more erratic migration patterns, with frequent changes in direction (Fig. 4.3H-J, Movie2). Although the total distance traveled was comparable to that seen in control embryos, the meandering course of cell migration in *itga5* morphants resulted in a marked reduction in net displacement (the straight-line distance from start to finish). Accordingly, the mean efficiency of

migration (net displacement/total distance) was only .49±.15 in *itga5* morphants compared to .71±.08 in control embryos (Fig. 4.3I; Table 3). Moreover, the range in angle of net displacement was much greater in all quadrants in *itga5* morphants (Fig. 4.3J). Second, inefficient cell migration led to aberrant partitioning of the *pax2a:GFP* domain in *itga5* morphants. Specifically, no cells from the first quadrant (0/6), and fewer than half of cells from the second quadrant (6/13), migrated into the otic placode (Fig. 4.3 I,J). This is in contrast to control embryos in which half (3/6) of cells in the first quadrant and 82% (9/11) of cells in the second quadrant converged into the otic placode (Fig. 4.3 F,G). Consequently, *itga5* morphants formed a smaller otic placode and a correspondingly enlarged anterior domain of non-otic cells. Third, we observed no examples of recruitment of neighboring cells into the *pax2a:GFP* domain in *itga5* morphants. That is, all cells tracked in *itga5* morphants (43/43 cells in 4 embryos) were both RFP-positive and GFP-positive throughout the recording period, whereas no neighboring RFP-positive cells were observed to enter the *pax2a:GFP* domain and become GFP-positive. However, using this approach it is not possible to track every single cell in the control and the morphant. Therefore, recruitment may be happening in *itga5* morphants but it is at a reduced level. Finally, unlike control embryos, *itga5* morphants showed a striking incidence of cell-lysis within the *pax2a:GFP* domain. For example, 12/43 (27%) of RFP-positive cells tracked in *itga5* morphants lysed during the course of recording (Fig. 4.3 C,D,H,I), whereas none of the 42 cells tracked in control embryos were observed to lyse (Fig. 4.3 F). In contrast, we detected no consistent changes in the rate of cell division in *itga5* morphants compared to controls based on the

pattern of BrdU incorporation (data not shown). Together these data show that *itga5* is required for normal migration and survival of cells in the otic/epibranchial domain. In

Table 3: Knockdown of *itga5* impairs the efficiency of directed cell migration.

Transgenic marker	Experimental condition	Net displacement (μm)±SD	Total distance (μm)±SD	Efficiency of migration (net/ total μm)±SD
pax2a:gfp (otic/epibranchial)	control	49.4±17.0	68.7±22.5	0.71±0.08
	*itga5*mo	32.1±12.5†	64.9±24.9†	0.49±0.15†
	*itga5*mo + *hs:fgf8*	28.8±11.3†	61.0±8.9†	0.46±0.17†
pax2a:gfp (otic/epibranchial)	control-mosaic*	54.9±11.1	68.8±13.4	0.79±0.04
	*itga5*mo-mosaic*	28.3±13.3†	71.0±19.3	0.40±0.17†
neuroD:gfp (trigeminal)	control	56.6±9.1	76.8±10.5	0.74±0.06
	*itga5*mo	44.4±17.0†	97.7±27.3†	0.45±0.13†
	*itga5*mo + *hs:fgf8*	35.9±21.2†	61.4±19.4†	0.54±0.20†
non-placodal cells	control	54.7±12.3	70.7±14.6	0.76±0.02
	*itga5*mo	40.4±6.2	61.3±11.4	0.66±0.10

* Indicates genotype of RFP-labeled cells transplanted into *pax2a:gfp* host embryo.
† Significantly different from control value based on t-test.

the absence of *itga5*, the otic placode is reduced in size by a combination of inefficient convergence, increased cell death, and faulty recruitment of new cells into the *pax2a* domain.

Retrospective tracking of epibranchial precursors

Although the above data provided detailed information about the otic placode, random RFP-labeling marked few cells in the non-otic domains (5/42 in control embryos, Fig. 4.3 F). However, we were able to track additional cells in the non-otic domain back to their origins based solely on GFP expression. Cells tracked in this way showed migration patterns consistent with those previously tracked by RFP-labeling (Fig. 4.4A). The majority of cells contributing to the anterior non-otic domain converged from the regions adjacent to the first two quadrants whereas all cells in the posterior domain converged from the fourth quadrant (Fig. 4.4 B). Surprisingly, the majority (15/19) of these cells originated from lateral regions well outside the domain of contiguous *pax2a:GFP* expression, first appearing as sparsely scattered GFP-positive cells before migrating into the non-otic domains (Fig. 4.4 A,B). Moreover, in keeping with their extreme lateral origins, these cells were recruited relatively late during the recording period. Whereas recruitment of otic cells usually occurred by 12 hpf (range, 11.7-12.5 hpf), recruitment of non-otic cells occurred around 12.7 hpf (range, 12.5-13.2 hpf). This is consistent with our previous findings that otic cells are specified earlier and, through upregulation of *fgf24*, subsequently induce epibranchial precursors from adjacent tissue (Padanad and Riley, 2011).

In *itga5* morphants, cell migration was highly erratic and the majority (24/27) of non-otic cells originated from within the contiguous domain of *pax2a:GFP* expression (Fig. 4.4 C,D). Additionally, both anterior and posterior non-otic domains were enlarged at the expense of the otic placode. Despite these abnormalities, the general mechanism

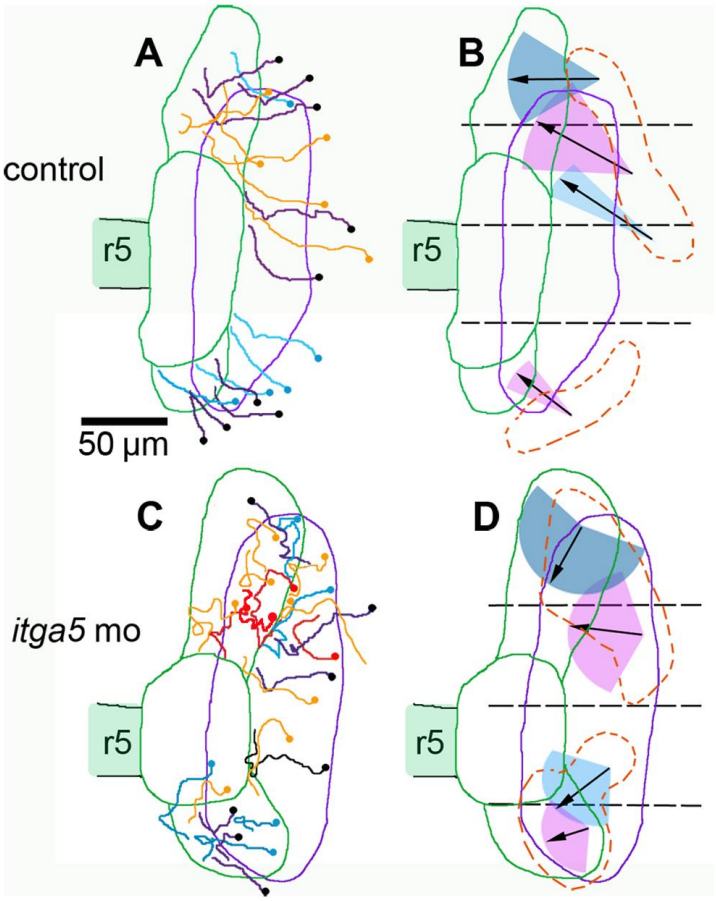

Figure 4.4: Trajectories of non-otic cells tracked in reverse. (**A, C**) Maps showing the trajectories of GFP positive cells pooled from the time-lapse movies in Fig. 3 of control embryos (A) and *itga5* morphants (C). Trajectories in orange indicate cells originally tracked by coexpression of GFP and RFP. All other trajectories represent cells tracked retrospectively by GFP alone. Dots indicate origins of tracked cells. Trajectories in red denote cells that died during recording (C). (**B, D**) Summaries of average migration patterns on non-otic cells in different quadrants in control embryos (B) and *itga5* morphants (D). The mean length of net displacement (arrows) and range of angle of net displacement (colored cones) are indicated. The dashed orange lines indicate regions from which non-otic cells originated. Initial and final positions of the *pax2a:GFP* domain are represented by the purple and green boundaries, respectively. The position of rhombomere 5 (r5) is indicated. Lateral is to the right and anterior is to the top. Scale bar, 50 µm.

of sequential induction of epibranchial precursors was found to operate relatively normally in *itga5* morphants based on expression of *fgf24* (not shown) and *sox3* (see below). Note we did not observe cell lysis amongst retrospectively tracked cells because this technique focused solely on cells that survived until the end of the recording period. Together, these data confirmed that *itga5* is required for normal migration and survival cells contributing to non-otic domains.

Cell autonomous requirement for *itga5* function

To examine whether the defect in morphogenesis of otic/epibranchial precursors is a direct effect of *itga5* knockdown, we transplanted *itga5* morphant cells into wild-type embryos and tracked their migration using time-lapse imaging from 11.5–14.5 hpf. As in non-mosaic *itga5* morphants, migration of isolated *itga5*-MO cells in wild-type host embryos was highly erratic (Fig. 4.5), with a migration efficiency of only 0.44±0.03 (n = 16; Table 3). Additionally, 19% of the tracked cells (n = 3/16) lysed during recording. In contrast, when wild-type cells were transplanted into wild-type hosts, migration efficiency was 0.71±0.08 (n = 7) and no cell lysis was detected. These data show that *itga5* is required cell autonomously for proper migration and survival of cells in the otic/epibranchial domain.

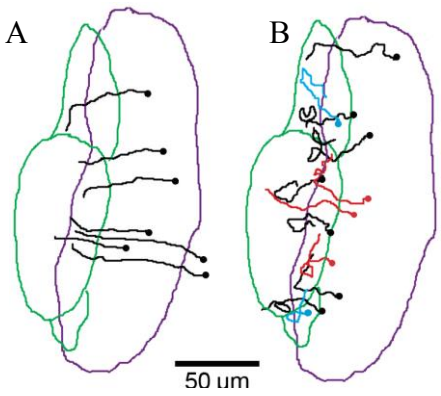

Figure 4.5: Cell-autonomous requirement for Itga5 in otic/epibranchial cells. (**A**) Trajectories of cells transplanted from a wild type donor into a wild type host and tracked by time-lapse from 11.5–14.5 hpf. Data show tracks of 7 cells from a single embryo. (**B**) Trajectories of cells transplanted from *itga5* morphant donors into wild type host embryos and tracked by time-lapse from 11.5–14.5 hpf. A total of 16 cells from 3 embryos were tracked, though some were not included on the map to avoid confusion. Red tracks represent cells that underwent lysis during the time-lapse. The purple and green boundaries represent the initial and final *pax2a* domain during time-lapse recording. Dots represent the initial positions of cells. Images show dorsal views with anterior to the top. Scale bar, 50 µm.

Morphogenesis of the trigeminal placode

We next conducted time-lapse analysis of morphogenesis of the trigeminal placode in *neuroD:EGFP* transgenic embryos, which begin to express GFP in trigeminal precursors by 11.5 hpf (Obholzer et al., 2008). Because of the small number and broad distribution of *neuroD:EGFP* cells, we could readily track most trigeminal precursors for the duration of recording and therefore did not require additional RFP plasmid injection. Consistent with endogenous gene expression data (Fig. 1), trigeminal cells in control embryos were initially scattered at 11.5hpf but then rapidly converged into a compact placode by 14 hpf (Fig. 4.6 A-C, Movie3). Tracks of individual cells were relative

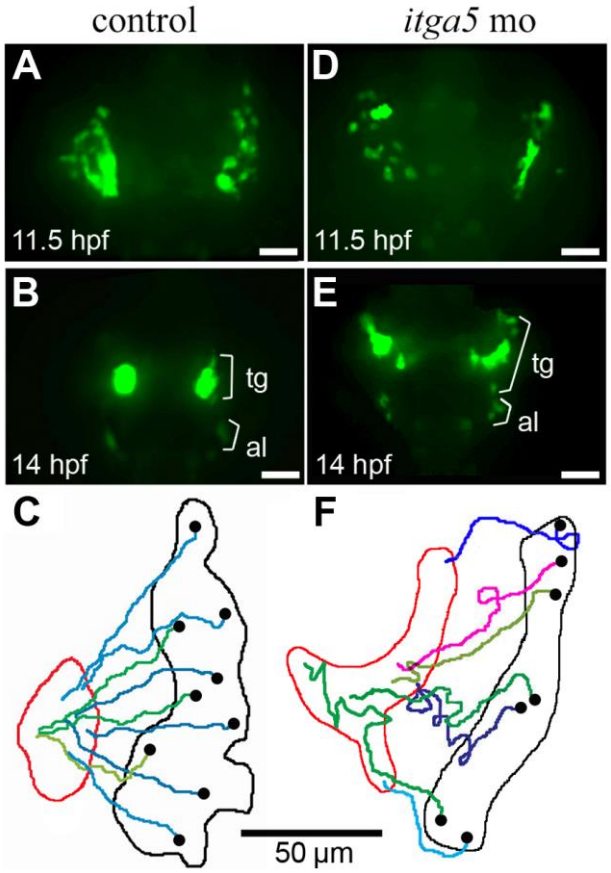

Figure 4.6: Convergence of trigeminal precursors is impaired in *itga5* morphants. (**A, B, D, E**) Images of time-lapse movies showing transgenic *neuroD:EGFP* expression in the first (11.5 hpf) and final (14 hpf) frames of a control movie (A, B) and *itga5* morphant movie (D, E). Positions of precursors of the trigeminal ganglion (tg) and anterior lateral line (al) are indicated. (**C, F**) Maps showing the trajectories of individual trigeminal precursors in the control embryo (C) and *itga5* morphant (F). Black and red boundaries mark the initial and final distribution, respectively, of *neuroD:EGFP*-positive trigeminal precursors. Black dots represent the initial and final positions, respectively, of individual cells. Images show dorsal views with anterior to the top, and summary figures show the right trigeminal field of each embryo, with lateral to the right. Scale bar, 50 µm.

straight and showed little deviation (Fig. 4.6 C). In *itga5* morphants, the initial distribution of *neuroD:EGFP* cells was normal at 11.5 hpf but subsequent convergence was severely impaired (Fig. 4.6 D-F, Movie4). Migration of trigeminal cells was highly erratic with frequent changes in direction (Fig. 4.6 F), hence the mean efficiency of migration was much smaller than normal (Table 3). Moreover, many cells failed to converge by 14 hpf (Figs. 4..1 J, 7E). Trigeminal cells did eventually converge to form poorly organized clusters by 15.5 hpf (not shown). Thus, *itga5* is required for efficient migration and convergence of trigeminal cells as it is for otic/epibranchial cells. However, we did not observe any cell death in *neuroD:EGFP* expressing trigeminal cells in *itga5* morphants. Thus the requirement for survival appears to be restricted to otic/epibranchial precursors.

itga5 regulates cell survival in the _pax2a_ otic/epibranchial domain

To confirm whether the cell-lysis observed during time-lapse imaging of otic/epibranchial precursors (Figs. 4.2, 4,3, 4.5) is due to apoptosis, we visualized apoptotic cells by staining with an antibody directed against activated Caspase-3. It was either performed in *pax2a:gfp* transgenic fish (in case of morphants) or double-immunostained for Pax2a antibody (in case of mutants). We observed more than two fold higher levels of apoptosis in *itga5* morphants (Fig. 4.7 A,B,E). Elevated apoptosis was limited to the otic/epibranchial domain and did not extend to more anterior ectoderm near the developing trigeminal placodes (data not shown). Similar results were obtained using Acridine Orange (data not shown). We also observed statistically significant

increase in the number of apoptotic cells in b926 mutants as compared to the controls (Fig. 4.2). These data indicate that *itga5* is specifically required for survival of cells in the otic/epibranchial domain.

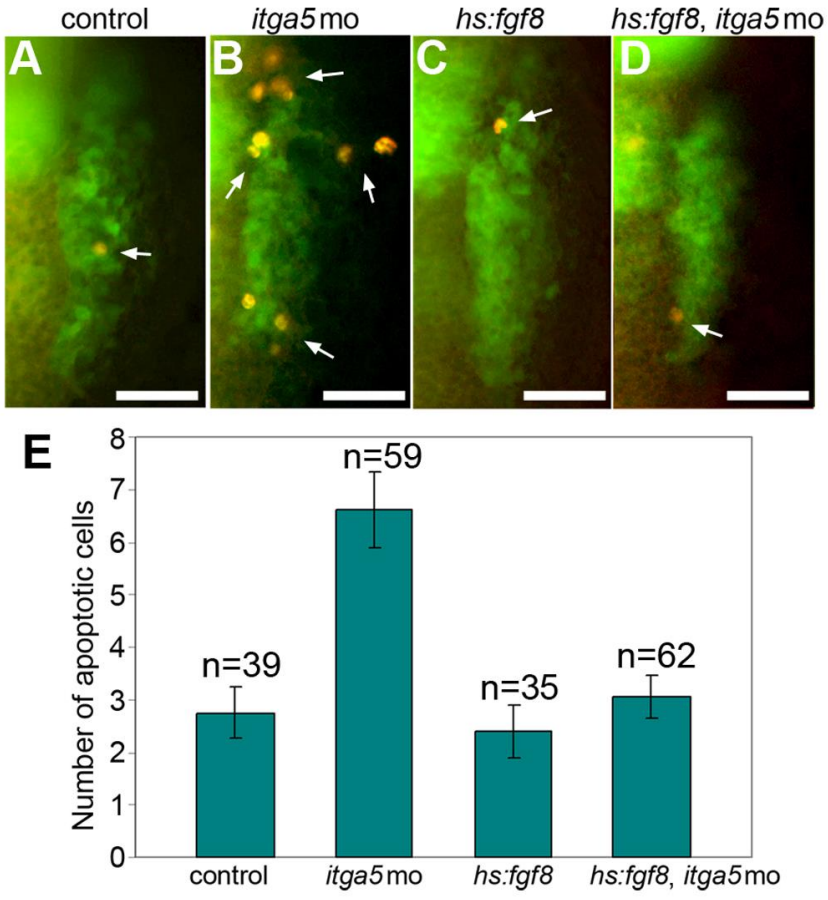

Figure 4.7: Elevated cell death in *itga5* morphants is rescued by *hs:fgf8*. (**A–D**) Transgenic *pax2a:GFP* embryos immunostained for GFP (green) and Caspase3 (red). Images show dorsal views (anterior up) of the right otic/epibranchial domain in a control embryo (A), *itga5* morphant (B), *hs:fgf8*/+ embryo (C) and *hs:fgf8*/+ embryo injected with *itga5*-MO (D). White arrows mark apoptotic cells. All embryos were heat shocked at 39°C for 30 minutes beginning at 11.5hpf and fixed at 13.5 hpf. Scale bar, 50 µm. (**E**) Mean number of Caspase3-positive cells in the otic/epibranchial domain in each of the four groups of embryos. Error bars indicate S.E.M.

***itga5* cooperates with Fgf to regulate otic/epibranchial survival and development**

Previous studies have shown that Integrin-ECM binding can promote cell survival through activation of MAPK and PI3K signal transduction. Because otic/epibranchial induction and maintenance requires Fgf signaling, which also operates via MAPK and PI3K activity, we hypothesized that *itga5* augments Fgf signaling to promote cell survival. To test this idea, we used a heat shock-inducible transgene, *hs:fgf8* (Millimaki et al., 2010), to elevate Fgf signaling in *itga5* morphants. Activation of *hs:fgf8* expression at 11.5 hpf in *itga5* morphants reduced the number of Caspase-3 positive apoptotic cells to normal by 13 hpf (Fig. 4.7D,E). These data support the hypothesis that *itga5* promotes cell survival in part through augmenting Fgf signaling.

We next tested whether *itga5* influences Fgf-dependent gene expression. Although genes in the Fgf-feedback pathway, including *sprouty4*, *pea3* and *erm* (Furthauer 2001; Raible and Brand 2001; Roehl and Nusslein-Volhard 2001) are often used as indicators for the presence of Fgf, they are not sensitive enough to detect modest reduction in the level of Fgf signaling (Maves et al., 2002) . However, we recently reported that *sox3* expression provides a sensitive readout of changing levels of Fgf signaling in the otic/epibranchial region, with two distinct threshold responses to Fgf (Padanad and Riley, 2011). Specifically, *sox3* is initially induced at a high level in the otic domain in response to moderate Fgf signaling during otic induction (Nikaido et al., 2007; Sun et al., 2007). Subsequently, in response to otic expression of *fgf24*, *sox3* expression downregulates to a discrete lower level in the otic domain and is induced at a higher level in abutting epibranchial tissue (Padanad and Riley, 2011). We therefore

reasoned that if *itga5* morphants experience decreased MAPK or PI3K signaling, expression of *sox3* should remain elevated in the otic domain. In support, *itga5* morphants showed equally heavy expression of *sox3* in the otic and epibranchial domains (Fig. 4.8 B). Similar changes were observed following low level misexpression of dominant-negative Fgf receptor (*hs:dnfgfr1*), while high level activation of *dnfgfr1* ablated *sox3* entirely (Fig. 4.8 E, F). In contrast, activation of *hs:fgf8* resulted in a low level of *sox3* expression throughout the otic-epibranchial domain in both control embryos and *itga5* morphants (Fig. 4.8 C, D). Thus, the effects of *itga5* knockdown on *sox3* expression mimic the effects of modest reduction of Fgf signaling and can be reversed by overexpression of *fgf8*, supporting the notion that *itga5* normally augments Fgf signaling.

Note that the above changes in *sox3* expression do not necessarily reflect changes in cell fate. For example, retention of high levels of *sox3* in the otic domain in *itga5* morphants, and in embryos weakly expressing *dnfgfr1,* does not indicate wholesale switching of otic to epibranchial fate since such embryos still produce substantial otic vesicles. Likewise, retention of elevated *sox3* in the otic domain of *fgf24* morphants does not impair otic development, nor does forced over-expression of *sox3* (Padanad and Riley, 2011). Thus, knockdown of *itga5* appears to cause only a modest reduction in cell signaling sufficient to alter *sox3* expression, but not cell fate, within the otic domain.

To further explore the relationship between *itga5* and MAPK signaling, we examined the genetic interaction between *itga5* and *erm*, a direct MAPK-target that helps mediate the effects of Fgf signaling (Raible and Brand 2001; Roehl and Nusslein-

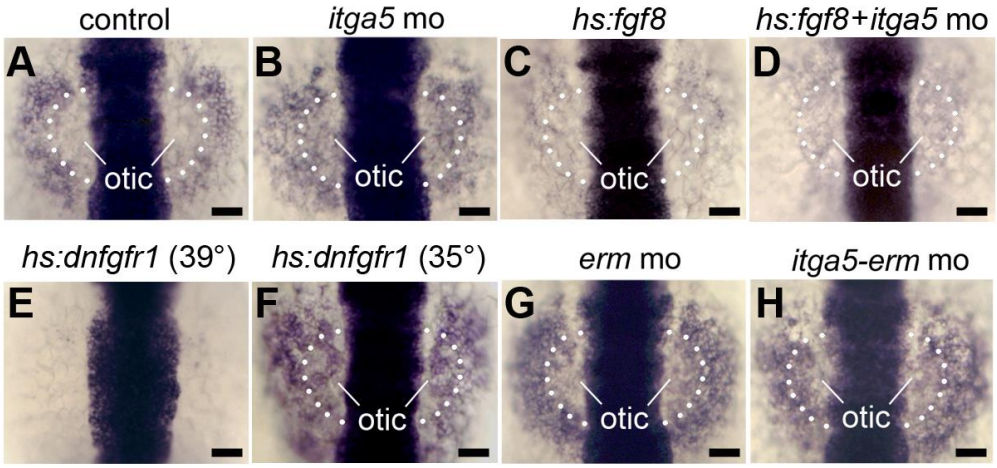

Figure 4.8: Similar effects of Itga5 and Fgf on *sox3* expression. (**A–H**) *sox3* expression at 12.5 hpf in a control embryo (A), *itga5* morphant (B), *Tg(hs:fgf8/+)* heat shocked at 37°C alone (C) or with *itga5* morpholino (D), *Tg(hs:dnfgfr1/+)* heat shocked at 39°C (E) or 35°C (F), *erm* morphant (G) and *itga5-erm* double morphant (H). The otic region where *sox3* normally downregulates is indicated. Scale bar, 50 μm.

Volhard 2001;Znosko et al., 2010). Because *erm* is partially redundant with *pea3*, knockdown of *erm* alone has negligible effects on gross morphology (Znosko et al., 2010; and our unpublished observations) with the exception of a variable incidence of otolith deficiencies in the otic vesicle (Fig. 4.9 G). In addition, early placodal development appears normal in *erm* morphants (Fig. 4.9 C), though otic expression of *sox3* shows slightly less pronounced downregulation compared to control embryos (Fig. 4.8 G). Thus *erm* morphants provide a sensitized background for detecting further reduction in MAPK signaling. As observed earlier, *itga5* morphants showed a reduced amount of otic tissue (Fig. 4.9 B, F), and simultaneously knocking down *erm* enhanced

this deficiency (Fig. 4.9 D, H). While *itga5* morphants produced abundant epibranchial neurons, albeit in a disorganized pattern (Fig. 4.9 J), *erm* morphants showed a marked deficiency of epibranchial ganglia (Fig. 4.9 K) and *erm-itga5* double morphants produced almost none at all (Fig. 4.9 L). Thus, *itga5* and *erm* work together to control otic and epibranchial development, possibly by acting through the same pathway.

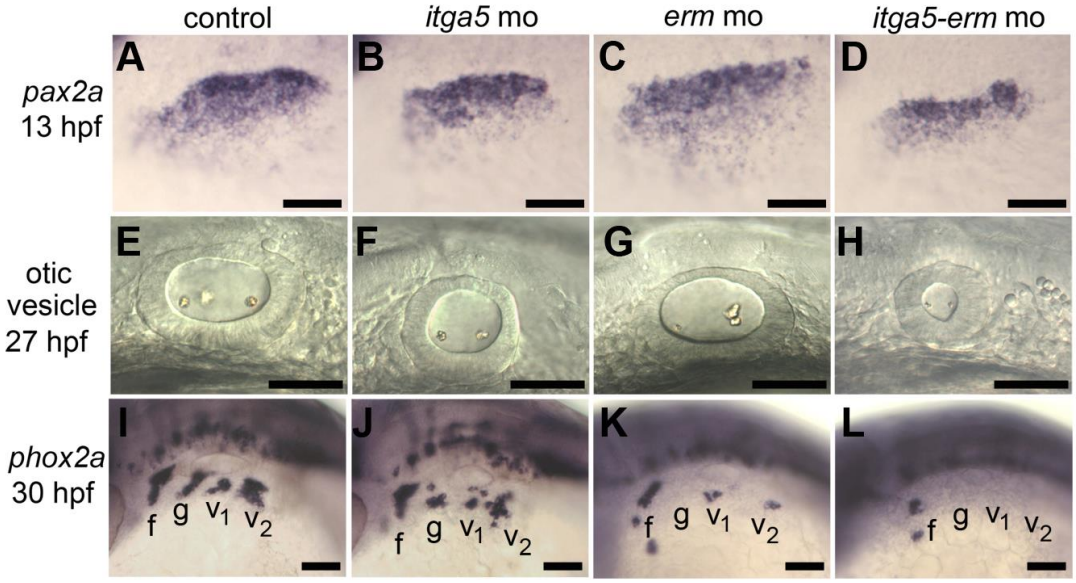

Figure 4.9: *itga5* and *erm* interact during otic and epibranchial development. (**A–D**) Otic/epibranchial expression of *pax2a* at 13 hpf. **(E–H**) Otic vesicle morphology in at 27 hpf. (**I–L**) *phox2a* expression in epibranchial ganglia at 30 hpf. Positions of facial (f), glossopharyngeal (g) and vagal (v1 and v2) ganglia are indicated. All images show lateral views with dorsal up and anterior to the left. Scale bar, 50 μm.

These data, together with the effects of *itga5*-MO on *sox3* expression and the ability of *hs:fgf8* to rescue the cell death phenotype in *itga5* morphants, support the idea that *itga5* normally augments Fgf signaling to promote cell survival and regulate differential gene expression in otic/epibranchial precursors. In contrast, *itga5* provides a unique function required for directed cell migration that cannot be replaced by elevating Fgf, but which is nevertheless likely to influence how many cells experience Fgf signaling (see Discussion).

Regulation of *itga5* expression

To elucidate a more complete picture of the pathway in which *itga5* acts, we sought to identify the upstream regulators of *itga5* expression. Expression of *itga5* shows elevated expression in a horseshoe-shaped pattern marking the preplacodal ectoderm at 10 hpf (Crump et al., 2004). By 11 hpf expression strongly upregulates in the anterior-most portion of the preplacodal domain (Fig. 4.10 A), which gives rise to the anterior pituitary, nasal and lens placodes (Toro and Varga, 2007). By 12 hpf expression expands in the otic/epibranchial domain and further intensifies by 13 hpf (Fig. 4.10 B). The spatial pattern of *itga5* expression strongly resembles that of *dlx3b* and *dlx4b*, which are the earliest preplacodal markers in zebrafish and are together required for proper development of many placodal derivatives (Kwon et al., 2010; Kaji and Artinger,2004; Solomon and Fritz 2002). We therefore examined whether *dlx3b/4b* genes are required for proper expression of *itga5*. Knockdown of *dlx3b/4b* did not prevent initiation of preplacodal expression of *itga5*, but subsequent upregulation and maintenance of *itga5*

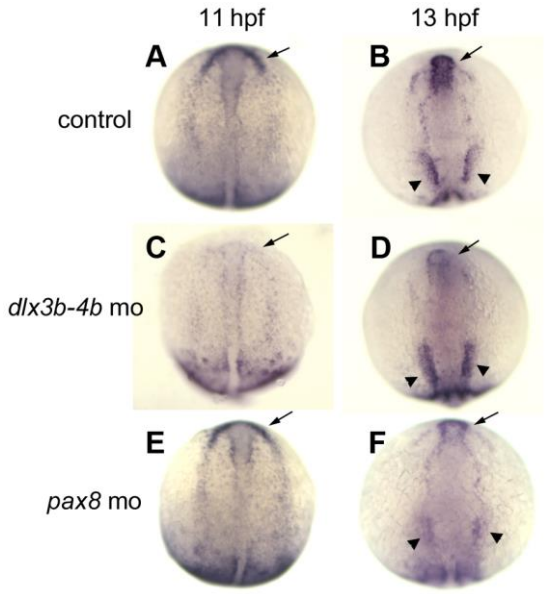

Figure 4.10: Differential spatial regulation of *itga5* by *dlx*3b/*4b* and *pax8*. (**A–F**) *itga5* expression at 11 hpf and 13 hpf in control embryos (A, B), *dlx3b-dlx4b* double morphants at (C, D), and *pax8* morphants (E, F). Regions where expression normally upregulates in precursors of anterior placodes (arrows) and otic/epibranchial precursors (arrowheads) are indicated. Images show dorsal views with anterior to the top.

in the anterior preplacodal domain were severely impaired (Fig. 4.10C, D). Surprisingly, however, expression of *itga5* in the otic/epibranchial ectoderm domain was relatively normal in *dlx3b/4b* double morphants (Fig. 4.10D). Because *pax8* regulates early aspects of otic and epibranchial development (Padanad and Riley, 2011; Hans et al., 2007; Mackereth et al., 2005) we examined expression of *itga5* in *pax8* morphants. Expression of *itga5* was normal in *pax8* morphants through 11 hpf (Fig. 4.10E) but expression failed to upregulate properly in the otic domain by 13 hpf (Fig. 4.10 F, and data not

shown). In contrast, *itga5* expression in the anterior preplacodal domain was relatively normal in *pax8* morphants. In summary, *dlx3b/4b* is required for upregulation and maintenance of *itga5* in anterior preplacodal ectoderm, whereas *pax8* is required for upregulation in the otic/epibranchial domain.

DISCUSSION

We have shown an essential role for *itga5* in proper formation of trigeminal, otic and epibranchial placodes. Cell motion analysis in GFP-transgenic backgrounds shows that cells normally converge from broad fields into compact placodes through highly directed migration. Overall, cells contributing to these diverse placodes originate from distinct regions with only limited overlap (Fig. 4.11 A). The data further show that the otic and epibranchial domains continue to expand after gastrulation through ongoing recruitment of cells from more lateral nonneural ectoderm (Fig. 4.11 B). In *itga5* morphants, cell migration is much less directional: Though the total distance traveled is comparable to normal, cells frequently change direction and backtrack, resulting in net lower displacement of cells leading to significant impairment of convergence and complete abrogation of recruitment. Loss of *itga5* also impairs patterning and cell survival in the otic/epibranchial domain. Several lines of evidence indicate that *itga5* interacts with Fgf signaling to regulate this region. First, misexpression of Fgf8 is sufficient to rescue the cell death phenotype in *itga5* morphants. Second, expression of *sox3* fails to downregulate in the otic domain in *itga5* morphants, mimicking the effects of reduced Fgf signaling (Padanad and Riley, 2010). Third, knockdown of *erm* enhances the

patterning defects in *itga5* morphants. Finally, proper expression of *itga5* requires the Fgf-target gene *pax8*. Together, these data suggest that *itga5* acts in a feed-forward loop to reinforce inductive Fgf signaling in the otic/epibranchial domain. Together, our data support a model in which *itga5* coordinates cell migration, differentiation and survival in posterior cranial placodes, in part by enhancing Fgf signaling (Fig. 4.11 C).

Role of Integrin in directed cell migration

Preplacodal ectoderm forms by the end of gastrulation and then quickly breaks into discrete placodes through directed cell migration (Bhattacharyya et al., 2004; Dutta et al., 2005; Knaut et al., 2005; Miyasaka et al., 2007; Toro and Varga, 207; Whitlock and Westerfield, 2000). Integrins are good candidates for regulating such morphogenetic processes, but there have been no previous studies of the role of Integrins in placodal development in any species. We chose to study *itga5* in zebrafish because it is initially expressed at a low level throughout the preplacodal ectoderm and later upregulates in various placodal derivatives as they form (Crump et al., 2004; Fig. 4.10). Surprisingly, placodes derived from the anterior portion of the preplacodal ectoderm (anterior pituitary, olfactory and lens placodes) appear to develop normally in *itga5* morphants. It is possible some other Integrin provides redundancy in this region, or later developmental processes compensate for early deficiencies in these tissues. In contrast, *itga5* knockdown impairs directed migration of precursors in posterior placodes, resulting in disorganization of trigeminal and epibranchial ganglia and significant deficiency of otic

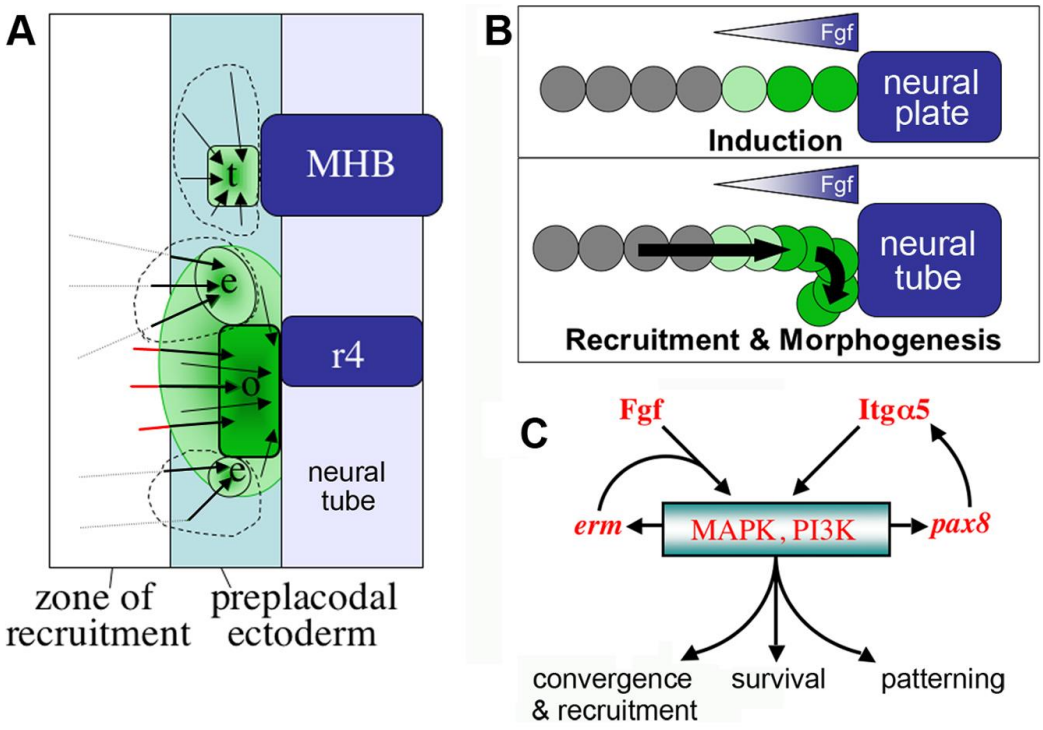

Figure 4.11: Model for regulation of posterior placode development by *itga5*. (**A**) Summary of cell migration during morphogenesis of trigeminal (t), epibranchial (e) and otic (o) placodes. Arrows indicate migration routes of cells tracked in *neuroD:EGFP* and *pax2a:GFP* expression domains (green). Dashed circles indicate the general areas from which trigeminal and epibranchial precursors were tracked. Most epibranchial precursors were not detected until relatively late (12.5–13.2 hpf) when they first activated *pax2:GFP* in a scattered pattern while still lateral to the contiguous domain of expression. We infer these cells originated from more lateral positions within the zone of recruitment (dashed tracks). RFP-positive otic cells were observed to migrate into the *pax2a:GFP* domain from nearby in the zone of recruitment (red tracks) between 11.7–12.5 hpf. Positions of the midbrain-hindbrain border (MHB) and rhombomere 4 (r4) are indicated. (**B**) A model for recruitment of otic/epibranchial cells. An initial otic domain (green) is induced by dorsally expressed Fgfs. Subsequently, *itga5*-dependent medial migration drives convergence of the otic field and draws new cells into range of inductive signaling. (**C**) Model for *itga5* in reinforcing Fgf signaling. Erm helps mediate Fgf signaling, which begets more *erm* expression. Fgf also activates *pax8*, which stimulates upregulation of *itga5* in the otic/epibranchial domain, further reinforcing Fgf signaling. Fgf acts primarily through the MAPK and PI3K pathways, and Itga5 facilitates these pathways through a variety of mechanisms (see text for details). Together these functional interactions control directed cell migration, cell survival, and gene expression within the otic/epibranchial field.

tissue. Interestingly, cells were observed to migrate long distances in *itga5* morphants adhesive gradients in the ECM (haptotaxis). Fibronectin-1 (Fn1) is an ECM component that strongly binds Itga5 and is expressed maximally by mesoderm just beneath the neural-nonneural border (Mould et al., 2009; Trinh and Stainier, 2004), possibly providing a cue for medial migration. Additionally, Integrin-ECM binding appears necessary for restricting pseudopod production to the leading edge of migratory cells (Petrie et al., 2009). Otherwise, cells tend to extend multiple pseudopods in random directions, resulting in frequent changes in direction similar to what we have observed in *itga5* morphants. Dynamic regulation of Integrins helps to stabilize leading pseudopods chemotaxis of many celll types (Chodniewicz and Klemke, 2004) and plays a vital role in modulating the response of T-lymphocytes to chemokines (Ward and Marello-Berg, 2009). The chemokine Sdf1 is required for focal migration of trigeminal precursors (Knaut et al., 2005), and knockdown of *itga5* causes a phenotype similar to loss of the Sdf1 receptor Cxcr4. Also, knockdown of cxcl4 or cxcr4 causes downregulation of integrin beta1 leading to migration defects in endodermal precursors during gastrulation (Nair and Schilling 2008). It is not known whether specific chemokines regulate convergence of otic or epibranchial cells. Otic placode cells express the chemokine Cxcl14 (Scyba) (Long et al., 2000), though knockdown of this gene causes no discernable defects (our unpublished observations). Epibranchial-specific chemokines are yet to be identified.

Role of Integrin in cell-signaling

Itga5 facilitates signaling associated with specification and survival of otic/epibranchial precursors, probably through multiple distinct mechanisms. First, *itga5*-dependent migration draws lateral cells into range of inductive Fgf signaling, thereby promoting recruitment of additional cells into these placodes (Fig. 4.11B). We showed previously that the number of *pax2a*-positive cells roughly doubles between 11 hpf and 14 hpf, and a similar fold-increase is seen in mutants blocked in cell division, leaving recruitment as the only means available to increase cell number (Riley et al., 2010). Second, Integrin-ECM binding is required in many cell types for proper nuclear import of phosphorylated MAPK/ERK (Aplin et al., 2001; Hirsch et al., 2002; James et al., 2007). Otherwise, ERK can continue to be phosphorylated yet accumulate ineffectually in the cytosol. Third, *itga5* could specifically amplify Fgf signaling through direct physical interactions. In mammalian vascular endothelial cells, for example, Integrin-αvβ3 binds Fgf1 or Fgf2 directly to form a ternary complex with FGFR1 and promotes receptor clustering (Mori et al., 2008; Rusnati et al., 1997; Tanghetti et al., 2002). Such binding interactions are required for sustained MAPK/ERK signaling. Itga5 can also stimulate PI3K (Hamidouche 2009), another signal transducer shared by the Fgf pathway that regulates cell migration and fate specification in a variety of cell types (Carballada et al., 2001; Ma et al., 2009; Montero et al., 2003).

In the case of otic/epibranchial development, *itga5* is not required for sustained Fgf signaling but appears necessary for achieving a full level of Fgf signaling. Although knockdown of *itga5* does not detectably alter expression of genes in the Fgf

synexpression group, such as *erm*, *pea3* or *sprouty4*, such genes are not suitable for detecting modest reduction in Fgf signaling (Padanad and Riley, 2011; Maves et al., 2002). Fortunately, *sox3* expression shows two distinct threshold-responses to Fgf signaling: Moderate Fgf signaling induces a high level of *sox3* expression in the epibranchial domain whereas elevated Fgf signaling downregulates *sox3* expression to a discrete lower level in the otic domain (Padanad and Riley, 2011). The finding that *sox3* expression is inappropriately maintained at a high level in the otic placode of *itga5* morphants (Fig. 4.8B) provides evidence that Fgf signaling is indeed diminished in this domain. Furthermore, reduced signaling in *itga5* morphants explains the elevated cell death seen throughout the otic/epibranchial domain, since activating *hs:fgf8* rescues this phenotype (Fig. 4.7). Nevertheless, it is interesting that *sox3* shows normal upregulation in the peripheral/epibranchial domain in *itga5* morphants (Fig. 4.8B). This process is Fgf-dependent and indicates that moderate Fgf signaling remains sufficient at the edge of the signaling range to properly regulate gene expression in the absence of *itga5* function. Thus, the effect of signaling on patterning can be separated to some extent from regulation of cell survival, with the latter being more sensitive to slight changes in signaling activity.

The link between cell fate specification and cell migration in the otic/epibranchial field is complex. We showed previously that otic and epibranchial fates are specified sequentially: The otic placode forms first and expresses *fgf24*, which then induces epibranchial development through upregulation of *sox3* expression in more lateral ectoderm (Padanad and Riley, 2011). Based on cell-tracking in the *pax2a:GFP*

domain, recruitment of otic and epibranchial cells occurs at correspondingly different times. Recruitment of otic cells occurs mostly between 11.5–12 hpf, whereas the majority of epibranchial cells are recruited between 12.5–13.3 hpf from a slightly more lateral domain. Given the 40-minute lag between onset of transcription to accumulation of GFP, these times agree well with dynamic changes in *sox3* expression in otic vs. epibranchial precursors (Padanad and Riley, 2011; Nikaido et al., 2007; Sun et al., 2007). Changes in these processes in *itga5* morphants provide some insight as to how morphogenesis and fate specification are coordinated. Because recruitment of new cells fails almost entirely in *itga5* morphants, fates are specified within a fixed population of *pax2a:GFP*-positive cells. Inefficient cell migration appears to contribute to a marked deficiency of otic cells and corresponding increase in non-otic domains. It is understandable that slow migration impedes peripheral cells from entering the otic domain in a timely manner, but why don't peripheral cells intercalate with otic cells at later times? There is possibly a timing mechanism that excludes new cells from the otic domain after some critical period. The transition is possibly related to how long cells are exposed to varying Fgf concentrations, which could co-regulate fate-specification with activation of genes that mediate contact-dependent repulsion. Further studies are needed to test these ideas.

CHAPTER V

SUMMARY AND CONCLUSIONS

This dissertation focuses on the elucidation of molecular mechanisms responsible for specification of PPE and its morphogenesis into individual placodes. PPE is a unique ectodermal domain of multipotent placodal progenitors that expresses transcription factors *six4.1, dlx3b* and *eya1* at the end of gastrulation (Akimenko et al., 1994; Sahly et al., 1999; Kobayashi et al., 2000). This domain eventually resolves into discrete cranial placodes at the neural-nonneural interface that make significant contributions to the peripheral nervous system. The study in Chapter II uncovers a novel genetic mechanism that shows temporally distinct roles for Bmp signaling during PPE specification: at late blastula stages Bmp sets up preplacodal competence throughout the ventral domain by activating transcription factors, *tfap2a*, *tfap2c, foxi1* and *gata3*. However, by the end of gastrulation, Bmp is completely inhibited for PPE specification. We also show an essential requirement for dorsally expressed growth factors: Fgf and Pdgf which act in concert with Bmp inhibitors and above mentioned competence factors to correctly position PPE at the neural-non neural interface (Kwon et al., 2010). Chapter III describes a self-sustaining genetic network of the competence factors that requires Bmp for activation but not for the subsequent maintenance. This genetic network restores PPE and individual placodal fates in the complete absence of Bmp signaling (Bhat et al., 2012). In Chapter IV we show that resolution of posterior PPE into trigeminal, otic and epibranchial placodes involves directed cell migration of placodal precursors.

Additionally, we show a novel requirement for the role of extracellular matrix binding protein, *integrin alpha5*, in directed cell migration of these posterior placodal precursors and its role in enhancing overall levels of Fgf signaling in otic and epibranchial precursors. This study also provides direct evidence for recruitment of cells from the adjacent epidermal domains into the placodes as a means to increase the number of otic and epibranchial precursors (Bhat and Riley, 2011). This dissertation on the whole provides important insights into placodal development from late blastula through mid-segmentation stages of zebrafish development which could stimulate more studies on placodal development.

BMP MORPHOGEN MODEL AND PPE DEVELOPMENT

Several studies on early ectodermal patterning indicate that high levels of Bmp specify epidermal (ventral) fates; low/no Bmp specify neural (dorsal) fates while neural crest, a dorsolateral fate, requires intermediate levels of Bmp signaling. These studies lead to the Bmp morphogen model for ectodermal patterning where different fates in the ectoderm are specified directly by distinct thresholds of Bmp signaling (Neave et al., 1997; Wilson et al., 1997; Marchant et al., 1998; Nyugen et al., 1998; Barth et al., 1999; Tucker et al., 2008; Brugmann et al., 2004; Glavic et al., 2004). However, the specification of PPE by intermediate levels of Bmp had been controversial. There were two major reasons: either the level of Bmp inhibition was not quantified making it difficult to assess if complete or partial attenuation of Bmp signaling is required or the experiments were conducted *in-vitro* which do not accurately recapitulate the in-vivo conditions (Brugmann et al., 2004;

Glavic et al., 2004; Litsiou et al., 2005; Ahrens and Schlosser, 2005; Esterberg and Fritz, 2008). To understand the role of Bmp during PPE specification directly *in-vivo*, we used a pharmacological inhibitor of Bmp signaling, Dorsomorphin, to control the degree of Bmp inhibition (Yu et al., 2008). We used both morphological and molecular methods to assess the degree of Bmp inhibition (See Table1; Fig2; Chapter I). We found that as expected, treatment with the full blocking dose of Bmp at late-blastula stages completely dorsalized the embryo with no evident NC, PPE or epidermal domains. When subjected to doses of DM that gave intermediate Bmp inhibition, neural crest fates expanded ventrally at the expense of nonneural domain similar to Bmp hypomorphic mutants. PPE, on the other hand, shows two distinct responses when exposed to intermediate DM concentration: either PPE domain was lost or bilateral domains of PPE upregulation were observed at the neural-non neural interface. These results are not consistent with a Bmp morphogen model which would predict that PPE would expand throughout the ventral ectoderm upon reduction in the overall levels Bmp in the embryo. Instead, our work shows a novel genetic mechanism for preplacodal specification: instead of getting specified by Bmp in a single step, PPE gets induced by a combination of different signals in a two-step model. The first step is established during late blastula-early gastrula stages where Bmp activates a set of four preplacodal competence factors, *tfap2a*, *tfap2c*, *foxi1* and *gata3* throughout the nonneural domain. These transcription factors render the whole nonneural domain competent to acquire preplacodal fate (Kwon et al, 2010; Bhat et al., 2012). In the second step of PPE specification, inductive factors from the dorsal specify PPE markers at the neural-nonneural interface at the end of

gastrulation. Consistent with reports in other model systems, Fgf ligands are the main inducers of PPE (Litsiou et al., 2005; Ahrens and Schlosser, 2005; Kwon et al., 2010). However, Bmp and Wnt ligands have to be completely attenuated for Fgf to induce PPE adjacent to the neural plate (Litsiou et al., 2005; Ahrens and Schlosser, 2005; Kwon et al., 2010; Brugmann et al., 2004). Our studies are not consistent with the Bmp morphogen model which predicts that a specific intermediate concentration of Bmp directly specifies PPE. Instead, Bmp sets up a bicompetent zone for epidermal and preplacodal fates in the ventral ectoderm during late blastula/early gastrula stages.

PROGRESSIVE RESTRICTION OF COMPETENCE DURING PLACODAL DEVELOPMENT

Placodal development is a long process beginning at late blastula stages and culminating in the formation of morphologically visible placodal structures by mid-segmentation (Grocott et al., 2012). As noted above, preplacodal competence is established during blastula stages by four Bmp-activated transcription factors, *tfap2a*, *tfap2c*, *foxi1* and *gata3* in zebrafish. In chick and Xenopus, the PPE competence persists in the ventral ectoderm even after the end of gastrulation (Glavic et al., 2004; Brugmann et al., 2004; Litsiou et al., 2005; Ahrens and Schlosser, 2004). The mechanism by which these transcription factors render the ventral ectoderm competent and the duration for which the competence persists in the ventral domain after gastrulation is currently not clear (Pieper 2012; Litsiou 2005; Glavic 2003, Ahrens and Schlosser, Brugmann 2004).

By the end of gastrulation, markers such as *six4.1, eya1* ad *dlx3b* are specifically upregulated at the neural-nonneural interface in PPE. Recent studies suggest that PPE fate acquisition is a necessary prerequiste for subsequent specification of individual placodes including otic placode. Using chick-quail grafts, Martin and Groves 2006 showed that the grafts from anterior and posterior regions of PPE but not from the nonneural ectoderm are competent to express otic markers in response to Fgf2, a necessary and sufficient signal for otic specification in chick. The nonneural explants activate otic markers only after the activation of PPE markers. Furthermore, misexpression of Fgf8 in zebrafish leads to a robust induction of otic and epibranchial markers only within the PPE (Padanad et al., 2012; Philips et al., 2004). Similar to the otic placode, trigeminal and olfactory placodal competence is also restricted to PPE (Bhattacharyya and Bronner-Fraser 2008; Baker et al., 1999). It seems likely from these experiments that the competence to acquire individual placodal fates is restricted to the preplacodal domain by virtue of expression of PPE markers in this domain. It would be interesting to find if prolonged activation of Fgf ligands would induce placode-specific markers in the ventral ectoderm after the PPE markers have been induced by Fgf and Bmp antagonists (See Chapter II). This necessity to acquire a preplacodal fate prior to differentiation into individual placodes could be essential for promoting proliferation, survival and neurogenesis in the cranial placodes (Kwon et al., 2010; Bhat et al., 2012; Bricaud and Collazo 2006; Chen et al., 2009; Ikeda et al., 2007; 2010; Brugman 2004; Li et al., 2003; Ozaki et al., 2004).

Although PPE is competent to acquire any placodal fate, posterior preplacodal domain can be more easily induced to express otic markers as compared to anterior preplacodal domain in response to overexpression of Fgf8/Fgf3, essential ligands for otic specification. Only prolonged overexpression of these ligands can induce otic markers in the anterior PPE (Padanad et al., 2012). Similarly, anterior pituitary precursors are more likely to get misspecified into lens placodal cells in response to Shh overexpression. These studies suggest that there is a bias within PPE to give rise to adjacent placodal fates in response to genetic perturbations (Bailey and Streit 2006). This bias could be influenced by localized signaling molecules that activate transcription factors encompassing adjacent placodal domains within PPE. For example, *msxB* is expressed in the PPE only from the prospective trigeminal to otic domain. Similarly, *otx2* and *gbx2* are expressed in the anterior and posterior domains of PPE respectively and form a sharp boundary at prospective trigeminal-otic precursor domains (Philips et al., 2006; Steventon et al., 2012). It would be interesting to determine if knockdown of anterior PPE marker, *otx2*, would enhance the ability of Fgf3/Fgf8 to activate otic markers in the anterior PPE. Our study along with others have also shown expression of *pax2a* in otic, epibranchial and lateral line placodes (Bhat and Riley, 2011; Ohyama et al., 2006; Nechiporuk et al., 2005) Altogether, there seems to be a progressive restriction of placodal competence from a broad nonneural domain to PPE and then subsequently to subdomains with the PPE.

POSSIBLE MECHANISMS FOR PREPLACODAL COMPETENCE

In Chapter II and III we show that overexpression of ventrally restricted competence factors causes PPE induction in the neural plate (dorsal) indicating that in the right inductive environment (neural plate) competence factor expression can lead to PPE gene expression. We also showed that competence mediated by these four transcription factors is relatively specific as other ventrally restricted Bmp targets, such as *p63*, is not required for PPE formation (Bakkers et al., 2002; Lee et al., 2002; Kwon et al., 2010). However, one of the intriguing observations was the temporal lag of about 4-5 hrs between the induction of the competence factors at the late blastula-early gastrula stages and the induction of PPE markers at the end of gastrulation. Understanding a possible reason for this delay will give us a better mechanistic understanding of how competence is induced. Therefore, we speculate a number of reasons for this delay in the induction of PPE:

i) Activation or repression of other factors: Possibly, the transcription factors *tfap2a*, *tfap2c*, *foxi1* and *gata3* mediate competence by activating and/or repressing other factors in the ventral ectoderm for optimal PPE specification at the end of gastrulation. These targets could be Fgf/Pdgf receptors which would have to be upregulated in the PPE domain to maximize Fgf/Pdgf signaling at the neural- non neural interface. However, it is not clear what might restrict the upregulation of Fgf/Pdgf receptors to neural-nonneural interface since the competence factors are expressed throughout the ventral domain. Another interesting candidate that could mediate competence could be *dlx3b*. As mentioned in previous chapters, *dlx3b* is a PPE marker that shows upregulation in the

PPE domain at the end of gastrulation. However, at mid-gastrula stages, *dlx3b* is expressed in the whole ventral ectoderm (Solomon et al., 2004; Solomon and Fritz 2002; Liu et al., 2003). Possibly, activation of *dlx3b* could be a necessary step for mediating preplacodal competence in the ventral ectoderm prior to its role in specifying different placodes (Pieper et al., 2011; Hans et al., 2007). Several experiments using both gain and loss of function approaches can be performed to understand if preplacodal competence is mediated through *dlx3b*. For example, if overexpression of *dlx3b* alone is unable to activate preplacodal markers in the ventral ectoderm post gastrulation, then it would indicate that *dlx3b* is a competence factor because it would not be sufficient to activate PPE markers in the absence of inducing factors. Also, if the inducing factors i.e. Fgf and Bmp antagonists can activate PPE markers in the absence of *dlx3b* on the ventral side, then dlx3b is either redundant or not essential for mediating preplacodal competence.

ii) Chromatin remodeling by Foxi1, Gata3: Mouse homologs of *foxi1* and *gata3*, FoxA3 and GATA4 respectively, render liver-specific gene, Alb-1, competent for subsequent induction by signaling molecules in the endoderm. These factors directly bind silent Alb-1 enhancer in undifferentiated liver progenitors keeping the chromatin at this specific genetic locus more accessible. This relatively more open conformation would prime Alb-1 for subsequent gene activation by inductive factors. Unlike most of the other transcription factors, Foxa3 and Gata4 binds more stably to nucleosomes than to free DNA, do not require prior acetylation on histones to bind the chromatin and can remodel compacted chromatin into a more open conformation (Cirillo et al., 2002; Cirillo and Zaret 1999). Therefore, these factors are called “pioneer transcription

factors" in the context of liver development in mice (Zaret and Caroll 2011; Zaret 2008). However, the generality of these transcription factors acting as chromatin remodellers during other development contexts is currently not clear. Nevertheless, we could still extend these findings into the developmental context of mediating preplacodal competence since these factors perform a similar function of providing competence to the cells to respond to inducing factors. After activation by Bmp, *foxi1* and *gata3* could bind the silent chromatin loci of *six*, *eya* and *dlx* genes in the ventral ectodermal cells. This would render these loci poised for subsequent gene activation by signaling molecules such as Fgf and Bmp antagonists (Philips et al., 2001; Kwon and Riley, 2010). Understanding the mechanistic basis of competence would help us in understanding one of the earliest steps during cell fate specification.

REDUNDANT AND NON REDUNDANT FUNCTIONS OF COMPETENCE FACTORS DURING PPE AND SPECIFIC PLACODAL DEVELOPMENT

Inspite of being structurally very distinct from each other, the four competence factors *tfap2a*, *tfap2c*, *foxi1* and *gata3* are functionally redundant for PPE specification (Kwon et al., 2010). Combinatorial knockdown of any two factors reduces but does not eliminate the PPE domain while simultaneous knockdown of all four factors leads to complete ablation of PPE. Conversely, PPE can be fully rescued upon overexpression of any two competence factors under conditions that otherwise reduce PPE induction. However, these factors have distinct non-redundant functions during the development of individual placodes. In the embryos where *tfap2a/c* are knocked down, overexpression

of *foxi1* and *gata3* can rescue only otic placode while more anterior placodes were not rescued (Bhat et al., 2012). Conversely, upon overexpressing *tfap2a* in *foxi1-gata3* morphant anterior placodes remained as expanded as *tfap2a* overexpressing embryos but the posterior placodes were not rescued. This epistasis analysis indicates that even though these competence factors are redundantly required for PPE specification, *foxi1* and *gata3* have a more specific role during the subsequent development of posterior placodes while they seem to be neither necessary nor sufficient for more anterior placodes such as olfactory, lens and anterior pituitary. These results are consistent with the requirement for *foxi1* to activate *pax8* even when Fgf8, an essential signal for otic specification, is overexpressed (Solomon et al., 2003; Mackereth et al., 2005; Nissen et al., 2003; Padanad et al., 2012). This special requirement for *foxi1* during otic induction could be because of *foxi1*'s role as a possible gene specific chromatin remodeller for *pax8* (see above). In the absence of *foxi1, pax8* locus could remain compacted and inaccessible making it impossible for Fgf signal transduction pathway to activate *pax8* (Padanad et al., 2012). Interestingly, after *foxi1* activates *pax8* in the otic domain towards the end of gastrulation (Solomon et al., 2004), *pax8* downregulates *foxi1* expression in the otic domain within next two hours suggesting that prolonged presence of *foxi1* is also inhibitory to otic development (Padanad and Riley, 2010).

THE ROLE OF GROWTH FACTORS DURING PPE AND OTIC PLACODE DEVELOPMENT

Several activating and repressing inductive factors correctly position the PPE at the neural-non neural border. Fgf is one of the most important pathways critical for the induction of PPE across vertebrates (Kwon et al., 2010; Ahrens and Schlosser, 2005; Litsiou et al., 2005). Fgf3 and Fgf8 are among the most abundant ligands found in the neural plate at the time of PPE induction at the end of gastrulation (Philips et al., 2001). Loss of Fgf signaling using SU5402, a drug that blocks the activity of Fgf receptors, causes almost complete loss of *six4.1,* in *Xenopus*while overexpression of Fgf8 causes ectopic expression of a subset of PPE markers in chick (Ahrens and Schlosser, 2005; Litsiou et al., 2005). In zebrafish, treatment of embryos with SU5402 shows reduced expression levels of *eya1* suggesting the presence of another factor that acts redundantly with Fgf pathway during placodal development (Kwon et al., 2010). Pdgf is another growth factor that shows intense expression in the cranial placodal domain towards the end of gastrulation and activates similar signal transduction pathway as Fgf (Liu et al., 2002; Montera et al., 2003). Therefore, we inhibited both Fgf and Pdgf pathways by pharmacological inhibitors, SU5402 and AG1295 respectively (Montera et al., 2003; Kudoh et al., 2004). Under these conditions *eya1* expression was ablated and *dlx3b* was significantly reduced (Kwon et al., 2010; Liu et al., 2002). Hence, our study identified another growth factor, Pdgf that acts redundantly with Fgf ligands to specify PPE ectoderm. It would be interesting to find if overexpression of Pdgf and Bmp inhibitors (see Chapter II) would lead to ectopic PPE induction in the ventral ectoderm.

In addition to acting as a PPE inducer, Fgf also acts to induce development of specific placodes such as otic and epibranchial placode. Fgf signaling is both necessary and sufficient for induction of both these placodes with epibranchial placodes being responsive to lower Fgf levels than otic placode (Bhat and Riley, 2011; Padanad et al., 2011; Padanad and Riley, 2011). During otic induction, Fgf activates *pax8* expression in the otic domain and *sox3* in both otic and epibranchial domains (Mackereth et al., 2004; Sun et al., 2007). *pax8* in turn amplifies overall levels of Fgf signaling in the otic domain by activating expression of *fgf24* and *integrin alpha5* in the otic domain (Padanad and Riley, 2011; Bhat and Riley, 2011; See Introduction). *fgf24* causes no otic phenotype but is essential for the induction of epibranchial placodes in the adjacent domain (Padanad and Riley, 2011). On the other hand, *itga5* loss of function results in a smaller otic placode and disorganized epibranchial ganglia (Bhat and Riley, 2011). We found that one of the reasons for the placodal defects in *itga5* morphants was elevated levels of cell death in the otic domain. We were able to rescue the cell death defects in *itga5* morphants to almost wild type levels by overexpression of Fgf signals (Bhat and Riley, 2011). Therefore, our study implicates an essential role for *itga5* in mediating survival of otic and epibranchial placodes.

RESOLUTION OF PPE INTO DISTINCT PLACODES BY LOCALIZED CELL MIGRATION

The contiguous horse-shoe shaped domain of PPE at the end of gastrulation gets resolved into morphologically visible placodes by mid-somitogenesis. Temporal changes

in gene expression of placode-specific markers and lineage tracing studies in anterior placodal domain indicate that morphogenesis of PPE into individual placodes involves directed migration of placodal precursors. We found that posterior placodal precursors also undergo directed cell migration from a broad initial domain into much condensed placodes and describe the novel function of Itga5 in this process. We made some interesting observations which are discussed below.

Cell shape changes

Placodal precursors of olfactory and trigeminal placodes undergo chemokine mediated directed cell migration into discrete focal condensations (Bhattacharya et al., 2004; Streit 2002; Knaut et al., 2003; Miyasaka et al., 2007). As noted above, similar migration events could be proposed for otic and epibranchial placodes based on temporal analysis of molecular markers (Philips et al., 2006; Streit 2002). However, direct visualization of otic and epibranchial placode formation from the precursor cells was not shown before. By time-lapse imaging of *pax2a:gfp* transgenic embryos (Picker et al., 2002), we showed that otic precursors converge from a broad initial domain in the PPE into condensed placodes. This transgenic line was also useful in lineage tracing epibranchial precursors, which activated Gfp during the course of time-lapse and hence were recruited relatively late into the preplacodal domain. These late recruited cells formed distinct clusters anterior and posterior to the otic placode at mid-somitogenesis. These clusters would undergo further morphogenesis to give rise to discrete epibranchial ganglia at 24hpf (McCaroll et al., 2012). We also confirmed that similar to otic

precursors, trigeminal precursors also converge from a broader initial domain into condensed placodal structures (Knaut et al., 2003; Bhat and Riley, 2011). Interestingly, during the course of time-lapse imaging we observed that individual trigeminal, otic and epibranchial precursors underwent amoebae-like random cell shape changes such that no two individual cells had similar shapes within the same frame and also between consecutive frames of the time-lapse. At the time of morphological otic and trigeminal placode formation, precursor cells acquired an epithelial phenotype with a columnar morphology. These dynamic cell shape changes combined with the condensation of the overall placodal domain indicate that cells undergo active cell rearrangements and changes in their relative positions during migration. Based on published reports, we can speculate two different scenarios for explaining the nature of cell migrations during placode morphogenesis:

i). Active rearrangement of epithelial cells: One of the processes where large-scale cellular rearrangements occur in the embryo leading to the establishment of embryonic axis is gastrulation. The cells in the ectodermal epithelia of gastrulating embryos undergo radial intercalation leading to the spread of epithelial cells over the yolk. This is accomplished by the cells actively remodelling their adherens junctions (Solnica-Krezel and Sepich 2012). Similar cellular movements are observed during tracheal and kidney development where epithelial cells undergo extensive cell rearrangements by actively remodeling their adherens junctions during branching morphogenesis. This results in extensive changes in their neighbour-neighbour relationships even though they are part of epithelia (Chi et al., 2009; Neumann and Affolter 2005). During kidney development

in zebrafish, the pronephric epithelial cells migrates anterior-ward extending filopodial protrusions at their basal side while still remaining connected by E-cadherin junctions at the apical sides (Vasilyev et al., 2009). Such collective epithelial cell migrations have also been described during the deposition of lateral line neuromasts in zebrafish (Nechipork and Raible 2008). Altogether, these recent and elegant studies show that during development, epithelial cells can exhibit more dynamic behaviors than previously thought. Therefore, in light of these studies it is possible that placodal precursors could be part of an epithelium undergoing extensive adherens junction remodeling and cell rearrangement while also extending cellular protrusions during migration.

ii) More experiments including sectioning the embryos and examining the expression of cadherins in otic and epibranchial precursors are required to resolve between these two mechanisms of cell migration: whether otic precursors are part of a loose mesenchyme that compacts into an epithelial placode or is it part of epithelia that undergoes active rearrangement by remodeling their adherens junctions. We can also speculate that the placodal precursors are part of immature epithelia where individual cells are not tightly linked like an epithelial sheet but are not completely mesenchymal either. This semi-epithelial state would allow the precursor cells to undergo active changes in their relative locations while still remaining connected to each other in the epithelia. We favor this possibility during otic placode morphogenesis.

Role of *integrin alpha 5* in posterior placodal assembly

The morphogenesis of a ball of cells at the blastula stage into a complex morphological adult form is achieved by controlled signaling and cell migration. One of the molecules that regulates these cell migration events during embryogenesis are Integrins. Integrins are implicated in mediating cell migration in several developmental contexts: neural crest delamination from dorsal neural tube, mesodermal cell migration during gastrulation, midgut morphogenesis in Drosophila, axon pathfinding, proper laminar organization of the brain (Marsden and DeSimone, 2001; Davidson et al., 2006; Hoang et al., 1998; Baum and Gariga 1997; Anton et al., 1999; Crump et al., 2004; Goh et al., 1997; Testaz and Duband 2001). Here, we described a role for Integrin alpha 5 in mediating posterior placodal assembly in zebrafish. In the time lapse recordings of posterior placodes, we observed that posterior placodal precursors migrate in relatively straighter trajectories in wild type embryos. In the embryos knocked down for *itga5*, the tracks of posterior placodal cells are circuitous and disoriented leading to smaller otic placode and disorganized trigeminal and epibranchial placodes (Bhat and Riley, 2011). This directed migration of precursor cells in wild type embryos suggest that the precursor cells are responding to some directional cue or a chemokine (Thelen 2001). Secreted chemokines such as Sdf1 and its receptor Cxcr4a are implicated in directional cell migration of primordial germ cells, posterior lateral line migration of neuromasts along the anterior-posterior axis of the embryo, migration of retinal ganglion axons from the optic stalk, mesendodermal cell migration in zebrafish, olfactory placode assembly (Shiau et al., 2008; Li et al., 2005; Raz 2004; David et al., 2002). Loss of sdf1a

chemokine in zebrafish also leads to defective assembly of trigeminal placode very similar to the defects we observed in *itga5* morphants (Knaut et al., 2005). Based on other published reports, I speculate that either Itga5 may be downstream of chemokine receptor Cxcr4b or there might be a cross talk between chemokine receptor and Itga5 on the cell surface (Hartmann et al., 2005; Nair and Schilling 2008). The latter is supported by the observation that downstream targets of both chemokine receptors and itga5 are similar. For example, both chemokine receptors and integrins lead to actin polymerization, activation of several G proteins and Ras-MAPK pathways. Knockdown of a chemokine expressed in otic placode, Cxcl14 (Long et al., 2000), gave no discernible otic phenotype possibly due to redundancy. We speculate that Itga5 could be acting downstream or together with chemokine signaling in posterior placodes to mediate proper assembly of placodes. Apart from secreted ligands, cells also migrate directionally in response to increasing gradients of extracellular matrix molecules, also called as haptotaxis. One of the major ECM proteins that Itga5 binds is fibronectin, which is expressed at high levels in the mesoderm and also in the ectoderm at the time of placodal morphogenesis (Trinh and Stainier 2004; Mould et al., 2009; unpublished observations). Thus, due to compromised binding to ECM, *itga5* morphant cells may not be able to respond to this adhesive gradient cue in the extra cellular environment.

Directional migration of cells also entails the establishment of polarity across the leading and trailing edges of the cell. Integrins regulates cell polarity by causing spatially restricted polymerization of actin monomers on the leading edge resulting in filopodial or lamellipodial protrusions propelling the cells in a directional manner (Liu

2000; Hynes, 2002; Schwatz and Ginsberg, 2002). Therefore, the defects in directional migration of placodal precursors in *itga5* morphants could result from de-localized synthesis of actin cytoskeleton causing cells to change their direction frequently during migration. Such defects have been shown to occur in *itga5* deficient mesoderm cells in *Xenopus* (Davidson et al., 2006; Bhat and Riley, 2011). Therefore, it is possible that defective migration is a consequence of delocalized synthesis of actin cytoskeleton.

Integrin binding to extracellular matrix can also regulate the localization of cell-cell adherens junctions to the apical side (Trinh and Staineir,2004). Due to defective cadherin localization in fibronectin mutants, the cardiac precursors do not migrate properly leading to cardiac bifidia. Recently, N-cadherin has also been implicated in the assembly of trigeminal and epibranchial ganglia (Shiau et al., 2008; Shiau et al., 2009). However, the relationship of N-cadherin to Integrins in this developmental context is unclear. One of the cadherins that is expressed in the otic precursors is E-cadherin. It would be interesting to find out if *itgs5* regulates membrane localization of E-cadherin which could subsequently lead to cell migration defects of otic precursors in *itga5* mutants.

Another interesting candidate that could mediate otic cell migration in addition to its established role in otic differentiation is Fgf (Philips et al., 2001; Philips et al., 2003; Padanad et al., 2012). Fgf has been implicated in mesodermal migration in *Drosophila*, lateral line migration in zebrafish and pronephric migration in mice (McMahon et al., 2010; Nechiporuk and Raible 2008; Chi et al., 2009; Sai and Ladher 2008). We found that *itga5* enhances overall levels of Fgf signaling in the otic/epibranchial domain (Bhat

and Riley, 2011). Reports in other developmental contexts suggest that integrins can enhance MAPK signaling by promoting phosphorylation of downstream components of MAPK pathway or by physically complexing with Fgf receptors (See Introduction). Consistent with these studies, we found that apoptosis in otic and epibranchial precursors of *itga5* morphants could be rescued to wild type levels by elevating overall Fgf signaling. However, the cell migration defects of *itga5* morphants were not rescued because of global overexpression of Fgf pathway. However, a localized ectopic source of Fgf signal could reveal whether Fgf also plays a role of a chemokine during otic placode morphogenesis. However, these experiments could get complicated because Fgf could lead to increased specification of new otic cells in the vicinity of the ectopic source given that Fgf is both necessary and sufficient for otic specification (Philips et al., 2001; Philips et al., 2004; Padanad et al., 2012).

Distinguishing otic and non-otic *pax2a* positive domains

In our time-lapse recordings, we observed partitioning of the final *pax2a* field into otic and non-otic domains. We found that the non-otic *pax2a* positive cells are recruited later (12.7-13.5hpf) into the non-otic domain suggesting some intrinsic differences in the late recruited non-otic *pax2a* positive cells (Bhat and Riley, 2011). Wnt signaling has recently been shown to favor the development of otic placode at the expense of epibranchial at these stages (Ohyama et al., 2006; McCaroll et al., 2012; Freter et al., 2008) while Fgf signaling is essential for both otic and epibranchial specification (Sun et al., 2007; Nechiporuk et al., 2007; Padanad and Riley 2011). It would be interesting to

find if a combination of Wnt and Fgf signals leads to the activation of different adhesion protein or upregulate already present E-cadherin in otic cells as compared to the late recruited epibranchial precursors. This would prevent non-otic cells from joining the otic placode. Such changes in the type of cadherins are most evident during mesodermal cell migration in *Drosophila* where these cells downregulate E-cadherin and upregulate N-cadherin during epithelial to mesenchymal transition (Oda et al., 1998). Eph receptor and ephrin ligands are another interesting candidates that mediate cell-cell repulsion during axon pathfinding, maintenance of rhombomeric and somitic boundaries (Cooke et al., 2005; Kemp et al., 2009; Murai and Pasquale 2003; Barrios et al., 2003). A similar ephrin mediated process may exclude newly recruited *pax2a* cells from the otic domain.

CONCLUSIONS

On the whole this dissertation unravels the molecular mechanism for PPE specification and the role of integrin alpha 5 in mediating the morphogenesis of posterior PPE into individual placodes. This work describes the importance of setting up genetic competence in progenitor cells for subsequent activation by secreted ligands. It also describes how signaling interactions between different tissues ensures correct and reproducible positioning and specification of tissues in spatially and temporally controlled manner. Mechanisms linking cell signaling with cell migration to ensure proper morphogenesis are also described. Future goals would be to determine other novel players that contribute to placode morphogenesis and specification and would aid in finding a cure for deafness and vestibular defects.

REFERENCES

Ahrens, K., Schlosser, G., 2005. Tissues and signals involved in the induction of placodal *Six1* expression in *Xenopus*laevis. Dev. Biol. 288, 40-59.

Akimenko, M. A., Ekker, M., Wegner, J., Lin, W., Westerfield, M., 1994. Combinatorial expression of three zebrafish genes related to Distal-less: part of a homeobox gene code for the head. J. Neurosci 14, 3475–3486.

Alvarez, Y., Alonso, M. T., Vendrell, V., Zelarayan, L. C., Chamero, P., et al., 2003. Requirements for FGF3 and FGF10 during inner ear formation. Development 130, 6329-38.

Andermann, P., Ungos, J., Raible, D., 2002. Neurogenin1 defines zebrafish cranial sensory ganglia precursors. Dev. Biol. 251, 45–58.

Anton, E. S., Kreidberg, J.A., Rakic, P., 1999. Distinct functions of alpha3 and alpha(v) integrin receptors in neuronal migration and laminar organization of the cerebral cortex. Neuron 22, 277–289.

Aplin, A. E., Stewart, S. A., Assoian, R. K., Juliano, R. L., 2001. Integrin-mediated adhesion regulates ERK nuclear translocation and phosphorylation of Elk-1. J. Cell Biol. 153, 273–82.

Artinger, K. M., Fedtsova, N., Rhee, J.M., Bronner-Fraser, M., Turner, E., 1998. Placodal Origin of Brn-3–Expressing Cranial Sensory Neurons. J. Neurobiol. 15, 572-585.

Bailey, A. P., Bhattacharyya, S., Bronner-Fraser, M., Streit, A., 2006. Lens specification is the ground state of all sensory placodes, from which FGF promotes olfactory identity. Dev. Cell 11, 505-517.

Bailey, A. P, Streit A., 2006. Sensory organs: making and breaking the pre-placodal region.Curr. Top Dev. Biol. 72, 167-204.

Baker, C. V. H., Bronner-Fraser, M., 2000. Vertebrate cranial placodes I. Embryonic induction. Dev. Biol. 232, 1-61.

Baker, C. V. H., Stark, M.R., Bronner-Fraser, M., 2002. Pax3-Expressing Trigeminal Placode Cells Can Localize to Trunk Neural Crest Sites but Are Committed to a Cutaneous Sensory Neuron Fate. Dev. Biol. 249, 219-236.

Bakkers, J., Hild, M., Kramer, C., Furutani-Seiki, M., Hammerschmidt, M., 2002. Zebrafish *ΔMp63* is a direct target of Bmp signaling and encodes a transcriptional repressor blocking neural specification in the ventral ectoderm. Dev. Cell 2, 617–627.

Barembaum, M., Bronner-Fraser, M., 2005. Early steps in neural crest specification. Semin. Cell Dev. Biol. 16; 642-646.

Barkai, N., Shilo, B-Z., 2009. Robust Generation and Decoding of Morphogen Gradients. Cold Spring Harb Perspect Biol. 1, a001990.

Barrios, A., Poole, R. J., Durbin, L., Brennan, C., Holder, N., et al., 2003. Eph/Ephrin Signaling Regulates the Mesenchymal-to-Epithelial Transition of the Paraxial Mesoderm during Somite Morphogenesis. Curr. Biol. 13, 1571–1582.

Barth, K. A., Kishimoto, Y., Rohr, K. B., Seydler, C., Schulte-Merker, S., et al., 1999. Bmp activity establishes a gradient of positional information throughout the entire neural plate. Development 126, 4977–4987.

Basch, M. L., Bronner-Fraser, M., Barcía-Castro, M. I., 2006. Specification of the neural crest occurs during gastrulation and requires Pax7. Nature 441, 218–222.

Bastidas, F., De Calisto, J., Mayor, R., 2004. Identification of neural crest competence territory: role of Wnt signaling. Dev. Dyn. 229, 109-117.

Baum, P. D., Garriga, G., 1997. Neuronal migrations and axon fasciculation are disrupted in ina-1 integrin mutants. Neuron. 19, 51-62.

Begbie, J., Brunet, J. F., Rubenstein, J. L., Graham, A., 1999. Induction of the epibranchial placodes. Development 126, 895–902.

Begbie, J., Graham, A., 2001. Integration between the epibranchial placodes and the hindbrain. Science 294, 595-598.

Bhattacharyya, S., Bailey, AP., Bronner-Fraser, M., Streit, A., 2004. Segregation of lens and olfactory precursors from a common territory: cell sorting and reciprocity of Dlx5 and Pax6 expression. Dev. Biol. 271, 403–414.

Bökel, C., Brown, N. H., 2002. Integrins in development: moving on, responding to, and sticking to the extracellular matrix. Dev. Cell 3, 311-321.

Brenner, D., Mak, T. W., 2009. Mitochondrial cell death effectors. Curr. Opin. Cell Biol. 21, 871–877.

Bricaud, O., Collazo, A., 2006. The transcription factor six1 inhibits neuronal and promotes hair cell fate in the developing zebrafish (Danio rerio) inner ear. J Neurosci. 26, 10438-10451.

Brower, D. L., Jaffe, S. M., 1989. Requirement for integrins during *Drosophila* wing development. Nature 342, 285–287.

Brugmann, S. A., Pandur, P. D., Kenyon. K. L., Pignoni F., Moody, S. A., 2004. Six1 promotes a placodal fate within the lateral neurogenic ectoderm by functioning as both a trancriptional activator and repressor. Development 131, 5871-5881.

Brugmann, S. A., Moody, S.A., 2005. Induction and specification of the vertebrate ectodermal placodes: precursors of the cranial sensory organs. Biol. Cell 97, 303–319.

Canning, C. C., Lee , L., Luo, ,S., Graham A., Jones, M., 2008. Neural tube derived Wnt signals cooperate with FGF signaling in the formation and differentiation of the trigeminal placodes. Neural Dev. 3, 35.

Carballada, R., Yasuo, H., Lemaire, P. H., 2001. Phosphatidylinositol-3 kinase acts in parallel to the ERK MAP kinase in the FGF pathway during *Xenopus* mesoderm induction. Development 128, 35–44.

Carmona-Fontaine, C., Acuna, G., Ellwanger, K., Niehrs, C., Mayor, R., 2007. Neural crests are actively precluded from the anterior neural fold by a novel inhibitory mechanism dependent on Dickkopf1secreted by the prechordal mesoderm. Dev. Biol. 309, 208-221.

Chen, B., Kim, E. H., Xu, P. X., 2009. Initiation of olfactory placode development and

neurogenesis is blocked in mice lacking both Six1 and Six4. Dev. Biol. 326, 75–85.

Chi, X., Michos, O., Shakya, R., Riccio, P., Enomoto, H., et al., 2008. Ret-Dependent Cell Rearrangements in the Wolffian Duct Epithelium Initiate Ureteric Bud Morphogenesis. Dev. Cell 17, 199-209.

Chiarugi, P., Giannoni, E., 2008. Anoikis: A necessary death program for anchorage-dependent cells. Biochem. Pharmaco. 76, 1352-1364.

Chodniewicz, D., Klemke, R. L., 2004. Guiding cell migration through directed extension and stabilization of pseudopodia. Exp. Cell. Res. 301, 31–37.

Cirillo, L. A., Lin, F. R., Cuesta, I., Friedman, D., Jarnik, M., Zaret, K. S., 2002. Opening of compacted chromatin by early developmental transcription factors HNF3 (FoxA) and GATA-4. Mol. Cell. 9, 279-289.

Cirillo, L. A., Zaret, K. S.,1999. An early developmental transcription factor complex that is more stable on nucleosome core particles than on free DNA. Mol. Cell. 4, 961-969.

Cooke, J. E., Kemp, H. A., Moens, C. B., 2005. EphA4 Is Required for Cell Adhesion and Rhombomere-Boundary Formation in the Zebrafish. Curr. Biol. 15, 536-542.

Cornell, R. A., Eisen, J. S., 2000. Delta signaling mediates segregation of neural crest and spinal sensory neurons from zebrafish lateral neural plate. Development 127, 2873-82.

Cornell, R.A., Eisen, J.S., 2002. Delta/Notch signaling promotes formation of zebrafish neural crest by repressing Neurogenin 1 function. Development 129, 2639-2648.

Crump, J. G., Swartz, M. E., Kimmel, C. B., 2004. An integrin-dependent role of pouch endoderm in hyoid cartilage development. Plos Biology 2, 1432–1445.

Culbertson, M. D., Lewis, Z. R., Nechiporuk, A.V., 2011. Chondrogenic and gliogenic subpopulations of neural crest play distinct roles during the assembly of epibranchial ganglia. Plos One 6, e24443.

David, N. B, Sapede, D., Saint-Etienne, L., Thisse, C., Thisse, B., et al., 2002. Molecular basis of cell migration in the fish lateral line: Role of the chemokine receptor CXCR4 and of its ligand, SDF1. Proc. Nat. Aca. Sci. 99, 16297–16302.

Davidson, L.A., Marsden, M., Keller, R., Desimone, D. W., 2006. Integrin alpha5beta1 and fibronectin regulate polarized cell protrusions required for *Xenopus* convergence and extension. Curr Biol. 16, 833-844.

de Crozé, N., Maczkowaiak, R., Monsoro-Burq, H., 2011. Reiterative AP2a activity controls sequential steps in the neural crest gene regulatory network. Proc. Natl. Acad. Sci. USA 108, 155-160.

De Robertis, E. M., 2006. Spemann's organizer and self regulation in amphibian embryos. Nat. Rev. 7, 296-301.

Dosch, R., Gwantka, V., Delius, H., Blumenstock, C., Niehrs, C., 1997. Bmp-4 acts as a morphogen in dorsoventral mesoderm patterning in Xenopus. Development 124, 2325-2334.

Duggan, C. D., DeMaria, S., Baudhuin, A., Stafford, D., Ngai, J., 2008. *Foxg1* is Required for Development of the Vertebrate Olfactory System. J. Neurosci. 28, 5229-5239.

Dutta, S., Dietrich, JE., Aspöck, G., Burdine, RD., Schier, A., et al., 2005. *pitx3* defines an equivalence domain for lens and anterior pituitary placode. Development 132, 1579–1590.

Esterberg, R., Fritz, A., 2008. *dlx3b/4b* are required for the formation of preplacodal region and otic placode through modulation of Bmp activity. Dev. Biol. 325, 189-199.

Faber, S. C., Dimanlig, P., Makarenkova, H. P., Shirke, S. Ko., K. Lang, R. A., 2001. Fgf receptor signaling plays a role in lens induction. Development 128, 4425–38.

Fan, T-J., Han, L-H., Cong, R-S., Liang, J., 2005. Caspase Family Proteases and Apoptosis. Acta Biochimica et Biophysica Sinica 37, 719–727.

Freter, S., Muta, Y., Mak, S. S., Rinkwitz, S., Ladher, R. K., 2008. Progressive restriction of otic fate: the role of FGF and Wnt in resolving inner ear potential. Development 135, 3415-3424.

Fürthauer, M., Reifers, F., Brand, M., Thisse, B., Thisse, C., 2001. *sprouty4* acts in vivo as a feedback-induced antagonist of FGF signaling in zebrafish. Development 128, 2175–2186.

Garcia, C. M., Huang, J., Madakashira, B. P., Liu, Y., Rajagopal, R., et al, 2011. The function of FGF signaling in the lens placode. Dev. Biol. 351, 176-185.

Giancotti, F. G., Ruoslahti, E., 1999. Integrin Signaling. Science 285, 1028-1033.

Gilcrease, M. Z., 2007. Integrin signaling in epithelial cells. Cancer Lett 247, 1–25.

Glavic, A., Maris Honore, S., Gloria Feijoo, C., Bastidas, F., Allende, M. L., Mayor, R., 2004. Role of BMP signaling and the homeoprotein Iroquois in the specification of the cranial placodal field. Dev. Biol. 272(1), 89-103.

Grocott, T., Tambalo, M., Streit, A., 2012. The peripheral sensory nervous system in the vertebrate head: a gene regulatory perspective. Dev. Biol. 370, 3-23.

Goh, K. L.,Yang , J. T., Hynes, R. O., 1997. Mesodermal defects and cranial neural crest apoptosis in alpha5 integrin-null embryos. Development. 124, 4309-4319.

Hamidouche, Z., Fromigue, O., Ringe, J., Haupl, T., Vaudin, P., et al., 2009. Priming integrin alpha5 promotes human mesenchymal stromal cell osteoblast differentiation and osteogenesis. Proc. Natl. Acad. Sci. 106, 18587–18591.

Hans, S., Liu, D., Westerfield, M., 2004. Pax8 and Pax2a function synergistically in otic specification, downstream of the Foxi1 and Dlx3b transcription factors. Development 131, 5091–5102.

Hans, S., Christison, J., Liu, D., Westerfield, M., 2007. Fgf-dependent otic induction requires competence provided by Foxi1 and Dlx3b. BMC Dev. Biol. 7, 5.

Hartmann, T. J, Burger, J. A., Glodek, A., Fujii3, N., Burger, M., 2005. CXCR4 chemokine receptor and integrin signaling co-operate in mediating adhesion and chemoresistance in small cell lung cancer (SCLC) cells. Oncogene 24, 4462–71.

Hehlgans, S., Haase, M., Cordes, N., 2007. Signalling via integrins: Implications for cell survival and anticancer strategies. Biochimica. Et Biophysica. Acta-Reviews on Cancer 1775, 163–180.

Herzog, W., Zeng, X., Lele, Z., Sonntag, C., Ting, J. W., Chang, C. Y., Hammerschmidt, M., 2003. Adenohypophysis formation in the zebrafish and its dependence on sonic hedgehog. Dev. Biol. 254, 36-49.

Hirsch, E., Barberis, L., Brancaccio, M., Azzolino, O., Xu, D. Z., et al., 2002. Defective Rac-mediated proliferation and survival after targeted mutation of the beta(1) integrin cytodomain. J. Cell Biol. 157, 481–492.

Hoang, B., Chiba, A., 1998. Genetic analysis on the role of integrin during axon guidance in *Drosophila*. J. Neurosci. 18 , 7847–7855.

Hoffman, T. L., Javier, A. L., Campeau, S.A., Knight, R. D., Schilling, T. F., 2007. Tfap2 transcription factors in zebrafish neural crest development and ectodermal evolution. J. Exp. Zool. 308B, 679-691.

Huang, X., Saint-Jeannet, J-P., 2004. Neural crest induction and the opportunities of life on the edge. Dev. Biol. 275, 1-11.

Hynes, RO., 2002. Integrins: bidirectional, allosteric signaling machines. Cell 110, 673-687.

Ikeda, K., Ookawara, S., Sato, S., Ando, Z., Kageyama, R., Kawakami, K., 2007. Six1 is essential for early neurogenesis in the development of olfactory epithelium. Dev. Biol. 311, 53–68.

Ikeda, K., Kageyama, R., Suzuki, Y., Kawakami, K., 2010. Six1 is indispensable for production of functional progenitor cells during olfactory epithelial development. Int. J. Dev. Biol. 54, 1453–1464.

James, B. P., Bunch, T. A., Krishnamoorthy, S., Perkins, L. A., Brower, D. L., 2007. Nuclear localization of the ERK MAP kinase mediated by *Drosophila* alphaPS2betaPS integrin and importin-7. Mol. Biol. Cell 18, 4190–4199.

Jin, H., Fisher, M., Grainger, R. M., 2012. Defining Progressive Stages in the Commitment Process Leading to Embryonic Lens Formation. Genesis 00, 1-13.

Jones, C. M, Smith, J. C., 1998. Establishment of a BMP-4 morphogen gradient by long-range inhibition. Dev. Biol. 194, 12-17.

Jülich, D., Geisler, R., Holley, S. A., 2005. Integrinalpha5 and delta/notch signaling have complementary spatiotemporal requirements during zebrafish somitogenesis. Dev. Cell 8, 575–586.

Kaji, T., Artinger, K. B., 2004. *dlx3b* and *dlx4b* function in development of Rohon-Beard sensory neurons and trigeminal placode in the zebrafish neurula. Dev. Biol. 276, 523–540.

Karis, A., Pata, I., van Doorninck, J. H., Grosveld, F., de Zeeuw, C. I., de Caprona, D., Fritzsch, B., 2001. Transcription factor GATA-3 alters pathway selection of olivochochlear neurons and affects morphogenesis of the ear. J. Comp. Neurol. 429, 615-630.

Katz, B. Z., Yamada, K. M., 1997. Integrins in morphogenesis and signaling. Biochimie. 79, 467-476.

Kawamura, K., Kouki, T., Kawahara, G., Kikuyama, S., Hypophyseal Development in Vertebrates from Amphibians to Mammals. General and Comparative Endocrinology 126, 130-135.

Kelsh, R. N., Dutton, K., Medlin, J., Wisen, J. S., 2000. Expression of zebrafish *fkd6* in neural crest-derived glia. Mech. Dev. 93, 161–164.

Kemp, H. A., Cooke, J. E., Moens, C. B., 2009. EphA4 and EfnB2a maintain rhombomere coherence by independently regulating intercalation of progenitor cells in the zebrafish neural keel. Dev Biol. 15, 313-326.

Kimmel, C. B., Ballard, W. W., Kimmel, S. R., Ullmann, B., Schilling, T. F., 1995. Stages of embryonic development of the zebrafish. Dev. Dyn. 203, 253-310.

Kishimoto, Y., Lee, KH., Zon, L., Hammerschmidt, M., Schulte-Merker, S., 1997. The molecular nature of zebrafish *swirl*: BMP2 function is essential during early dorsoventral patterning. Development 124, 4457–4466.

Knaut. H., Blader, P., Strähle, U., Schier, A. F., 2005. Assembly of trigeminal sensory ganglia by chemokine signaling. Neuron 47, 653–666.

Knight, R. D., Nair, S., Nelson, S. S., Afshar, A., Javidan, Y., et al., 2003. *lockjaw* encodes a zebrafish *tfap2a* required for early neural crest development. Development 130, 5755-5768.

Knight, R. D., Javidan, Y., Zhang, T., Nelson, S., Schilling, T. F., 2005. AP2-dependent signals from ectoderm regulate craniofacial development in the zebrafish. Development 132, 3127-3138.

Kobayashi, M., Osanai, H., Kawakami, K., Yamamoto, M., 2000. Expression of three zebrafish Six4 genes in the cranial sensory placodes and the developing somites. Mech Dev 9, 151–155.

Koshida, S., Kishimoto, Y., Ustumi, H., Shimizu, T., Furutani-Seiki, M., et al., 2005. Integrinalpha5-dependent fibronectin accumulation for maintenance of somite boundaries in zebrafish embryos. Dev. Cell 8, 587–598.

Krauss, S., Johansen, T., Korzh, V., Fjose, A., 1991. Expression of the zebrafish paired box genes *pax[zf-b]* during early neurogenesis. Development 113, 1193–1206.

Kollmar, R., Nakamura, SK., Kappler, JA., Hudspeth, AJ., 2001. Expression and phylogeny of claudins in vertebrate primordia. Proc. Natl. Acad. Sci. 98, 10196–10201.

Kudoh, T., Concha, ML., Houart, C., Dawid, IB., Wilson, SW., 2004. Combinatorial Fgf and Bmp signalling patterns the gastrula ectoderm into prospective neural and epidermal domains. Development 131, 3581–3592.

Kulesa, P. M.**,** Gammill, L. S., 2010. Neural crest migration: patterns, phases and signals. Dev. Biol. 344, 566-568.

Kwon, H. J., Riley, B. B., 2009. Mesendodermal signals required for otic induction: Bmp-antagonists cooperate with Fgf and can facilitate formation of ectopic otic tissue. Dev. Dyn. 238, 1582-1594.

Kwon, H. J., Bhat, N., Sweet, E. M., Cornell, R. A., Riley, B. B., 2010. Identification of early requirements for preplacodal ectoderm and sensory organ development. PLoS Gen. 6(9), e1001133.

Ladher, R.K., Anakwe, K.U., Gurney, A.L., Schoenwolf, G.C., Francis-West, P.H., 2000. Identification of synergistic signals initiating inner ear development. Science 290, 1965–1968.

Ladher, R. K., O'Neill, P.O., Begbie, J., 2010. From shared lineage to distinct functions: the development of the inner ear and epibranchial placodes. Development 137, 1777-1785.

Lassiter, R. N., Dude, C. M., Reynolds, S. B, Winters, N. I., Baker, C.V.H, et al., 2007. Canonical Wnt signaling is required for ophthalmic trigeminal placode cell fate determination and maintenance. Dev. Biol. 308, 392-406.

Lee, H., Kimelman, D., 2002. A dominant-negative form of *p63* is required for epidermal proliferation in zebrafish. Dev. Cell 2, 607–616.

Lee, S. A., Shen, E. L., Fiser, A., Sali, A., Guo, S., 2003. The zebrafish forkhead transcription factor Foxi1 specifies epibranchial placode-derived sensory neurons. Development 130, 2669-2679.

Léger, S., Brand, M., 2002. Fgf8 and Fgf3 are required for zebrafish ear placode induction, maintenance and inner ear patterning. Mech. Dev. 119, 91–108.

Lewis, J. L., Bonner, J., Modrell, M., Ragland, J. W., Moon, R. T., et al., 2004. Reiterated Wnt signaling during zebrafish neural crest development. Development 131, 1299-1308.

Li, Q., Shirabe, K., Thisse, C.,Thisse, B., Okamoto, H., et al., 2005. Chemokine Signaling Guides Axons within the Retina in Zebrafish. J. Neurosci. 25, 1711-1717.

Li, W., Cornell, R. A., 2007. Redundant activities of Tfap2a and Tfap2c are required for neural crest induction and development of other non-neural ectoderm derivatives in zebrafish embryos. Dev. Biol. 304, 338-354.

Litsiou, A., Hanson, S., Streit, A., 2005. A balance of FGF, BMP and WNT signalling positions the future placode territory in the head. Development 132, 4051-4062.

Liu, S., Calderwood, D.A., Ginsberg, M. H., 2000. Integrin cytoplasmic domain-binding proteins. J. Cell Sci. 113, 3563–3571.

Liu, L., Korzh, V., Bablsubramaniyan, N. V., Ekker, M., 2002. Platelet-derived growth factor A (*pdgf-a*) expression during zebrafish embryonic development. Dev. Genes Evol. 212, 298–301.

Liu, D., Chu, H., Maves, L., Yan, Y. L., Morcos, P. A., et al., Postlethwait, J. H., Westerfield, M., 2003. Fgf3 and Fgf8 depdendent and independent transcription factors are required for otic plaocde specification. Development 130, 213-2224.

Long, Q. M., Quint, E., Lin, S., Ekker, M., 2000. The zebrafish *scyba* gene encodes a novel CXC-type chemokine with distinctive expression patterns in the vestibulo-acoustic system during embryogenesis. Mech. of Dev. 97, 183–186.

Luo, T., Lee, Y. H., Saint-Jeannet, J. P., Sargent, T. D., 2003. Induction of neural crest in *Xenopus*by transcription factor AP2α. Proc. Natl. Acad. Sci. USA 100, 532-537.

Ma, H., Blake, T., Chitnis. A., Liu, P., Balla, T., 2009. Crucial role of phosphatidylinostitol 4-kinase IIIalpha in development of zebrafish pectoral fin is linked to phosphoinositide 3-kinase and FGF signaling. J. Cell Sci. 122, 4303–4310.

Mackereth, M. D., Kwak, S. J., Fritz, A., Riley, B. B., 2005. Zebrafish *pax8* is required for otic placode induction and plays a redundant role with Pax2 genes in the maintenance of the otic placode. Development 132, 371–382.

Mancilla, A., Mayor, R.,1996. Neural crest formation in *Xenopuslaevis*: mechanisms of *Xslug* induction. Dev. Biol. 177, 580-589.

Marchant, L., Linker, C., Ruiz, P., Guerrero, N., Mayor, R., 1998. The inductive properties of mesoderm suggest that the neural crest cells are specified by a BMP gradient. Dev. Biol. 198, 319–329.

Maroon, H., Walshe, J., Mahmood, R., Kiefer, P., Dickson, C., Mason, I., 2002. Fgf3 and Fgf8 are required together for formation of the otic placode and vesicle. Development. 129, 2099–2108.

Marsden, M., DeSimone, D.W., 2001. Regulation of cell polarity, radial intercalation and epiboly in Xenopusnovel roles for integrin and fibronectin. Development 128, 3635–3647.

Martin-Bermudo, M. D., Brown, N. H., 1999. Uncoupling integrin adhesion and signalingthe betaPS cytoplasmic domain is sufficient to regulate gene expression in the *Drosophila* embryo. Genes Dev. 13, 729–739.

Martin-Bermudo, M. D., 2000. Integrins modulate the Egfr signaling pathway to regulate tendon cell differentiation in the *Drosophila* embryo. Development 127, 2607–2615.

Martin, K., Groves, A. K., 2006. Competence of cranial ectoderm to respond to Fgf signaling suggests a two-step model of otic placode induction. Development. 133, 877-887.

Maves, L., Jackman, W., Kimmel, C. B., 2002. FGF3 and FGF8 mediate a rhombomere 4 signaling activity in the zebrafish hindbrain. Development 129, 3825–3837.

Mayer, U., Saher, G., Fassler, R., Bornemann, A., Echtermeyer, F., et al., 1997. Absence of integrin alpha 7 causes a novel form of muscular dystrophy. Nat. Genet. 17, 318–323.

Mayor, R., Morgan, R., Sargent, M. G., 1995. Induction of the prospective neural crest of *Xenopus*. Development 121, 767-777.

McCabe, K. L., Shiau, C. E., Bronner-Fraser, M., 2007. Identification of Candidate Secreted Factors Involved in Trigeminal Placode Induction. Dev. Dyn. 236, 2925–2935.

McCabe, K. L., Bronner-Fraser, M., 2008. Essential role for PDGF signaling in ophthalmic trigeminal placode induction. Development 135, 1863-1874.

McCarroll, M. N., Lewis, Z. R., Culbertson, M. D., Martin, B. L., Kimelman, D., et al., 2012. Graded levels of Pax2a and Pax8 regulate cell differentiation during sensory placode formation. Development. 139, 2740-2750.

McLarren, K. W., Litsiou, A., Streit, A., 2003. DLX5 positions the neural crest and preplacode region at the border of the neural plate. Dev. Biol. 259, 34-47.

McLennan, R., Teddy, J. M., Kasemeier-Kulesa, J. C., Romine, M. H., Kulesa, P. M., 2010. Vascular endothelial growth factor (VEGF) regulates cranial neural crest migration *in vivo*. Dev Biol. 339, 114-125.

McLennan, R., Dyson, L., Prather, K. W., Morrison, J.A., Baker, R. E., et al., 2012. Multiscale mechanisms of cell migration during development: theory and experiment Development 139, 2935-2944.

McMahon, A., Supatto, W., Fraser, S. E., Stathopoulos, A. 2008. Dynamic analyses of *Drosophila* gastrulation provide insights into collective cell migration. Science. 322, 1546-1550.

Millimaki, B. B., Sweet, E. M., Riley, B. B., 2010. Sox2 is required for maintenance and regeneration, but not initial development, of hair cells in the zebrafish inner ear. Dev Biol 338, 262–267.

Minoux, M., Rijli, F. M., 2010. Molecular mechanisms of cranial neural crest cell migration and patterning in craniofacial development. Development 137, 2605-2621.

Miyasaka, N., Knaut, H., Yoshihara, Y., 2007. Cxcl12/Cxcr4b chemokine signaling is required for placode assembly and sensory axon pathfinding in the zebrafish olfactory system. Development 134, 2459–2468.

Monsoro-Burq, A. H., Fletcher, R. B., Harland, R. M., 2003. Neural crest induction by paraxial mesoderm in *Xenopus*embryos requires FGF signals. Development 130, 3111-31124.

Montera, JA., Kilian, B., Chan, J., Bayliss, PE., Heisenberg, CP., 2003. Phosphoinositide 3-kinase is required for process outgrowth and cell polarization of gastrulating mesendodermal cells. Curr. Biol. 13, 1279–1289.

Montero-Balaguer, M., Lang, M. R., Weiss Sachdev, S., Knappmeyer, C., Stewart. R A., et al., 2006. The *mother superior* mutation ablates *foxd3* activity in neural crest progenitor cells and depletes neural crest derivatives in zebrafish. Dev. Dyn. 235, 3199–3212.

Mori, S., Wu, C. Y., Yamaji, S., Saegusa, J., Shi, B., et al., 2003. Direct binding of integrin alphavbeta3 to FGF1 plays a role in FGF1 signaling. J. Biol. Chem. 283, 18066–18075.

Mould, A. P., Koper, E. J., Byron, A., Zahn, G., Humphries, M. J., 2009. Mapping the ligand-binding pocket of integrin alpha5beta1 using a gain-of-function approach. Biochem. J. 424, 179–89.

Mullins, M. C., Hammerschmidt, M., Kane, D. A., Odenthal, J., Brand, M., et al., 1996. Genes establishing dorsoventral pattern formation in the zebrafish embryo: the ventral specifying genes. Development 123, 81–93.

Murai, K. K., Pasquale, E. B., 2003. Eph'ective signaling: forward, reverse and crosstalk. J. Cell Sci. 116, 2823-2832.

Nair, S., Schilling, T. F., 2008. Chemokine Signaling Controls Endodermal Migration During Zebrafish Gastrulation. Science. 322, 89-92.

Nakayama, T., Cui, Y., Christian, J. L., 2000. Regulation of BMP/Dpp signaling during embryonic development. Cell. Mol. Life Sci. 57, 943–956.

Neave, B., Rodaway, A., Wilson, S. W., Patient, R., Holder, N., 1995. Expression of zebrafish GATA 3 (*gata3*) during gastrulation and neurulation suggests a role in the specification of cell fate. Mech. Dev. 51, 169-182.

Neave, B., Holder, N., Patient, R., 1997. A graded response to BMP-4 spatially coordinates patterning of the mesoderm and ectoderm in the zebrafish. Mech Dev 62, 183–195.

Nechiporuk, A., Linbo, T., Raible, D.W., 2005. Endoderm-derived Fgf3 is necessary and sufficient for inducing neurogenesis in the epibranchial placodes in zebrafish. Development 132, 3717–3730.

Nechiporuk, A., Linbo, T., Poss, K. D., Raible, D. W., 2007. Specification of epibranchial placodes in zebrafish. Development 134, 611-623.

Nechiporuk, A., Raible, D. W., 2008. FGF-Dependent Mechanosensory Organ Patterning in Zebrafish. Science 320, 1774-1777.

Neumann, M., Affolter, M., 2006. Remodelling epithelial tubes through cell rearrangements: from cells to molecules. EMBO reports 7, 36-40.

Newman Jr., S. M., Wright, T. R., 1981. A histological and ultrastructural analysis of developmental defects produced by the mutation, lethal (1)myospheroid, in *Drosophila* melanogaster. Dev. Biol. 86, 393–402.

Nguyen, V. H., Schmid, B., Trout, J., Connors, S. A., Ekker, M., Mullins, M. C., 1998. Ventral and lateral regions of the zebrafish gastrula, including the neural crest progenitors, are established by a *bmp2b/swirl* pathway of genes. Dev. Biol. 199, 93-110.

Nikaido, M., Doi, K., Shimizu, T., Hibi, M., Kikuchi, Y., et al., 2007. Initial specification of the epibranchial placode in zebrafish embryos depends on the fibroblast growth factor signal. Dev Dyn 236, 564–571.

Nikitina, N., Sauka-Spengler, T., Bronner-Fraser, M., 2008. Dissecting early regulatory relationships in the lamprey neural crest gene network. Proc. Natl. Acad. Sci. USA 105, 20083-20088.

Nissen R. M., Yan, J., Amsterdam, A., Hopkins, N., Burgess, S. M., 2003. Zebrafish *foxi one* modulates cellular responses to Fgf signaling required for the integrity of ear and jaw patterning. Development 130, 2543-2554.

Obholzer, N., Wolfson, S., Trapani, J. G., Mo, W., Nechiporuk, A., et al., 2008. Vesicular glutamate transporter 3 is required for synaptic transmission in zebrafish hair cells. J Neourosc 28, 2110–2118.

O'Brien, E. O., d'Alencon, C., Bonde, G., Li, W., Schoenebeck, J., Allende, M. L., Gelb, B. D., Yelon, D., Eisen, J., Cornell, R. A., 2004. Transcription factor Ap-2α is necessary for development of embryonic melanophores, autonomic neurons and pharyngeal skeleton in zebrafish. Dev. Biol. 265,246-261.

Oda, H., Tsukita, S., Takeichi, M., 1998. Dynamic Behavior of the Cadherin-Based Cell–Cell Adhesion System during *Drosophila* Gastrulation. Dev. Biol. 203, 435-450.

Ohyama, T., Mohamed, O. A., Taketo, M. M., Dufort, D., Groves, A. K., 2006. Wnt signals mediate a fate decision between otic placode and epidermis.Development. 133, 865-75.

Ozaki, H., Nakamura, K., Funahashi, J., Ikeda, K., Yamada, G., et al., 2004. Six1 controls patterning of the mouse otic vesicle. Development 131, 551–562.

Padanad, M. S., Riley, B. B., 2011. Pax2/8 proteins coordinate sequential induction of otic and epibranchial placodes through differential regulation of *foxi1, sox3* and *fgf24*. Dev. Biol. 351, 90–98.

Padanad, M. S., Bhat, N., Guo, B., Riley, B. B., 2012. Conditions that influence the response to Fgf during otic placode induction. Dev. Biol. 364, 1-10.

Pandit, T., Jidigam, V. K., Gunhaga, L., 2011. BMP-induced L-Maf regulates subsequent BMP-independent differentiation of primary lens fibre cells. Dev. Dyn. 8, 1917-1928.

Patthey, C., Gunhaga, L., Edlund, T., 2008. Early development of the central and peripheral nervous systems is coordinated by Wnt and Bmp signals. PLoS ONE 3, 31625.

Patthey, C., Gunhaga, L., Edlund, T., 2009. Wnt-regulated temporal control of BMP exposure directs the choice between neural plate border and epidermal fate. Development 136, 73-83.

Petrie, R. J., Doyle, A. D., Yamada, K. M., 2009. Random versus directionally persistent cell migration. Nat. Rev. Mol. Cell Biol. 10, 538–549.

Pfeffer, P.L., Gerster, T., Lun, K., Brand, M., Büsslinger, M., 1998. Characterization of three novel members of the zebrafish Pax2/5/8 family: dependency of Pax5 and Pax8 expression on the Pax2.1 (noi) function. Development 125, 3063–3074.

Picker, A., Scholpp, S., Bohli, H., Takeda, H., Brand, M., 2002. A novel positive transcriptional feedback loop in midbrain-hindbrain boundary development is revealed through analysis of the zebrafish *pax2.1* promoter in transgenic lines. Development 129, 3227–3239.

Pieper, M., Ahrens, K., Rink, E., Peter, A., Schlosser, G., 2012. Differential distribution of competence for panplacodal and neural crest induction to non-neural and neural ectoderm.Development. 139, 1175-1187.

Phillips, B. T., Bolding, K., Riley, B. B., 2001. Zebrafish *fgf3* and *fgf8* encode redundant functions required for otic placode induction. Dev. Biol. 235, 351-365.

Phillips, BT., Kwon, H. Y., Melton, C., Houghtling, P., Fritz, A., et al., 2006. Zebrafish *msxB*, *msxC* and *msxE* function together to refine the neural-nonneural border and regulate cranial placodes and neural crest development. Dev Biol 294, 376–390.

Pieper, M., Ahrens, K., Rink, E., Peter, A., Schlosser, G., 2012. Differential distribution of competence for panplacodal and neural crest induction to non-neural and neural ectoderm. Development 139, 1175-1187.

Pogoda, H. M., Hammerschmidt, M., 2009. How to make a teleost adenohypophysis: molecular pathways of pituitary development in zebrafish. Mol. Cell. Endocrinology 312, 2-13.

Pulkkinen, L., Kimonis, V. E., Xu, Y., Spanou, E. N., McLean, W.H., et al., 1997. Homozygous *alpha6 integrin* mutation in junctional epidermolysis bullosa with congenital duodenal atresia. Hum. Mol. Genet., 6, 669–674.

Pyati, U. J., Webb, A. E., Kimelman, D., 2005. Transgenic zebrafish reveal stage-specific roles for Bmp signaling in ventral and posterior mesoderm development. Development 132, 2333–2343.

Raible, F., Brand, M., 2001. Tight transcriptional control of the ETS domain factors Erm and Pea3 by Fgf signaling during early zebrafish development. Mech. Dev. 107, 105–117.

Raz, E., 2004. Guidance of primordial germ cell migration. Curr. Opin. Cell Biol. 16, 169–173.

Rembold, M., Lahiri, K., Foulkes, N. S., Wittbrodt, J., 2006. Transgenesis in fish: efficient selection of transgenic fish by co-injection with a fluorescent reporter construct. Nature Protocols 1, 1133-1139.

Reversade, B., De Robertis, E. M., 2005. Regulation of ADMP and BMP2/4/7 at opposite embryonic poles generates a self-regulating morphogenetic field. Cell 123, 1147–1160.

Riley, B. B., Phillips, B, 2003. Ringing in the new ear: resolution of cell interactions in otic development. Dev. Biol. 261, 289-312.

Riley, B. B., Sweet, E. M., Heck, R., Evans, A., McFarland, K. N., et al., 2010. Characterization of *harpy/Rca1/emi1* Mutants: Patterning in the Absence of Cell Division. Dev. Dyn. 239, 828–843.

Roehl, H., Nusslein-Volhard, C., 2001. Zebrafish *pea3* and *erm* are general targets of FGF8 signaling. Curr. Biol. 11, 503–507.

Rogers, K. W., Schier, A. F., 2011. Morphogen gradients: from generation to interpretation. Annu. Rev. Cell Dev. Biol. 27, 377-407.

Rusnati, M., Tanghetti, E., Dell'Era, P., Gualandris, A., Presta, M., 1997. alphavbeta3 integrin mediates the cell-adhesive capacity and biological activity of basic fibroblast growth factor (FGF-2) in cultured endothelial cells. Mol. Biol. Cell 8, 2449–2461.

Sahly, I., Andermann, P., Petit, C., 1999. The zebrafish *eya1* gene and its expression pattern during embryogenesis. Dev. Genes Evol 209, 399–410.

Sai, X., Ladher, R. K., 2008. FGF signaling regulates cytoskeletal remodeling during epithelial morphogenesis. Curr Biol. 18, 976-981.

Schlosser, G., 2006. Induction and specification of cranial placodes. Dev. Biol. 294, 303–351.

Schlosser, G., 2010. Making senses: development of vertebrate cranial placodes. Int. Rev. Cell Mol. Biol. 283, 129-234.

Schwartz, M. A., Ginsberg, M. H., 2002. Networks and crosstalk: integrin signalling spreads. Nat Cell Biol. 4, 65-68.

Sheng, G., Stern, CD., 1999. *Gata2* and *Gata3*: novel markers for early embryonic polarity and for non-neural ectoderm in the chick embryo. Mech Dev 87, 213–219.

Shoji, W., Yee, C. S., Kuwada, J. Y., 1998. Zebrafish Semaphorin Z1a collapses specific growth cones and alters their pathway in vivo. Development 125, 1275-1283.

Shiau, C. E, Lwigale, P. Y., Das, R. M, Wilson, S. A, Bronner-Fraser M., 2008. Robo2-Slit1 dependent cell-cell interactions mediate assembly of the trigeminal ganglion. 11, 269-276.

Shiau, C. E., Bronner-Fraser, M., 2009. N-cadherin acts in concert with Slit1-Robo2 signaling in regulating aggregation of placode-derived cranial sensory neurons. Development 136, 4155-64.

Shigetani, Y., Howard, S., Guidato, S., Furushima, K., Abe, T., et al., 2008. Wise promotes coalescence of cells of neural crest and placode origins in the trigeminal region during head development. Dev. Biol. 319, 346-358.

Sidi, S., Sanda, T., Kennedy, R. D., Hagen, A. T., Jette, C. A., et al., 2008. Chk1 suppresses a caspase-2 apoptotic response to DNA damage that bypasses p53, Bcl2, and Caspase-3. Cell 133, 864–877.

Sjödal, M., Edlund, T., Gunhaga, L., 2007. Time of exposure to BMP signals plays a key role in the specification of the olfactory and lens placodes ex vivo. Dev. Cell 13, 141-149.

Solnica-Krezel, L., Sepich, D. S., 2012. Gastrulation: making and shaping germ layers. Annu. Rev. Cell Dev. Biol. 10, 687-717.

Solomon, K. S., Fritz, A., 2002. Concerted action of two *dlx* paralogs in sensory placode formation. Development 129, 3127-3136.

Solomon, K.S., Kudoh, T., Dawid, I. B., Fritz, A., 2003. Zebrafish *foxi1* mediates otic placode formation and jaw development. Development 130, 929-940.

Solomon, K. S., Kwak, S. J., Fritz, A., 2004. Genetic interactions underlying otic placode induction and formation. Dev. Dyn. 230, 419-433.

Spemann, H., Mangold, H., 1924. Über die Induktion von Embryonalanlagen durch Implantation artfremder Organisatoren. W. Roux' Arch. f. Entw. d. Organis.u. mikrosk. Anat. 100, 599-638.

Sun, S. K., Dee, C. T., Tripathi, V. B., Rengifo, A., Hirst, C.S., et al., 2007. Epibranchial and otic placodes are induced by a common Fgf signal, but their subsequent development is independent. Dev. Biol. 303, 675–686.

Steventon, B., Carmona-Fontaine, C., Mayor, R., 2005. Genetic network during neural crest induction: from cell specification to cell survival. Semin Cell Dev. Biol. 16, 647-654.

Steventon, B., Araya, C., Linker, C., Kuriyama, S., Mayor, R., 2009. Differential requirements of BMP and Wnt signalling during gastrulation and neurulation define two steps in neural crest induction. Development 136, 771-779.

Steventon, B., Mayor, R., 2012. Early neural crest induction requires an initial inhibition of Wnt signals. Dev. Biol. 365, 196-207.

Steventon, B., Mayor, R., Streit, A., 2012. Mutual repression between Gbx2 and Otx2 in sensory placodes reveals a general mechanism for ectodermal patterning. Dev. Biol. 367, 55-65.

Streit, A., 2007. The preplacodal region: an ectodermal domain with multipotential progenitors that contribute to sense organs and cranial sensory ganglia. Int. J. Dev. Biol. 51(6-7), 447-461.

Streit, A., Stern, C. D., 1999. Establishment and maintenance of the border of the neural plate in the chick: involvement of FGF and BMP. Mech. Dev. 82, 51-66.

Stuhlmiller, T. J., García-Castro, M. I., 2012. Current perspectives of the signaling pathways directing neural crest induction. Cell Mol. Life Sci. 22, 3715-3737.

Sun, S. K., Dee, C. T., Tripathi, V. B., Rengifo, A., Hirst, C. S., Scotting, P. J., 2007. Epibranchial and otic placodes are induced by a common Fgf signal, but their subsequent development is independent. Dev. Biol. 303(2), 675-686.

Swindell, EC., Zilinski, C. A., Hashimoto, R., Shah, R., Lane, M. E., 2008. Regulation and function of *foxe3* during early zebrafish development. Genesis 46, 177–183.

Tanghetti, E., Ria, R., Dell'Era, P., Urbinati, C., Rusnati, M., et al., 2002. Biological activity of substrate-bound basic fibroblast growth factor (FGF2): recruitment of FGF receptor-1 in endothelial cell adhesion contacts. Oncogene 21, 3889–3897.

Taverna, D., Disatnik, M. H., Rayburn, H., Bronson, R. T, Yang, J., et al., 1998. Dystrophic muscle in mice chimeric for expression of alpha5 integrin. J. Cell Biol. 143, 849-59.

Testaz, S., Duband, J. L., 2001. Central role of the alpha4beta1 integrin in the coordination of avian truncal neural crest cell adhesion, migration, and survival Dev. Dyn. 222, 127–140.

Thelen, M., 2001. Dancing to the tunes of chemokines. Nat. Immuno. 2, 129-134.

Thermes, V., Grabher, C., Ristoratore, F., Bourrat, F., Choulika, A., Wittbrodt, J., Joly, J. S., 2002. *I-SceI* meganuclease mediates highly efficient transgenesis in fish. Mech. Dev. 118, 91-98.

Trinh, L. A., Stainier, D. Y. R., 2004. Fibronectin regulates epithelial organization during myocardial migration in zebrafish. Dev. Cell 6, 371–382.

Toro, S., Varga, Z. M., 2007. Equivalent progenitor cells in the zebrafish anterior preplacodal field give rise to adenohypophysis, lens, and olfactory placodes. Sem. Cell Dev. Biol. 18, 534–542.

Toyofuku, T., Yoshida, J., Sugimoto, T., Yamamoto, M., Makino, N., et al., 2008. Repulsive and attractive semaphorins cooperate to direct the navigation of cardiac neural crest cells. Dev. Biol. 32, 251-262.

Tribulo, C**.,** Aybar, M. J**.,** Nguyen, V. H**.,** Mullins, M. C**.,** Mayor, R., 2003. Regulation of Msx genes by a Bmp gradient is essential for neural crest specification. Development 130, 6441-6452.

Tucker, J. A., Mintzer, K.A., Mullins, M. C., 2008. The BMP signaling gradient patterns dorsoventral tissues in a temporally progressive manner along the anteroposterior axis. Dev. Cell 14, 108-119.

Van Otterloo, E., Li, W., Garnett, A., Cattell, M., Meulemans Medeiros, C., Cornell, R. A., 2012. Novel Tfap2-mediated control of *soxE* expression facilitated the evolutionary emergence of the neural crest. Development 139, 720-730.

Vasilyev, A., Liu, Y., Mudumana, S., Mangos, S., Lam, P-Y., et al., 2009. Collective Cell Migration Drives Morphogenesis of the Kidney Nephron. Plos Biol. 7, e1000009.

Vendrell, V., Carnicero, E., Giraldez, F., Alonso, M. T., Schimmang, T., 2000. Induction of inner ear fate by FGF3. Development 127, 2011–2019.

Vidal, F., Aberdam, D., Miquel, C., Christiano, A. M., Pulkkinen, L., et al., 1995. Integrin beta 4 mutations associated with junctional epidermolysis bullosa with pyloric atresia. Nat. Genet. 10, 229–234.

Villanueva, S., Glavic, A., Ruiz, P., Mayor, R., 2002. Posteriorization by FGF, Wnt, and retinoic acid is required for neural crest induction. Dev. Biol. 241, 289-301.

Wang, W. D., Melville, D. B., Monteror-Balaguer, M., Hatzopoulos, A. K., Knapik E. W., 2011. Tfap2a and Foxd3 regulate early steps in the development of the neural crest progenitor population. Dev. Biol. 360, 173-185.

Ward, S. G., Marelli-Berg, F. G., 2009. Mechanisms of chemokine and antigen-dependent T-lymphocyte navigation. Biochem. J. 418, 13–27.

Wawersik, S., Evola, C., Whitman, M., 2004. Conditional BMP inhibition in *Xenopus*reveals stage-specific roles for BMPs in neural and neural crest induction. Dev. Biol. 277, 425-442.

Whitfield, T. T., Riley, B. B., Chiang, M.-Y., Phillips, B., 2002. Development of the zebrafish inner ear Dev. Dyn. 223, 427-458.

Whitlock, K. E., Westerfield, M., 2000. The olfactory placodes of the zebrafish form by convergence of cellular fields at the edge of the neural plate. Development 127, 3645–3653.

Wilson, P. A., Lagna, G., Suzuki, A., Hemmati-Brivanlou, A., 1997. Concentration-dependent patterning of the *Xenopus*ectoderm by BMP4 and its signal transducer Smad1. Development 124, 3177–3184.

Woda, J. M., Pastagia, J., Mercola, M., Artinger, K. B., 2003. Dlx proteins position the neural plate border and determine adjacent cell fates. Development 130, 331-342.

Wright, T. J, Mansour, S. L., 2003. Fgf3 and Fgf10 are required for mouse otic placode induction. Development 130. 3379-90.

Yabe, T., Shimizu, T., Muraoka, O., Bae, Y. K., Hirata, T., Nojima, H., Kawakami, A., Hirano, T., Hibi, M., 2003. Ogon/Secreted Frizzled functions as a negative feedback regulator of Bmp signaling. Development 130, 2705-2716.

Yam, J., Xu, L., Crawford, G., Wang, Z., Burgess, SM., 2006. The forkhead transcription factor Foxi1 remains bound to condensed mitotic chromosomes and stably remodels chromatin structure. Mol. Cell. Biol. 26, 155–168.

Yu, P. B., Hong, C. C., Sachidanandan, C., Babitt, J. L., Deng, D. Y., Hoyng, S. A., Lin, H. Y., Bloch, K. D., Peterson, R., 2008. Dorsomorphin inhibits Bmp signals required for embryogenesis and iron metabolism. Nature Chem. Biol. 4, 33-41.

Zaret, K. S., Carroll, J. S., 2011. Pioneer transcription factors: establishing competence for gene expression. Genes Dev. 25, 2227-2241.

Zaret, K.S., 2008. Genetic programming of liver and pancreas progenitors: lessons for stem-cell differentiation. Nat. Rev. Genet. 9, 329-340.

Zelarayan, L.C., Vendrell, V., Alvarez, Y., Domínguez-Frutos, E., Theil, T., et al., 2007. Differential requirements for FGF3, FGF8 and FGF10 during inner ear development. Dev. Biol. 308, 379-391.

Znosko, W. A., Yu, S., Thomas, K., Molina, G. A., Li. C., et al., 2010. Overlapping. functions of Pea3 ETS transcription factors in FGF signaling during zebrafish development. Dev. Biol. 342, 11–12.

Zygar, C. A., Cook Jr., T. L., Grainger, R. M., 1998. Gene activation during early stages of lens induction in Xenopus. Development 125, 3509-3519.